



**Prokhorov General Physics Institute
of the Russian Academy of Sciences**



**22th International Workshop
Complex Systems of Charged Particles and
Their Interactions with Electromagnetic Radiation**



CSCPIER

Moscow, Russia, April 6-10, 2026



УДК 533.9
ББК 22.333
В77

ISBN 978-5-6048157-4-8

Book of abstracts of 22th International Workshop Complex Systems of Charged Particles and Their Interactions with Electromagnetic Radiation, April 6-10, 2026, Prokhorov General Physics Institute of the Russian Academy of Sciences, Moscow, Russia. – M: GPI RAS, 2026. – 124 p.

The book of abstracts includes materials from the 22th International Workshop Complex Systems of Charged Particles and Their Interactions with Electromagnetic Radiation (April 6-10, 2026). The workshop's reports present modern results in plasma physics, laser physics and the interaction of radiation with matter.

Compiled by: Gusein-zade N.G., Bogachev N.N., Tarakanova E.N.,
Andreev S.E., Stepin V.P., Khudov A.V., Fomichev O.V.

ISBN 978-5-6048157-4-8



© Prokhorov General Physics Institute
of the Russian Academy of Sciences
© Authors, 2026

**22th International Workshop
Complex Systems of Charged Particles and
Their Interactions with Electromagnetic Radiation**

Program

Moscow, Russia, April 6-10, 2026

22th International Workshop
Complex Systems of Charged Particles and
Their Interactions with Electromagnetic Radiation

Moscow, Russia, April 6-10, 2026

PROGRAM

April 7, (Monday) 2026

9:30-10:00 Gathering of the CSCPIER-2026 participants

10:00-10:15 Opening Ceremony of the CSCPIER-2026

SECTION 1. BASIC ASPECTS OF PLASMA SCIENCE. 6 April 2026 (Monday)

10:15-10:45

THERMODYNAMIC LIMIT OF THE COULOMB SYSTEM IN THE MODEL OF A BOUNDED ONE-COMPONENT PLASMA (*Invited*)

D.I. Zhukhovitskii, E.E. Perevoshchikov

10:45-11:00

ROBUST ENHANCEMENT OF PLASMA SEPARATION FOR AN ENSEMBLE OF NON-INTERACTING IONS UNDER REALISTIC FIELD FLUCTUATIONS

I.V. Voronov, A.P. Oiler, A.V. Timofeev, R.A. Usmanov

11:00-11:15

SHORT-RANGE ORDERING IN CRYSTALLIZED MIXTURES OF ATOMIC NUCLEI AND THE PHASE DIAGRAM OF C/O MIXTURE

D.A. Baiko

11:15-11:30

RECOVERING ELECTRON SPECTRA WITH DEEP NEURAL NETWORKS

V.Y. Kozhevnikov, A.V. Kozyrev, V.F. Tarasenko, D.V. Beloplotov, E.Kh. Baksht, D.A. Sorokin, M.I. Lomaev

11:30-11:45 Coffee Break

11:45-12:15

TUNNELING OF ELECTROMAGNETIC RADIATION THROUGH A PLASMA LAYER: TUNNELING TIME ASYMPTOTICS AND HARTMAN EFFECT (*Invited*)

D.V. Novitsky, M.S. Usachonak, L.V. Simonchik, S.V. Gaponenko

12:15-12:30

PHYSICAL ORIGIN OF NON-SPECTRAL MATRIX EFFECTS IN RF PLASMAS AND THEIR SUPPRESSION VIA PLASMA PARAMETER CONTROL

T.K. Nurubeyli, N.Sh.Jafar

12:30-12:45

UNSTABLE HIGH FREQUENCY RADIATION IN INHOMOGENEOUS PLASMA IN PRESENCE OF DRIFT WAVE TURBULENCE

Paramananda Deka, Banashree Saikia

12:45-13:00

INTERACTION OF SURFACE WAVES AND GENERATION OF ACOUSTICS IN A MICROWAVE ATMOSPHERIC PRESSURE PLASMA JET

Suryasunil Rath, Satyananda Kar

13:00-13:15

TOWARDS A UNIFIED MODEL OF DC DISCHARGES WITH LIQUID (WATER) ELECTRODES

A.I. Saifutdinov, V.A.Purin, A.A. Saifutdinova

13:15-13:30

STRUCTURE OF THE ELECTROMAGNETIC FIELD IN AN ECR DISCHARGE IN A RESONATOR EXCITED BY A ROD ANTENNA

S.A. Dvinin, D.V. Chuprov, Z.A. Qodirzoda, D.K. Solihzoda

13:30-14:30 Lunch

14:30-15:00

THERMODYNAMIC FUNCTIONS OF NON-IDEAL PLASMA OF INDIUM (*Invited*)

A.V. Ivanov, A.M. Kondratyev, A.D. Rakhel, A.S. Shumikhin

15:00-15:15

PHONON-ROTON SPECTRUM IN ONE-COMPONENT PLASMA

S.A. Trigger

15:15-15:30

THE CLASSICAL CHARGED PARTICLE MOTION IN AXISYMMETRICAL NON-UNIFORM MAGNETIC FIELD

S.A. Maslov, S.A. Trigger

15:30-15:45

STEADY-STATE ULTRACOLD PLASMA

A.A. Bobrov, S.A. Saakyan, B.B. Zelener

15:45-16:00

TWO ELECTRON LOSS MECHANISMS OF ULTRACOLD PLASMA IN CONSTANT HOMOGENEOUS CROSSED ELECTRIC AND MAGNETIC FIELDS

E. V. Vikhrov, B.B. Zelener, B. V. Zelener

16:00-16:15

CONDUCTOR-INSULATOR CROSSOVER IN ULTRACOLD PLASMAS

Yu.V. Dumin, L.M. Svirskaya

16:15-16:30 Coffee Break

16:30-17:00

ON THE SCALING OF ANEUTRONIC PROTON – BORON FUSION IN A NANOSECOND VACUUM DISCHARGE (*Invited*)

Yu.K. Kurilenkov, A.V. Oginov, S.N. Andreev, S.Yu. Gus'kov, I.S. Samoylov

17:00-17:15

POSSIBILITIES OF IMPLEMENTING THE PROTON–BORON-11 NUCLEAR FUSION REACTION IN PULSED SYSTEMS WITH A MAGNETIC FIELD

A.Yu. Chirkov, E.G. Vovkivsky

17:15-17:30

ANOMALOUS ELECTRON FLUXES IN A PLASMA WITH ION-ACOUSTIC TURBULENCE AND POSSIBILITY OF CALCULATION OF CURRENT DENSITY IN HOLLOW CATHODES

A.A. Shelkovoy, S.A. Uryupin

17:30-17:45

NONLINEAR ION-ACOUSTIC WAVES IN NONISOTHERMAL PLASMA

S.V. Kuznetsov

17:45-18:00

TO THE MOST PROBABLE DISTRIBUTIONS OF STRUCTURELESS PARTICLES IN HIGHER-LEVEL STRUCTURAL UNITS AS APPLIED TO THE PHYSICS OF PHASE TRANSITIONS

M.Yu. Romanovsky

SECTION 2 COMPLEX PLASMAS. 7 April 2026 (Tuesday)

10:00-10:30

LOCALIZED OSCILLATIONS OF A LINEAR PLASMA CRYSTAL (Invited)

A.M. Ignatov

10:30-10:45

MICROPARTICLE SEPARATION BY RECTANGULAR-VOLTAGE PAUL TRAP IN AIR

M.S. Dobroklonskaya, L.M. Vasilyak, V.Ya. Pecherkin, V.I. Vladimirov

10:45-11:00

SELF-ORGANIZATION OF ACTIVE BROWNIAN PARTICLES IN AN ANISOTROPIC LINEAR STRUCTURE DEPENDING ON EXTERNAL PARAMETERS IN DC DISCHARGE

A.V. Erilin, E. A. Kononov, M. M. Vasiliev, O. F. Petrov

11:00-11:15

DYNAMICS OF ACTIVE BROWNIAN MOTORS IN COMPLEX COLLOIDAL SYSTEM IN VISCOUS MEDIUM

R.V. Senoshenko, E.A. Kononov, M.M. Vasiliev, O.F. Petrov

11:15-11:30

THE BEHAVIOUR OF SMALL SYSTEMS OF JANUS PARTICLES IN GAS-DISCHARGE PLASMA

X.G. Koss, K.A. Mizeva, D.A. Zamorin, M.M. Vasiliev, O.F. Petrov

11:30-12:00 Coffee Break

12:00-12:30

COMPETING MECHANISMS OF DUSTY PLASMA ROTATION IN A MAGNETIC FIELD (*Invited*)

V.Yu. Karasev, E.S. Dzlieva, M.A. Gasilov, L.A. Novikov, S.I. Pavlov

12:30-12:45

DUST PARTICLE ROTATION IN PLASMA AROUND ITS OWN AXIS

L.G. Dyachkov, E.S. Dzlieva, L.A. Novikov, S.I. Pavlov, M.S. Golubev, V.Yu. Karasev

12:45-13:00

EXPERIMENTAL STUDY OF DUSTY PLASMA FORMATION IN A LOW-PRESSURE CAPACITIVE RF DISCHARGE

M.E. Viktorov, S.V. Sintsov, D.A. Sergeev, I.M. Kraev, E.I. Preobrazhensky, A.V. Vodopyanov

13:00-13:15

INFLUENCE OF THE EXTERNAL ELECTROSTATIC POTENTIAL WELL CONFIGURATION ON THE FORM OF THE DUST PARTICLE STRUCTURES (*Online*)

A.V. Fedoseev, M.V. Salnikov, M.M. Vasiliev, O.F. Petrov

13:15-13:30

DISPERSION OF THE POWDER-GAS INTERFACE BY MICROWAVE RADIATION

R.I. Golyatina, S.A. Maiorov

13:30-13:45

EFFECT OF THE NATURE OF CERIUM-CONTAINING COMPOUNDS ON THE MICROWAVE SYNTHESIS OF LUMINESCENT MATERIALS

N.S. Akhmadullina, A.K. Kozak, N.N. Skvortsova, A.S. Sokolov, O.N. Shishilov

13:45-14:30 Lunch

14:30-15:00

DUSTY PLASMA IN THE SOLAR SYSTEM: SPECIFIC DUSTY PLASMA EFFECTS (*Invited*)

S.I. Popel, L.M. Zelenyi

15:00 -15:15

ON THE POSSIBILITY OF EXISTENCE OF NONLINEAR DUST ACOUSTIC PERTURBATIONS NEAR COMETS

Yu.S. Reznichenko, S.I. Popel, A.Yu. Dubinskii

15:15 -15:30

ON DUSTY PLASMAS IN JOVIAN MAGNETOSPHERE

S.I. Kopnin, S.I. Popel

15:30-15:45

EXPERIMENTAL INVESTIGATION OF REGOLITH SIMULANT DYNAMICS IN A FLOW OF CHARGED PLASMA PARTICLES

I.A. Shashkova, I.A. Kuznetsov, G.V. Koynash, S.I. Popel, G.G. Dol'nikov, A.N. Lyash, M.E. Abdelaal, A.V. Zakharov

15:45-16:00

ON NONLINEAR WAVE STRUCTURES IN ELECTRON-POSITRON-ION DUSTY PLASMAS

Yu.N. Izvekova, S.I. Popel

16:00-16:15

ON A POSSIBILITY OF DUSTY PLASMA FORMATION IN VENUSIAN IONOSPHERE

A.Yu. Dubinsky, S.I. Popel, Yu.S. Reznichenko

16:15 — 16:30

DUST ION-ACOUSTIC WAVES FROM THE INTERACTION OF A COMET'S TAIL WITH THE PLASMA OF THE ZODIACAL SOLAR CLOUD

T.I. Morozova, S.I. Popel

16:30-16:45 Coffee Break

16:45-18:00

An excursion of the laboratory at the Center for Plasma and Microwave Technologies at the Prokhorov General Physics Institute of the Russian Academy of Sciences

SECTION 3 LASER PLASMAS. 8 April 2026 (Wednesday)

10:00-10:30

GENERATION OF ELLIPTICALLY POLARIZED RADIATION BY GAS MEDIA IN TWO-COLOR LASER FIELDS (*Invited*)

S.Yu. Stremoukhov

10:30-10:45

LASER INDUCED DYNAMICS OF THE CONTINUUM STATE ELECTRONS AND SUBSEQUENT HARMONIC GENERATION IN SOLIDS

K.V. Lvov, S.Yu. Stremoukhov

10:45-11:00

HARMONICS GENERATION FROM RELATIVISTIC LASER STRUCTURED PLASMA

A.A. Andreev, K.Y. Platonov, M.V. Sedov, I.M. Ustinov

11:00-11:15

REFRACTIVE INDEX ULTRAFAST ANISOTROPY IN GASEOUS MEDIA INDUCED BY ULTRA-SHORT LASER PULSES

K.A. Galyuk, A.A. Ushakov, P.A. Chizhov

11:15-11:30

THE ROLE OF AIS IN THE MULTIPHOTON IONIZATION PROCESSES

S.N. Yudin, M.M. Popova, E.V. Gryzlova, A.N. Grum-Grzhimailo

11:30-11:45

COMPTON IONIZATION OF HYDROGEN BEAM BY A TWISTED PHOTON WITH USE OF THE COLTRIMS DETECTOR

Yu. V. Popov, K.A. Kouzakov, K. A. Bornikov

11:45-12:00 Coffee Break

12:00-12:30

METAMATERIALS AND OPTOACOUSTICS, LASER-INDUCED DEFORMATION OF SOLIDS, BERYLLIUM OPTICS AND FINE FOCUSING OF HARD X-RAYS FROM XFEL (*Invited*)

N.A. Inogamov

12:30-12:45

X-RAY GENERATION IN A MICROCLUSTER MEDIUM IRRADIATED BY AN ULTRASHORT LASER PULSE

D. A. Gozhev, S.G. Bochkarev, O.E. Vais, M.G. Lobok, V.Yu. Bychenkov

12:45-13:00

FEATURES OF THE CREATION AND CONTROL OF SUBWAVELENGTH MICROSTRUCTURES IN THE PROCESS OF DIRECT LASER WRITING IN THE VOLUME OF TRANSPARENT DIELECTRICS

A. V. Bogatskaya, E.A. Volkova, M. P. Verteletskaya, A. M. Popov

13:00-13:15

EFFECT OF LASER ENERGY DENSITY ON ABLATION EFFICIENCY OF ZINC SULFIDE NANOPARTICLES

A.V. Kharkova, D.A. Kochuev, A.A. Voznesenskaya, D.N. Bukharov

13:15-13:30

TIME DELAY OF REFLECTED AND TRANSMITTED LASER PULSE AT LASER ACTION ON A DENSE PLASMA SLAB

A.A. Frolov

13:30 -13:45

SCALABLE QUANTUM NEUROMORPHIC ARCHITECTURES BASED ON QUANTUM MEMRISTORS

A.S. Frolova, S.Yu. Stremoukhov, P.A. Forsh, I.A. Kovalishin, D.M. Rusakov, M.I. Shakirov, K.Yu. Khabarova, N.N. Kolachevsky

13:45 -14:00

ANALYTICAL ANALYSIS OF A QUANTUM MEMRISTOR ON AN ULTRACOLD $^{171}\text{YB}^+$ ION

I.A. Kovalishin, S.Yu. Stremoukhov, P.A. Forsh, K.Yu. Khabarova, N.N. Kolachevsky

14:00-14:30 Lunch

14:30-15:00

LASER AND BEAM PLASMA PARTICLE-IN-CELL SIMULATION IN A RELATIVISTIC REFERENCE FRAME (*Invited*)

A.G. Zhidkov

15:00-15:15

PROPAGATION OF A MONOENERGETIC BEAM OF RELATIVISTIC ELECTRONS IN VACUUM

D.E. Iankhotov, S.V. Kuznetsov, N.E. Andreev

15:15-15:30

ION WEIBEL INSTABILITY DIRECTLY OBSERVED IN FEMTOSECOND LASER-PLASMA EXPANSIO

A.V. Korzhimanov, R.S. Zemskov, S.E. Perevalov, A.V. Kotov, A.A. Murzanev, A.I. Korytin, K.F. Burdonov, V.N. Ginzburg, A.A. Kochetkov, S.E. Stukachev, I.V. Yakovlev, I.A. Shaikin, A.A. Kuzmin, A.A. Nechaev, V.I. Kocharovskiy, A.A. Soloviev, A.A. Shaykin, A.N. Stepanov, M.V. Starodubtsev, E.A. Khazanov

15:30-15:45

ENHANCEMENT OF QUASI-STATIONARY MAGNETIC FIELDS BY ORDERS OF MAGNITUDE VIA OPTIMIZATION OF THE PLASMA TRANSVERSE DENSITY PROFILE IN THE REGIME OF RELATIVISTIC SELF-CHANNELING

V.A. Kuleshova, A.V. Korzhimanov

15:45-16:00

LASER-DRIVEN AUTORESONANT ACCELERATION OF THERMAL ELECTRONS IN MAGNETIZED PLASMA CHANNELS

Iu.K. Gagarin, Ph.A. Korneev

16:00-16:15

ON SCALINGS OF ACCELERATION OF ELECTRONS AND GENERATION OF SHORT WAVELENGTH RADIATION IN LASER PLASMA AND SOLID TARGETS

M.E. Veysman, I.R. Umarov, N.E. Andreev

16:15-16:30 Coffee Break

16:30-17:00

ROLE OF PLASMA WAVES IN RESCATTERING PROCESSES IN INTENSE LASER FIELDS (*Invited*)

V. V. Strelkov, S. A. Bondarenko, I. V. Smetaniⁿ

17:00-17:15

TOWARDS GENERATING ELECTRON-POSITRON AVALANCHE PRE-CURSORS AT MULTI-PETAWATT LASER FACILITIES

A. A. Mironov

17:15-17:30

MEASURING ULTRA-STRONG FIELDS VIA PAIR PRODUCTION IN LASER PLASMA

A.A. Andreev, I.A. Alexandrov

17:30-17:45

ACCELERATION/DECELERATION AND TWISTING OF ATOMS BY CIRCULARLY POLARIZED LASER PULSES

V.S. Melezhik

17:45-18:00

RELATIVISTIC TUNNEL IONIZATION OF HIGHLY CHARGED IONS BY LASER RADIATION OF EXTREME INTENSITY

D.D. Baranov, S.V. Popruzhenko

18:00-18:15

RADIATION OF RELATIVISTIC ELECTRONS CREATED IN IONIZATION OF ATOMIC GASES BY LASER BEAMS OF EXTREME INTENSITY

N.V. Makarenko, S.V. Popruzhenko

SECTION-3 LASER PLASMAS. 9 April 2026 (Thursday)

10:00-10:30

PLASMA SPECTRUM SIMULATION: INFLUENCE OF EQUILIBRIUM PLASMA COMPOSITION AND LOWERING OF IONIZATION POTENTIALS (*Invited*)

M. Kuzmanović, M. Ristić, N. Krstevski

10:30-10:45

EXPERIMENTAL INVESTIGATION OF ⁸³KR ISOMERIC STATES POPULATION IN FEMTOSECOND LASER PLASMA

S.N. Ryazantsev, S.S. Makarov, I.Yu. Skobelev

10:45-11:00

CALCULATION OF THE GENERATION OF KR NUCLEAR ISOMERS IN THE INTERACTION OF HIGH-POWER LASER PULSES WITH A GAS CLUSTER JET

M.V.Sedov, I.Yu. Skobelev

11:00-11:15

OBSERVATION AND INTERPRETATION OF X-RAY EMISSION SPECTRA OF LASER PLASMA OF KRYPTON CLUSTERS

R.K. Kulikov, S.S. Makarov, S.N. Ryazantsev, I.Yu. Skobelev

11:15-11:30

DIAGNOSTICS OF PREPLASMA PROFILES WITH REFLECTION SPECTRA OF A RELATIVISTICALLY-INTENSE FEMTOSECOND LASER PULSE

A.R. Poletaeva, N.D. Bukharskii, Ph.A. Korneev, I.P. Tsygvintsev

11:30-11:45

PLASMODYNAMIC ESTIMATION OF A MULTILAYER TARGET UNDER THE INFLUENCE OF EXTERNAL WIDE BAND RADIATION

V.V. Kuzenov, A.G. Polyanskiy, S.V. Ryzhkov

11:45-12:00

THE IMPACTING LASER RADIATION DIFFRACTION INFLUENCE ON PHOTOEMISSION OF ELECTRONS FROM A METAL NEEDLE

A.V. Borovskiy, A.L. Galkin

12:00-12:30 Coffee Break

SECTION 5. SOLID STATE PLASMAS. 9 April 2026 (Thursday)

12:30-13:00

CONTROL OF ELECTROMAGNETIC CHARACTERISTICS OF SEMICONDUCTOR AND NANOCOMPOSITE STRUCTURES USING PLASMAS OF THEIR OWN FREE CHARGE CARRIERS (*Invited*)

V.Yu. Timoshenko

13:00-13:15

EFFECT OF FREE CHARGE CARRIER PLASMA IN ANISOTROPIC SILICON NANOSTRUCTURES ON THEIR OPTICAL PROPERTIES

Y. Deng, A.V. Ikonnikov, V.Yu. Timoshenko

13:15-13:30

FIELD EMISSION OF ELECTRONS FROM DISPERSED HYBRID DIAMOND-GRAPHITE FILM STRUCTURES

R.K. Yafarov

13:30-13:45

FEATURES OF AVALANCHE AND FIELD IONIZATION IN THE VOLUME OF TRANSPARENT DIELECTRICS IN PROCESS OF DIRECT LASER WRITING BY ULTRASHORT LASER PULSES

M.P. Verteletskaya, A.V. Bogatskaya, A.M. Popov

13:45-14:15 Lunch

14:15-14:45

CORRELATION EFFECTS IN INDUCED BINARY DIPOLAR SYSTEMS IN A DOUBLE-PLATE GEOMETRY (*Invited*)

E.A. Allahyarov, H. Lowen

14:45-15:00

EXCITATION OF TERAHERTZ SURFACE PLASMONS AT THE INTERFACE BETWEEN JOSEPHSON SANDWICH AND DIELECTRIC

A.S. Malishevskii, S.A. Uryupin

15:00-15:15

PLASMONIC INTERBAND HYBRIDIZATION IN HGTE QUANTUM WELLS

Yu.B. Vasilyev

15:15-15:30

QUANTUM FLUCTUATIONS OF THE NUMBER OF CURRENT CARRIERS AND ELECTRIC CHARGE IN QUASI-ONE-DIMENSIONAL SYSTEMS IN THE POLAR CRYSTAL MODEL

L.M. Svirskaya

15:30-16:00 Coffee Break

SECTION 4. GENERAL PLASMAS. 9 April 2026 (Thursday)

16:00-16:30

DIAGNOSTICS OF ATMOSPHERIC PLASMAS USING ATOMIC EMISSION LINE PROFILES (*Invited*)

B. Obradović, G. Sretenović, N. Cvetanović, S. Ivković, V. Kovačević, I. Krstić, M. Kuraica

16:30-16:45

ELECTRICAL BEHAVIOUR OF SUB-ATMOSPHERIC ALTERNATING CURRENT PLASMA FOR CARBON DIOXIDE CONVERSION TO ALTERNATIVE FUEL PRODUCTION

Pratyay Chattopadhyay, Satyananda Kar

16:45-17:00

CONTROL OF REACTIVE SPECIES DOSES THROUGH GROUND RESISTANCE MODULATION IN A SUB RADIO FREQUENCY ATMOSPHERIC PRESSURE PLASMA JET INTERACTION WITH LIQUID: IMPLICATION ON DYE DEGRADATION KINETICS AND CHANGES IN PHYSICOCHEMICAL PROPERTIES OF LIQUID

Aishik Basu Mallick, G. Veda Prakash, Satyananda Kar, Ramesh Narayanan

17:00-17:15

PLASMA-CHEMICAL STUDY OF A NONEQUILIBRIUM MICROWAVE DISCHARGE IN DIELECTRIC POWDERS

Z. A. Zakletskii

17:15-17:30

SPATIAL DISTRIBUTION OF ELECTRIC FIELD STRENGTH IN GAS MIXTURES WITH HELIUM IN AN ATMOSPHERIC PRESSURE GLOW DISCHARGE WITH DIFFERENT CATHODE SHAPES

A.V. Kazak, P.A. Ivanova, L.V. Simonchik, M.U. Tomkavich

17:30-17:45

VACUUM ULTRAVIOLET RADIATION OF THE PLASMA JET

V. P. Krainov, B.M. Smirnov

17:45-18:00

PROCESSING OF ION FLOW FOR PLASMA SEPARATION

D.D. Tiubaev, A.P. Oiler, A.V. Timofeev, R.A. Usmanov

SECTION 4. GENERAL PLASMAS. April 10 2026 (Friday)

10:00-10:30

MECHANISM OF HIGHLY-IONIZED PLASMA FILAMENT GROWTH IN A PULSED NANOSECOND DISCHARGE IN ATMOSPHERIC AIR (*Invited*)

E.V. Parkevich, A.I. Khirianova, K.V. Shpakov, T.F. Khirianov, K.S. Vinogradova, A.A. Tarasenko, D.V. Antonov, S.Yu. Gavrilov, N.A. Popov

10:30-10:45

FEATURES OF THE FORMATION OF A PULSED DISCHARGE IN HELIUM IN A POINT-TO-PLANE GAP

G.B. Ragimkhanov, A.A. Trenkin, A.N. Belonogov

10:45-11:00

FORMATION OF A PULSED DISCHARGE IN ATMOSPHERIC-PRESSURE HELIUM IN A PLANE-PARALLEL GEOMETRY UNDER CONDITIONS OF GAS PREIONIZATION

V.S. Kurbanismailov, G.B. Ragimkhanov, Z.R. Khalikova

11:00-11:15

INFLUENCE OF WATER VAPOR ON PLASMA PROPERTIES OF PULSE-PERIODIC DISCHARGE IN NON-UNIFORM ELECTRIC FIELD AT AIR

V.F. Tarasenko, D.V. Beloplotov, A.N. Panchenko, D.A. Sorokin

11:15-11:30

TRANSPORT PROPERTIES OF ELECTRON DRIFT IN A MIXTURE OF XENON AND WATER VAPOR

S.A. Maiorov, G.B. Ragimkhanov, R.I. Golyatina,

11:30-11:45

CREATION OF LUMINOUS CHARGED PARTICLES USING CAPILLARY AND CORONA DISCHARGES

V. L. Bychkov, A.A. Logunov, K.N. Kornev, D.V. Bychkov, O.S. Surkont

11:45-12:00 Coffee Break

12:00-12:30

ON MECHANISM PROVIDING THE TRAJECTORY TWIST OF SURFACE STREAMER IN A BARRIER DISCHARGE UNDER TRANSVERSE MAGNETIC FIELD (*Invited*)

Yu. Akishev, N. Dyatko, V. Karalnik, I. Kochetov, A. Petryakov

12:30-12:45

EXPERIMENTAL INVESTIGATION OF THE X- AND O-MODE ANOMALOUS ABSORPTION IN THE PLASMA FILAMENT

M.S. Usachonak, L.V. Simonchik, A.Yu. Popov, E.Z. Gusakov

12:45-13:00

EXPERIMENTAL DEMONSTRATION OF TEMPORAL COMPRESSION OF HIGH-CURRENT PULSED ELECTRON BEAM IN THE SYSTEM WITH VIRTUAL CATHODE

D.A. Adamyants, A.E. Donets, V.I. Rogozhin, A.A. Ravaev, A.B. Buleyko, O.T. Loza, I.R. Muftakhov

13:00-13:15

THE INFLUENCE OF THE INTRINSIC NOISE OF A RELATIVISTIC ELECTRON BEAM ON THE PARAMETERS OF ITS PROPAGATION

S.E. Andreev, I.L. Bogdankevich, N.G. Gusein-zade

13:15-13:30

CALCULATION OF NONLINEAR SPECTRA OF CHERENKOV INSTABILITIES OF DENSE ELECTRON BEAMS IN ELECTRODYNAMIC SYSTEMS OF PLASMA MICROWAVES

A.V. Ershov, M.V. Kuzelev

13:30-13:45

SELF-EXCITATION OF A PLASMA MICROWAVE AMPLIFIER USING AN NON-UNIFORM ABSORBE

I.N. Kartashov, M.V. Kuzelev, A.V. Tumanov

13:45-14:30 Lunch

14:30-15:00

POSSIBILITIES OF ATOMIC-LAYER ETCHING IN INDUCTIVELY COUPLED PLASMA FOR THE CREATION OF NANOELECTRONIC DEVICES (*Invited*)

A.V. Miakonkikh, R.R. Khalilullin, V.O. Kuzmenko

15:00-15:15

NUMERICAL INVESTIGATION OF CLAMP EFFECT ON SPACE CHARGE LAYER FORMATION AND IMPACT ON ETCH UNIFORMITY

R.R. Khalilullin, V.O. Kuzmenko, A.V. Miakonkikh

15:15-15:30

MICROWAVE GYROTRON-INDUCED COATING FORMATION ON TUNGSTEN PLATES FROM METAL AND DIELECTRIC POWDERS

T.E. Gayanova, E.A. Obraztsova, A.V. Stepanova, A.S. Sokolov, E.V. Voronova, V.D. Stepakhin, N.N. Skvortsova

15:30-15:45

SYNTHESIS OF SODIUM-MANGANESE OXIDE MATERIALS VIA MICROWAVE DISCHARGE: FIRST EXPERIMENTAL RESULTS

M.E. Donets, T.E. Gayanova, N.N. Skvortsova, N.S. Akhmadullina, V.D. Borzosekov, D.V. Malakhov, E.A. Korneeva, N.Yu. Samoylova

15:45-16:00

EFFECTIVE LENGTH OF A PLASMA ANTENNA ON A PLASMA COLUMN

I.M. Minaev, V.I. Zhukov, O.V. Tikhonovich, D.M. Karfidov, I.L. Bogdankevich

16:00-16:15

STRUCTURE AND DYNAMICS OF A SURFACE-WAVE-SUSTAINED MICROWAVE DISCHARGE IN LOW-PRESSURE ARGON

V.P. Stepin, V.I. Zhukov, D.M. Karfidov, S.E. Andreev, I.L. Bogdankevich, N.N. Bogachev

16:15-16:30 Coffee Break

16:30-17:00

PLASMA SCIENCE AND TECHNOLOGY IN BRAZIL: FOUR PILLARS FROM FUSION AND SPACE PLASMAS TO ATMOSPHERIC-PRESSURE APPLICATION (*Invited*)

R.S. Pessoa, G. Petraconi Filho, D.M. Leite, A.L.J. Pereira, A.S. da Silva Sobrinho, H.S. Maciel

17:00-17:15

PLASMA TECHNOLOGIES IN AERODYNAMICS

S.V. Ryzhkov, V.V. Kuzenov

17:15-17:30

INTERACTION OF POWERFUL HIGH-FREQUENCY RADIO EMISSION WITH PLASMA IN THE LOWER AND UPPER IONOSPHERE - EXPERIMENTAL RESULTS

N.V. Bakhmetieva, I.N. Zhemyakov, E.E. Kalinina, O.K. Khromin

17:30-17:45

INVESTIGATION OF SPORADIC E-STRUCTURES AND WAVE PHENOMENA IN THE EARTH'S LOWER IONOSPHERE BASED ON ANALYSIS OF RADIO OCCULTATION MEASUREMENTS

V.N. Gubenko, I.A. Kirillovich, V.E. Andreev

17:45-18:00 Closing Ceremony of the CSCPIER-2026

**22th International Workshop
Complex Systems of Charged Particles and
Their Interactions with Electromagnetic Radiation**

Book of abstracts

Moscow, Russia, April 6-10, 2026

THERMODYNAMIC LIMIT OF THE COULOMB SYSTEM IN THE MODEL OF A BOUNDED ONE-COMPONENT PLASMA

D.I. Zhukhovitskii¹, E.E. Perevoshchikov^{1,2}

¹*Joint Institute of High Temperatures, RAS, Moscow, Russian Federation, dmr@ihed.ras.ru*

²*Moscow Institute of Physics and Technology, Dolgoprudny, Moscow Region, Russian Federation*

The classical one-component plasma (OCP) bounded by a spherical surface reflecting ions (BOCP) is studied using molecular dynamics (MD). Simulations performed for a series of sufficiently large BOCPs made it possible to establish the size dependences for the investigated quantities and extrapolate them to the thermodynamic limit. Estimated limit of the total electrostatic energy per ion u is very close to the Debye–Hückel model at the Coulomb coupling parameter $\Gamma = 0.1$ and to the Madelung constant u_0 at $\Gamma = 1000$, and it is lower by nearly 0.5% than the modern Monte Carlo (MC) simulation data obtained by different authors for intermediate Γ . This energy difference far exceeds the relative error of the calculations, which is about 0.1%. We attribute this to the non-vanishing effect of boundary conditions in both OCP and BOCP cases. Based on the excess interatomic energy and the excess ion–background energy, we calculate the wide-range ionic equation of state inaccessible for conventional MC and MD simulations of the OCP with periodic boundary conditions (PBC). The corresponding ionic compressibility factor (Fig. 1, left panel) vanishes at high Γ , in accordance with [1].

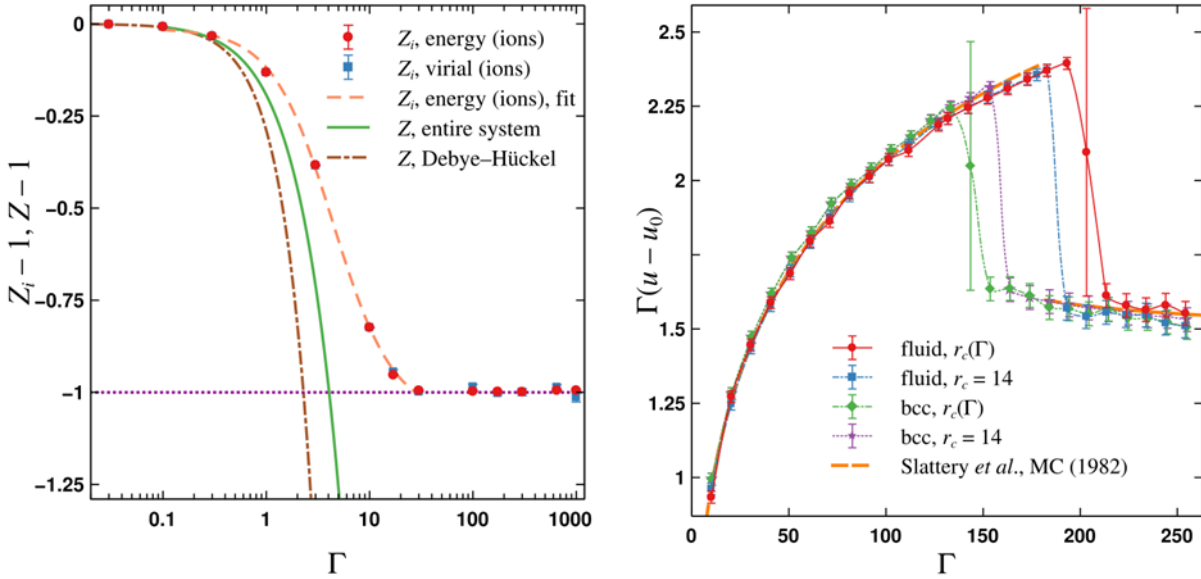


Fig. 1. Left panel: Ionic compressibility factor Z_i determined for BOCP from MD simulation as compared to the renormalized compressibility factor Z for OCP with PBC and to the Debye–Hückel model. Right panel: Thermal fraction of the potential energy as a function of Γ for OCP from LAMMPS calculations. The metastable region is located between abrupt changes of u indicated by almost vertical lines. Orange dashed line shows the data from [2].

We utilize the ionic equation of state to propose an improved cutoff radius $r_c(\Gamma)$ for the interionic forces implemented in LAMMPS. We demonstrate that the kinetic and interfacial quantities determined for the classical OCP may be ambiguous. To check this, we perform a simulation of the OCP metastable region and find that its width depends sensitively on the cutoff radius decreasing with the increase of the latter (Fig. 1, right panel).

References

- [1]. Zhukhovitskii D. I. and Perevoshchikov E. E. *High Temp.* **62** (4) 484-493 (2024).
- [2]. Sattery W. L., et al. *Physical Review A* **26** (4) 2255-2258 (1982).

ROBUST ENHANCEMENT OF PLASMA SEPARATION FOR AN ENSEMBLE OF NON-INTERACTING IONS UNDER REALISTIC FIELD FLUCTUATIONS

I.V. Voronov, A.P. Oiler, A.V. Timofeev, R.A. Usmanov

*Joint Institute for High Temperatures of the Russian Academy of Sciences, Izhorskaya 13
Bldg 2, Moscow 125412, Russia*

Plasma mass separation in crossed electric and magnetic fields represents a promising technique for processing nuclear waste, isotope enrichment, and rare-earth element extraction. Prior single-particle studies demonstrated that introducing a localized Gaussian perturbation into a linear electric potential profile can substantially improve the spatial separation of ion species with different charge-to-mass ratios [1]. The present work extends this result to physically realistic conditions by considering ensembles of ions with distributed initial conditions and by explicitly accounting for realistic electromagnetic field fluctuations.

We consider a cylinder of radius R with a uniform axial magnetic field B_z and a radial electric field derived from either a linear potential $U_0(r)$ or a combined potential

$$U(r) = U_0(r) + A \exp\left(-\frac{(r - r_1)^2}{2\sigma_1^2}\right),$$

where the Gaussian term introduces a localized nonlinearity. Two equally charged ion species with different masses are initialized in a localized region near the cylinder wall; their in-plane velocities are sampled from a Maxwellian at temperature T and shifted by a drift velocity. Particle trajectories are computed using the Boris pusher. Separation is quantified by the metric

$$Q = \frac{|\langle\theta_1\rangle - \langle\theta_2\rangle|}{\sigma_{\theta_1} + \sigma_{\theta_2}},$$

where θ is the deposition angle and $\langle\cdot\rangle$, σ denote ensemble mean and standard deviation [2].

To assess robustness, we propagate parameter uncertainties via automatic differentiation (JAX) and define a reliability score

$$Z = \frac{Q - Q^*}{\sqrt{\sigma_Q^2 + \sigma_{Q^*}^2}},$$

where Q^* is the best separation attainable in the linear potential within prescribed (U_0, B_z) bounds. Requiring $Z \geq 1.645$ ensures 95% confidence that $Q \geq Q^*$ for the adopted fluctuation levels [3]. A scan over (A, r_1, σ_1) shows that the combined potential can reliably increase separation by $\approx 10\%$ relative to Q^* across a broad range of operating parameters (U_0, B_z) and initial-condition spreads. However, when reliability targets are tightened, field fluctuations are stronger, or initial-condition distributions are broader, the robustly admissible region in (A, r_1, σ_1) becomes empty, implying that predictable improvement is not always achievable.

Sensitivity analysis indicates that electric-potential fluctuations dominate the uncertainty of Q , while magnetic-field fluctuations contribute least to the total uncertainty, suggesting that stabilizing the potential is the most effective route to increasing robustness. The proposed framework provides practical criteria for selecting field parameters that maximize separation under quantified uncertainty and can be extended to include inter-particle interactions.

The study was supported by grant No. 25-79-30008 from the Russian Science Foundation, <https://rscf.ru/project/25-79-30008/>

References

- [1]. Oiler A. P., et al. *Molecules* **27**(20), 6824 (2022).
- [2]. Smirnov V. S., et al. *Phys. Plasmas* **27**(11), 113503 (2020).
- [3]. Valinurov M. A., et al. *Plasma Phys. Rep.* **49**(5), 649–655 (2023).

SHORT-RANGE ORDERING IN CRYSTALLIZED MIXTURES OF ATOMIC NUCLEI AND THE PHASE DIAGRAM OF C/O MIXTURE

D.A. Baiko

Ioffe institute, Saint Petersburg, Russia, baiko.astro@mail.ioffe.ru

Mixtures of bare atomic nuclei on a nearly uniform neutralizing electron background are a realistic model of matter in the interior of white dwarfs and crusts of neutron stars. Despite tremendous progress in understanding their phase diagrams achieved mainly via first-principle simulations [1-4], structural, thermodynamic, and kinetic properties of these mixtures are poorly understood. We develop a semi-analytic model of the crystal state of such binary mixtures based on the concept of mutual short-range ordering of nuclei of two sorts. We derive an analytic formula for the electrostatic energy of the crystal mixtures, including the crucial effect of static displacements of the nuclei from the ideal lattice nodes, and analyze a dependence of the crystal mixture residual entropy on the order parameters. Furthermore, we perform free energy minimization with respect to the order parameters for C/O mixtures at all relevant compositions and temperatures. The resulting C/O phase diagram is in a reasonable agreement with that obtained in the most advanced first-principle study (Fig. 1). The proposed theory opens up a path to analyze ordering and construct phase diagrams of ternary mixtures (e.g., C/O/²²Ne) which are of great practical interest in astrophysics.

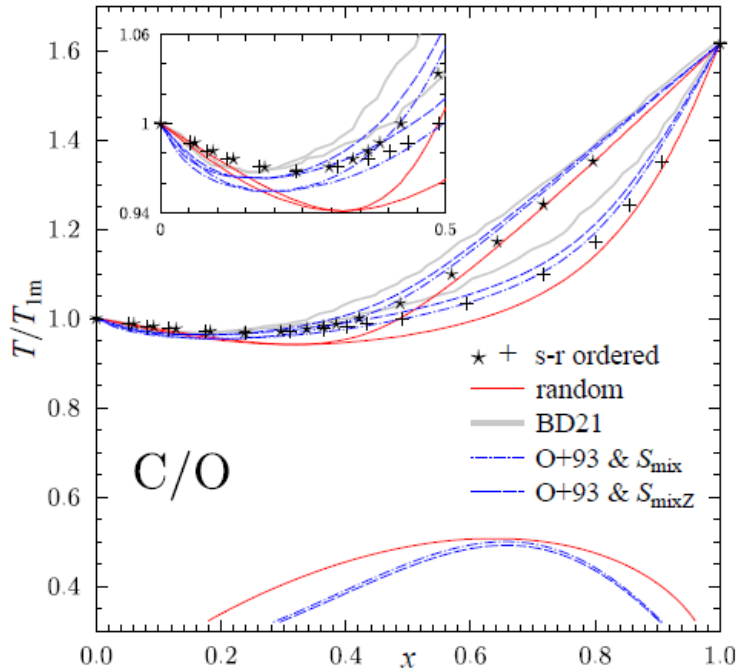


Fig. 1. C/O phase diagram for a short-range ordered crystal (symbols), fully disordered crystal (solid), based on simulations [4] (thick solid grey), based on the energy model [1] with the residual entropy equal to S_{mix} (dot-dashed) or S_{mixZ} (dashed) [5]

References

- [1]. Ogata S., et al. *Phys. Rev. E* **48**: 1344 (1993)
- [2]. Horowitz C. J., et al. *Phys. Rev. Lett.* **104**: 231101 (2010).
- [3]. Medin Z., Cumming A. *Phys. Rev. E* **81**: 036107 (2010).
- [4]. Blouin S., Daligault J. *Phys. Rev. E* **103**: 043204 (2021).
- [5]. Baiko D. A. *Mon. Not. Roy. Astron. Soc.* **517**: 3962 (2022).

RECOVERING ELECTRON SPECTRA WITH DEEP NEURAL NETWORKS

V.Yu. Kozhevnikov, A.V. Kozyrev, V.F. Tarasenko, D.V. Beloplotov, E.Kh. Baksht,
D.A. Sorokin, M.I. Lomaev

Institute of High Current Electronics SB RAS, Tomsk, Russia, kozhevnikov@hcei.ru

Experimental determination of particle energy distribution functions in subnanosecond electron beams is a critically important problem in modern pulsed power physics. The standard approach involves the attenuation curve method, which requires solving a Fredholm integral equation of the first kind. This task is a classic ill-posed inverse problem where small variations in experimental data can lead to unstable or unphysical solutions [1]. While the Arsenin-Tikhonov regularization methodology has been traditionally used, it often introduces numerical artifacts, such as negative excursions or spurious peaks, and typically assumes that the integral kernel is known exactly [2], [3].

This paper presents a deep learning-based methodology (PINN) for reconstructing electron energy spectra, which explicitly accounts for measurement uncertainties in both the experimental attenuation curves and the integral operator kernel [4]. The proposed framework utilizes two coupled neural networks: a spectrum approximation network and an adaptive kernel correction network. As a mesh-free technique, it operates directly on raw, sparse experimental datasets without extra interpolation or preprocessing.

The methodology was validated using experimental data for vacuum and atmospheric-pressure gas-filled diodes from a number of experimental papers. The results demonstrate that the neural network approach successfully resolves non-trivial two-peak spectral structures and reliably identifies populations of "anomalous" high-energy electrons. Unlike traditional regularization [1], this method ensures strict non-negativity of the reconstructed spectrum and avoids classical artifacts, providing a robust tool for pulsed electronics and accelerator physics.

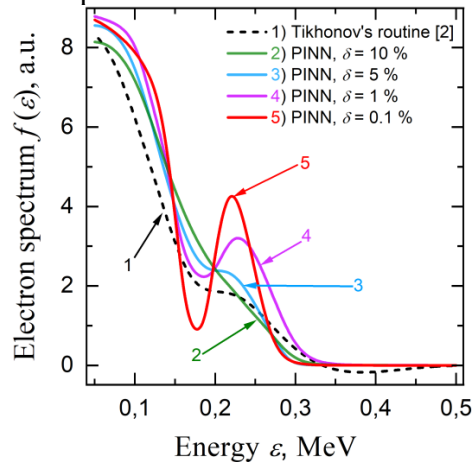


Fig. 1. An example of the PINN-reconstructed energy spectrum: 1 – solution of the incomplete ill-posed problem [2]; 2–5 – the solutions of the full inverse problem using the proposed deep-learning method.

The work was carried out within the framework of the State Task of the Ministry of Science and Higher Education of the Russian Federation on themes FWRM-2026-0008 and FWRM-2026-0009.

References

- [1]. Tikhonov A. N. and Arsenin V. I. *Solutions of ill-posed problems*. Washington, New York (1977).
- [2]. Kozyrev A. V., Kozhevnikov V. Yu., et al. *Russ. Phys. J.* **53** 361-368 (2010).
- [3]. Baksht E. Kh., et al. *J. Phys. D: Appl. Phys.* **43** 305201 (2010).
- [4]. Tabata T. and Ito R. *Nucl. Instrum. Method.* **127** 429-434 (1975).

TUNNELING OF ELECTROMAGNETIC RADIATION THROUGH A PLASMA LAYER: TUNNELING TIME ASYMPTOTICS AND HARTMAN EFFECT

D.V. Novitsky, M.S. Usachonak, L.V. Simonchik, S.V. Gaponenko

*B.I. Stepanov Institute of Physics, National Academy of Sciences of Belarus, Minsk, Belarus,
E-mail: dvnovitsky@gmail.com*

Tunneling is a well-known quantum phenomenon arising due to wave-like nature of quantum objects. It turns out that a similar effect can be observed for classical electromagnetic radiation propagating with imaginary wavenumber due to evanescence or negative permittivity. The latter variant naturally occurs in plasma below the plasma frequency, where the medium has extremely low transparency for electromagnetic waves.

In this work, we study theoretically and experimentally the problem of tunneling time for electromagnetic radiation propagating through a plasma layer in the limit of low transparency. The issue of tunneling time remains controversial due to different definitions and interpretations of time values used by different researchers [1]. We show that asymptotically (in the low-frequency limit – $\omega \ll \omega_p$) the tunneling time through the plasma layer does not depend on radiation frequency and is inversely proportional to the plasma frequency. This result is obtained analytically for the phase (Wigner) time in the continuous-wave limit [2] and is supported by numerical simulations of electromagnetic pulse propagation giving the same asymptotic values value for both phase and center-of-gravity times [3]. The obtained asymptotics for plasma principally differ from the other cases of electromagnetic tunneling usually demonstrating the inverse dependence of the tunneling time on radiation frequency.

Our calculations also demonstrate the electromagnetic analogue of the quantum-mechanical Hartman effect. This effect consists in tunneling time independence of the layer thickness in the limit of very low layer transparency and is observed as saturation of the tunneling time with layer thickness. Although this implies paradoxical evidence of superluminal radiation propagation, we give it an interpretation compatible with the standard relativity notions. Finally, it is shown that one can use the delay of not only transmitted, but also of reflected pulses to obtain tunneling times. The approach based on high-intensity reflected radiation is advantageous from a practical point of view.

The theoretical results are supported by experiments with microwaves propagating through periodic structures based on gas-discharge plasmas. The experimental scheme is based on the approach developed in Ref. [4] and consists of the rectangular waveguide with the periodically placed gas-discharge tubes. Interaction of microwave radiation with this electromagnetic crystal can be tuned simply by changing the discharge current and, hence, the electron density inside the plasma tubes. The phase time for microwaves was determined from the transmission spectra for different discharge currents. In the low-frequency range, the phase-time dependence on the electron density is in accordance with the expected from theory inverse-square-root relation.

We believe that the features of radiation tunneling reported here are important for both fundamental understanding of this phenomenon and for practical study of plasma media.

References

- [1]. Winful H. G. *Phys. Rep.* **436** (1-2) 1-69 (2006).
- [2]. Gaponenko S. V., Novitsky D. V. *Phys. Rev. A* **106** (2) 023502 (2022).
- [3]. Novitsky D., Usachonak M., Simonchik L., Gaponenko S. *Phys. Rev. A* **111** (3) 033529 (2025).
- [4]. Arkhipenko V. I. et al. *J. Appl. Phys.* **116** (12) 123302 (2014).

PHYSICAL ORIGIN OF NON-SPECTRAL MATRIX EFFECTS IN RF PLASMAS AND THEIR SUPPRESSION VIA PLASMA PARAMETER CONTROL

T.K.Nurubeyli^{1,2}, N.Sh.Jafar¹

¹*Institute of Physics of the Ministry of Science and Education of Republic of Azerbaijan, H. Javid Avenue, 131, Baku, AZ-1073, Azerbaijan, t.nurubeyli@physics.science.az, nurlanajafarr@gmail.com*

²*Azerbaijan State Oil and Industry University, Azadliq Avenue, 20, Baku, AZ-1010, Azerbaijan, omartarana@gmail.com*

Nonspectral matrix effects in RF inductively coupled plasmas originate from fundamental plasma-physical processes that disturb ionization equilibrium and energy balance rather than from spectral overlap. High matrix concentrations (e.g., HCl and HNO₃) increase plasma loading, consume energy for desolvation and atomization, and reduce effective plasma temperature in the analytical zone. As a result, elements with higher first ionization potential (φ_i^+) experience stronger signal suppression compared to easily ionized elements. In addition, redistribution of high-temperature regions and changes in analyte residence time alter ion formation kinetics and enhance ion–electron recombination [1].

Increasing RF generator power restores plasma temperature and improves radial energy transport toward the central channel. At elevated power (1430–1550 W), the plasma reaches a stable thermodynamic regime where ionization efficiency becomes nearly independent of matrix composition, and discrimination between low- and high-ionization-potential elements is minimized.

Optimization of nebulizer argon flow further stabilizes plasma conditions. Reduced flow (~1.00 L/min) decreases convective cooling, limits formation of oxide and doubly charged ions, and stabilizes electron density, thereby compensating matrix-induced ionization shifts. Excessive gas flow, in contrast, enhances plasma cooling and increases nonspectral effects.

Sampling geometry also affects ion extraction efficiency. Proper sampling depth ensures ion collection from a thermally stabilized plasma region where ionization equilibrium is maximized. Deviations from optimal conditions shift extraction toward lower-temperature zones and increase discrimination of high φ_i^+ elements. Adjustment of sample uptake rate influences aerosol size distribution and plasma loading, indirectly affecting ionization efficiency [2].

The lens–extractor potential primarily controls ion transmission rather than ion formation. Within moderate negative potentials (–10 to –20 V), ion transport efficiency is optimized without amplifying matrix effects.

Thus, nonspectral matrix effects are plasma-thermodynamic phenomena caused by perturbations in temperature, electron density, and ionization kinetics. Their suppression is achieved through controlled optimization of RF power, gas flow, and sampling conditions, which stabilizes plasma equilibrium and eliminates ionization-potential-based discrimination across different matrices [3].

References

- [1]. T.K. Nurubeyli, N.S. Jafar, G.N. Mammadova, *International Journal of Mass spectrometry*, vol. 507, 117355, 2025
- [2]. T.K. Nurubeyli, N.Sh. Jafar, K.N. Ahmadova, *Methods and Objects of Chemical Analysis*, vol. 20, № 1, pp. 39–45, 2025
- [3]. T.K. Nurubeyli, A.M. Hashimov, N.S. Jafar, *International Journal on Technical and Physical Problems of Engineering*, vol. 17, № 1, pp. 59–68, 2025

UNSTABLE HIGH FREQUENCY RADIATION IN INHOMOGENEOUS PLASMA IN PRESENCE OF DRIFT WAVE TURBULENCE

Paramananda Deka¹, Banashree Saikia²

¹*Department of Mathematics, Dibrugarh University, Dibrugarh-786004, Assam, India*

²*Department of Mathematics, Sibsagar University, Sivasagar-785665, Assam, India*

The ubiquitous presence of drift wave turbulence in magnetically confined inhomogeneous plasmas provides a significant reservoir of energy in the system that can be transferred to high-frequency electromagnetic modes through nonlinear wave particle interaction process. This study investigates the excitation of unstable high-frequency radiation in the presence of drift wave turbulence energy which may act as pump wave through a nonlinear wave-particle, specifically the plasma maser effect, in an inhomogeneous plasma system [1, 2].

A kinetic formulation, based on the Vlasov-Poisson system of equations is employed to describe the interaction between low-frequency drift wave turbulence and a high-frequency test wave. Following the linear response theory[3] for turbulent plasmas, the unperturbed particle distribution function incorporates the density inhomogeneity through a gradient parameter $\lambda = \left[\left(\frac{1}{f_{0j}} \frac{df_{0j}}{dy} \right) \right]_{y=0}$ under the local approximation. The nonlinear dispersion relation for the high-frequency mode is derived, accounting for both direct coupling and polarization coupling contributions arising from the modulated field. The growth rate is evaluated by analyzing the imaginary part of the nonlinear dispersion relation under the condition that the drift wave satisfies the Cherenkov resonance condition $\omega = \mathbf{k} \cdot \mathbf{v}$ [4], while the high-frequency mode is treated as non-resonant [5].

The analysis reveals that the growth rate is proportional to the energy density of the drift wave turbulence and exhibits a strong dependence on the density gradient parameter. The polarization coupling term is identified as the dominant contributor to the growth, consistent with previous findings on plasma maser interactions in inhomogeneous systems. Using parameters, characteristic of tokamak edge plasmas, the normalized growth rate is estimated to be of the order $\gamma/\Omega \sim 10^{-3}$, which is comparable to or exceeds typical damping rates such as Landau damping, suggesting the viability of this mechanism for generating high-frequency radiation in fusion-relevant plasmas [6,7].

The findings highlight the critical role of density inhomogeneity in enhancing the plasma maser effect, leading to efficient up-conversion of low-frequency turbulent energy into high-frequency electromagnetic radiation. This mechanism may provide a plausible explanation for anomalous high-frequency emissions observed in tokamaks and magnetospheric plasmas, such as auroral kilometric radiation. The results underscore the importance of incorporating gradient effects in predictive models of wave instabilities in confined plasma systems.

References

- [1]. Deka, P. N., Borgohain, A. *Phys. Plasmas* **18** (4) 042311 (2011).
- [2]. Singh, M., Deka, P. N. *Phys. Plasmas* **12** (10) 102304 (2005).
- [3]. Nambu, M. *Laser Part. Beams* **1** (4) 427-454 (1983).
- [4]. Deka, P. N., Borgohain, A. *Phys. Plasmas* **18** (4) 042311 (2011).
- [5]. Saikia, B., Deka, P. N. *East Eur. J. Phys.* (3) 122-132 (2023).
- [6]. Saikia, B., Deka, P. N. *J. Korean Phys. Soc.* (2023).
- [7]. Saikia, B., Deka, P. N., Karmakar, P. K. *Fundam. Plasma Phys.* **16** 100104 (2025).

INTERACTION OF SURFACE WAVES AND GENERATION OF ACOUSTICS IN A MICROWAVE ATMOSPHERIC PRESSURE PLASMA JET

Suryasunil Rath, Satyananda Kar

Atmospheric pressure research laboratory (APRL), Department of Energy Science and Engineering, Indian Institute of Technology Delhi, Hauz Khas, New Delhi, India,
suryasunilrath918@gmail.com

The interaction of surface waves strongly influences plasma stability and energy transport in microwave atmospheric pressure plasma jets (MW-APPJs)[1][2]. This study investigates surface-wave interaction and its role in acoustic wave generation in a MW-APPJ operated in continuous-wave mode. Audible acoustic emissions were observed at microwave powers of 220-360 W and 570-620 W under argon flow rates of 3-12 lpm, with controlled air swirl and water cooling. Acoustic signals were analyzed using Fast Fourier Transform, while plasma fluctuations were characterized by optical emission spectroscopy, gas temperature measurements, and high-speed imaging. The results indicate that interference between surface waves near the applicator induces periodic plasma instabilities, producing pressure perturbations responsible for acoustic emission. These findings clarify plasma wave acoustic coupling mechanisms in MW-APPJs[3].

References

- [1]. S. Rath and S. Kar, "Microwave atmospheric pressure plasma jet: A review," *Contrib. to Plasma Phys.*, vol. 65, no. 2, p. e202400036, 2025, doi: 10.1002/ctpp.202400036.
- [2]. S. Rath, P. Das, P. M. Pandey, and S. Kar, "Uncertainty-Aware Machine Learning-Based Prediction of Plasma Parameters in a Microwave Atmospheric Pressure Plasma Jet," *Phys. Chem. Chem. Phys.*, p., 2026, doi: 10.1039/D5CP04364F.
- [3]. S. Rath and S. Kar, "Generation of sound waves in a continuous-wave mode microwave atmospheric pressure plasma jet," *Ph`ys. Fluids*, vol. 37, no. 11, p. 117113, 2025, doi: 10.1063/5.0293788

TOWARDS A UNIFIED MODEL OF DC DISCHARGES WITH LIQUID (WATER) ELECTRODES

A.I. Saifutdinov, V.A. Purin, A.A. Saifutdinova

*Kazan National Research Technical University named after A.N. Tupolev, Kazan, Russia,
as.uav@bk.ru*

This paper presents a self-consistent model of low-current glow discharges with a liquid-phase anode. This model is based on an extended fluid description of the plasma and takes into account gas heating, heating of the metal cathode and liquid-phase anode, and the evaporation of water molecules into the discharge gap.

Numerical simulations were performed for three cases. In the first, it was assumed that the discharge was initiated in argon, with water molecules initially virtually absent from the discharge gap. The set of particles considered was taken from [1], and the plasma-chemical reactions from [2, 3]. For this case, the dynamics of the evaporation of water molecules into the discharge gap and the change in plasma-forming charged particles from electrons and argon molecular ions to the water cluster ion $H_9O_4^+$ and the negative ion OH^- , respectively, were demonstrated. In the second series of calculations, a case was considered in which it was assumed that water molecules were present in the discharge gap and their concentration corresponded to the saturated vapor pressure at an initial liquid anode temperature of 293 K. It was shown that the dominant positive ion species in the discharge over virtually the entire time interval is the cluster ion $H_9O_4^+$. The concentrations of electrons and negative OH^- ions are virtually equal, and competition between the dominant species is observed at different time intervals up to several tens of milliseconds. Over a time interval above 1 s, OH^- is the dominant negatively charged particle. However, the electron concentration is only a few times lower than the negative ion concentration, since electrons are necessary to maintain the discharge and form negative ions.

In the third case, it was assumed that the discharge was initiated in helium, and the concentration of water molecules in the discharge gap was set to correspond to the saturated vapor pressure at an initial liquid anode temperature of 293 K. An extended set of plasma-chemical processes, taken from [2, 3], was considered. Numerical calculations yielded a temporal evolution of the discharge parameters that demonstrated complex quasi-periodic behavior caused by a sequential change in the dominant charge transfer mechanisms and thermal processes at the electrodes. The following phases can be identified. Analysis showed that this is a consequence of the nonlinear interaction of two time scales:

1) Fast electronic processes ($\tau \sim 10^{-6}$ – 10^{-3} s), which determine the balance between ionization and attachment.

2) Slow thermal processes ($\tau \sim 10^{-3}$ – 10^1 s), associated with the heating of the electrodes and the evaporation of water molecules into the discharge gap, which irreversibly shift the plasma to a state of ion-ion conductivity.

The spatial alternation of the e^-/OH^- ratio varies along the discharge gap, further enriching the dynamics, promoting its quasi-periodic rather than strictly oscillatory nature. Furthermore, based on the calculations performed, a reduced set of plasma-chemical reactions was created, on the basis of which two-dimensional simulations were performed.

Work supported by the RSF, grant No. 25-21-20063

References

- [1]. Saifutdinov A. I., Purin V. A., Saifutdinova A. A. // Plasma Physics Reports. 2025. V.51. no. 12 P. 1521-1541.
- [2]. Van Gaens W., Bogaerts A. // Journal of Physics D: Applied Physics. 2013. V. 46. no. 27. P. 275201
- [3]. Van Gaens W., Bogaerts A. // J. Phys. D: Appl. Phys. 2014. V 47. 079502

STRUCTURE OF THE ELECTROMAGNETIC FIELD IN AN ECR DISCHARGE IN A RESONATOR EXCITED BY A ROD ANTENNA

S.A. Dvinin^{1,2}, D.V. Chuprova², Z.A. Qodirzoda³, D.K. Solihzoda

¹Lomonosov Moscow State University, Moscow, Russian Federation, DvininSA@my.msu.ru

²RUDN University, Moscow, Russian Federation

³Tajik National University, Dushanbe, Tajikistan

Discharges in a magnetic field [1, 2], including discharges at electron cyclotron resonance (ECR) have a number of advantages when creating technological installations operating at low gas pressure. Moreover, the sources can operate effectively over a wide range of electron densities. In [3], [4], the structure of the field in a magnetic trap initiated by a resonator excited by a slot antenna was studied. This work is devoted to constructing a mathematical model of a microwave discharge in a magnetic field, implemented in the RAPIRA facility (RUDN University).

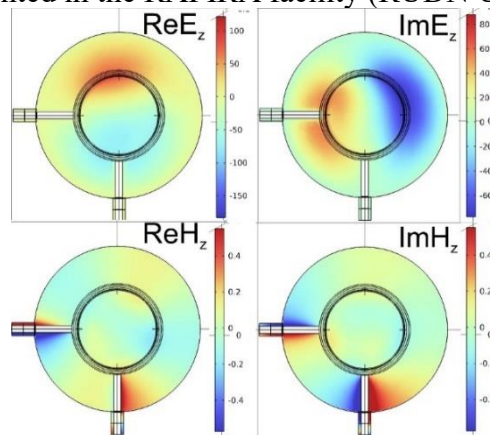


Fig. Distribution of the z-component of the electric (V/m) and magnetic (A/m) field in space in the excitation plane of the resonator.

The discharge is generated in a long quartz tube with a diameter of 60 mm and a length of approximately 2 m. The magnetic field in a trap configuration is provided by three coils, each of which can generate a field with an induction of up to 2 kG. The microwave field initiating the discharge is excited in a cylindrical resonator, along the axis of which the quartz tube runs. Unlike the works [3, 4] two metal rod antennas is used. Spatial characteristics of the electromagnetic field and their changes with constant magnetic field and electron density are calculated using Comsol Multiphysics package in the cold plasma approximation.

The figure shows an example E_z and H_z distribution in a resonator at an electron density of $4 \cdot 10^{10} \text{ cm}^{-3}$. In general, the evolution of the spatial distribution of the microwave field with changing electron density is similar to that calculated in [3, 4], with the exception of the possibility of exciting waves propagating not only azimuthally but also in z-direction, due to the finite size of the exciting plasma rods. The impedance of each rods is also calculated as a function of the electron density.

The research was carried out with the support of the Ministry of Science and Higher Education of the Russian Federation (State Assignment No. FSSF-2026-0043) within the framework of the federal project “Development of technologies for controlled thermonuclear fusion and innovative plasma technologies”.

References

- [1]. Gammino S., Selona L., Giavola G., Maimone F. and Mascali D. *Review of scientific instruments* **81**: 02B313 (2010).
- [2]. Fu S., Ding Z., Ke Y., Tian L. *IEEE Transactions on plasma science* **48** (3): 676-684 (2020).
- [3]. Dvinin S.A., Korneeva M.A. *Phys. Plasmas* **33**, 022105 (2026).
- [4]. Dvinin S.A., Korneeva M.A. *Phys. Plasmas* **33**, 022104 (2026).

THERMODYNAMIC FUNCTIONS OF NON-IDEAL PLASMA OF INDIUM

A.V. Ivanov, A.M. Kondratyev, A.D. Rakhel, A.S. Shumikhin

*Joint Institute for High Temperatures of the Russian Academy of Sciences, Izhorskaya st. 13
Bd. 2, Moscow, 125412, Russia, E-mail: rakhel@ihed.ras.ru*

The technique of pulsed Joule heating of tamped metal foils [1] makes it possible to obtain a homogeneous dense plasma and study its thermodynamic properties. During the experiment, the time dependences of the specific volume of the metal under study, pressure, internal energy and enthalpy, as well as the electrical resistivity are measured. In this experiment the transition of the metal sample to the plasma state occurs during its thermal expansion at supercritical pressures, so no separation into liquid and gaseous phases occurs in this process. When the specific volume of the metal increases to 3–5 times its normal value, it undergoes a continuous metal-nonmetal transition at a temperature of ~ 1 eV and a pressure of ~ 1 GPa [2]. The non-metallic state in this case is a dense plasma, that is, a fluid with a specific volume above the critical value and the resistivity of $\sim 10 \mu\Omega$ m. The degree of ionization of this plasma reaches values of ~ 1 , and it is strongly non-ideal: for it, the average potential energy of the Coulomb interaction between neighboring ions is of the order of their kinetic energy.

Currently, there is no generally accepted theory of such plasmas, which is partly explained by the lack of sufficiently accurate experimental data on thermodynamic properties of non-ideal plasmas. The results of measurements [1], obtained on dense lead plasma for relatively wide ranges of specific volume and pressure with an error of no more than 10%, make it possible to verify the predictions of existing models of non-ideal plasma. The chemical model [3], obtained from the exact expansion of the plasma equation of state in powers of activity in the grand canonical ensemble, has demonstrated satisfactory agreement with the experimental data [1].

The aim of this work is to perform a detailed comparison of the predictions obtained using the model [3] with the measured results obtained for three types of dense plasma (lead plasma, eutectic lead-bismuth alloy plasma, and indium plasma) to establish its accuracy and applicability limits. The focus is on indium plasma, since the second ionization potential of indium atom is almost three times higher than the first, so there is a fairly wide temperature range in which the degree of ionization of the plasma is close to unity. This property of indium plasma allows us to test the accuracy of plasma composition calculations using this chemical model.

References

- [1]. Apfelbaum E.M., Kondratyev A.M., Rakhel A.D. *Žurnal èksperimental'noj i teoretičeskoj fiziki* **165** (6), 876-888 (2024).
- [2]. Kondratyev A. M., Korobenko V. N., and Rakhel A. D. *J. Phys.: Condens. Matter* **34**, 195601 (2022).
- [3]. Shumikhin A.S. *Eur. Phys. J. D.* **79**. 112 (2025).

PHONON-ROTON SPECTRUM IN ONE-COMPONENT PLASMA

S.A. Trigger

Joint Institute for High Temperatures RAS, Moscow, Russia

The spectrum of phonon-roton excitations is very general and is not directly related to the phenomenon of Bose condensation, but is a common feature of disordered systems with strong interactions. The existence of phonon-roton spectra in liquids has been confirmed by numerous experiments on X-ray and neutron scattering (references and examples are given, for example, in [1-2]). The occurrence of a rotonic minimum in the spectrum associated with strong interparticle interaction in liquids can be described by the generalized Feynman formula [3]. It is also applicable to single-component systems of charged particles, in particular to an electron gas in a compensating background. It is found that the calculation using the generalized Feynman formula leads to the appearance of a second minimum of the roton type in the spectrum, associated with a well-defined second maximum in the electron-electron structural factor with a strong Coulomb interaction.

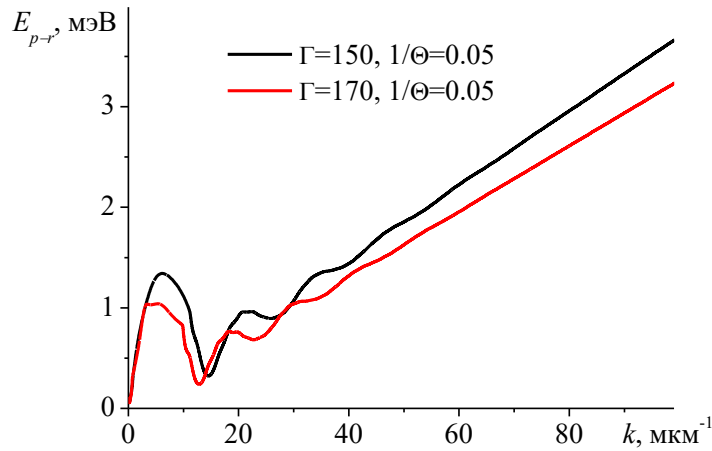


Fig. 1. Phonon-roton energy E_{p-r} for OCP plasma for the interaction $\Gamma=150$ (upper curve) $\Gamma=170$ (lower curve) and degeneracy $1/\Theta=0.05$ calculated by use the generalized Feynman relation: Eq. (12) in [3].

The presence of a minimum in the spectrum of excitations is not yet a confirmation of the existence of well-defined excitations. The existence of such excitations requires a small attenuation. Currently, there are no reliable methods for calculating the decay decrement for Coulomb fluids with strong interparticle interaction. Comparison of the characteristic frequency of the roton minimum $\sim 3.2 \cdot 10^{14} \text{ sec}^{-1}$ and the respective value $k v_T \sim 8 \cdot 10^{13} \text{ sec}^{-1}$ permits to assume that collisionless damping is small. The collision damping, roughly estimated using the given diffusion coefficient [4], is also small. The found spectrum $E_{p-r}(p)$, as well as the experimentally observed maxima of the dynamic structure factor $S(p, E)$, satisfying to the Landau criterion of superfluidity $\min_p [E(p)/p] > 0$ does not lead to the appearance of superfluidity. This indicates that the Landau criterion is necessary but not precise enough for the existence of the superfluid state.

References

- [1]. Burkel E. *Inelastic Scattering of X-rays with Very High Energy Resolution*. Berlin: Springer, 129 p. (1991).
- [2]. Belyayev A.M., Bobrov V.B., Trigger S.A. *J. Phys.: Cond. Matt.* **1:48** 9665 (1989).
- [3]. Trigger S.A. *High Temperatures* **63:3** 766 (2025).
- [4]. Khrapak S.A. *Phys.Rep.* **1050** 1 (2024).

THE CLASSICAL CHARGED PARTICLE MOTION IN AXISYMMETRICAL NON-UNIFORM MAGNETIC FIELD

S.A. Maslov^{1,2}, S.A. Trigger¹

¹*Joint Institute for High Temperatures of the Russian Academy of Sciences, Moscow, Russia,
 e-mail: sergm90@mail.ru, satron@mail.ru*

²*Lomonosov Moscow State University, Moscow, Russia*

The report researches motion of single classical charged particle in axisymmetric magnetic field $\mathbf{B}=B_0\exp(-\beta\rho)\mathbf{e}_z$. In cylindrical coordinates the particle motion of mass m and charge q in such magnetic field can be described by the equation system [1, 2] with initial conditions

$$\begin{aligned} \ddot{\rho} &= u_\theta^2 / \rho + qu_\theta B_0 \exp(-\beta\rho) / (mc), & \rho\ddot{\theta} &= -2u_\rho u_\theta / \rho - qu_\rho B_0 \exp(-\beta\rho) / (mc), \\ \rho(0) &= \rho_0, & \theta(0) &= 0, & u_\rho(0) &= 0, & mcu_\theta(0) &= -WqB_0\rho_0 \exp(-\beta\rho_0). \end{aligned} \quad (1)$$

The authors determine the particle trajectories satisfying to (1) for different values of dimensionless parameters W and $A=\beta\rho_0$, using numerical Runge – Kutta method. In dependence of initial velocity (corresponding to W) and radial exponential decreasing rate of magnetic field the particle can move along the circle or non-periodic curve in limited region, or go to infinite dimensionless distance $R=\rho/\rho_0$ [2] from the symmetry axis (Fig. 1). Lyapunov exponents reflect the stability or instability of motion along the circle, the chaotic nature of non-periodic trajectories lying in the ring region and the regularity of curves going to infinity.

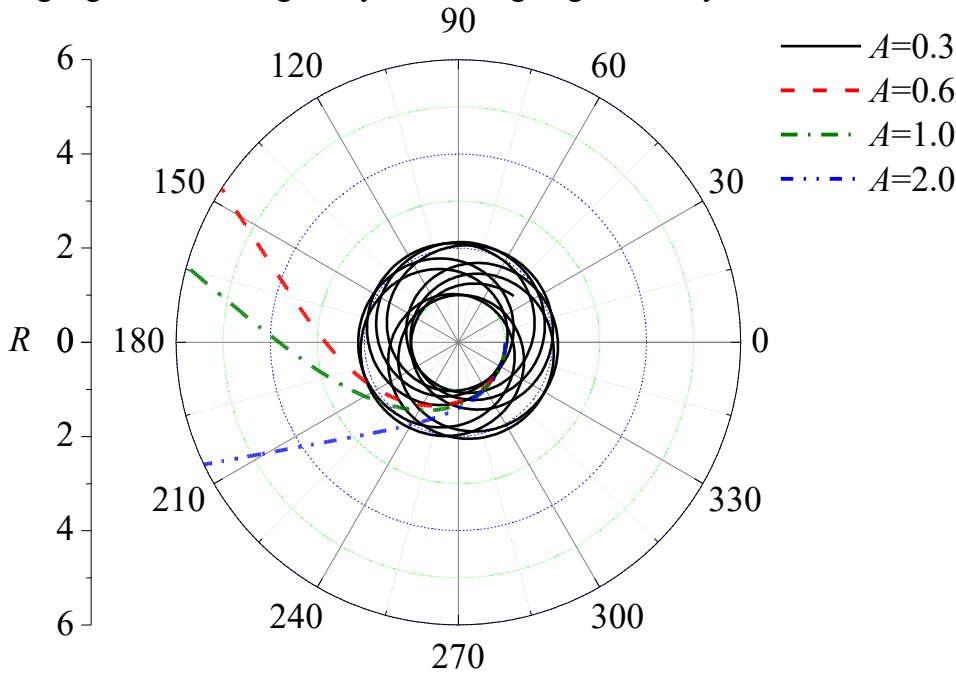


Fig. 1. Particle trajectories at $W=1.3$ for some values of A . The angle θ is given in degrees.

References

- [1]. Babusci D., Dattoli G., and Sabia E. *J. Phys. Math.* **3** 110601 (2011).
- [2]. Maslov S. A., Trigger S.A. *Teplofizika Vysokikh Temperatur* **63**(6) 766-769 (in Russian, 2025).

STEADY-STATE ULTRACOLD PLASMA

A.A. Bobrov, S.A. Saakyan, B.B. Zelener

*Joint Institute for High Temperatures, Russian Academy of Sciences, Moscow, Russia,
abobrov@inbox.ru*

We report on creation of a steady-state ultracold plasma by continuously ionizing calcium atoms in a magneto-optical trap (MOT) [1]. First, about 5×10^7 of Ca 40 atoms were cooled in the MOT to about 1 mK at $4s^2-4s4p$ transition. Then the 390 nm continuous laser was turned on, ionizing the Ca atoms from the upper state ($4s4p$) of the cooling transitions. In the result the steady state plasma was formed inside the cold Ca atoms cloud. The charged particles were not trapped in the MOT, therefore they leave the plasma cloud, but they were constantly replaced by the new electrons and Ca⁺ ions due to the continuous ionization.

Plasma parameters were studied using laser-induced fluorescence of calcium ions observed in the optical range. The experimental results are well described by a simple theoretical model that includes electro neutrality and compensation for the continuous source of charged particles by hydrodynamic ion outflow and three-body recombination:

$$\begin{aligned} \frac{dN_i}{dt} &\sim S - N_i \frac{v}{R_{eff}} - N_i v_{TBR} \\ k_B \frac{dT_e}{dt} &= \frac{S}{N_e} \left(\frac{2}{3} E_e - k_B T_e \right) + \frac{2}{3} v_{TBR} E^*, \end{aligned}$$

where N_i is the Ca⁺ ions number (equal to the electrons number N_e), S is the plasma source (equal to the Ca atoms loss in the MOT, which was measured in the experiment), T_e is the electrons temperature, $v = \sqrt{k_B T_e / M_i}$ is the ions hydrodynamic velocity (M_i is the Ca atom mass), R_{eff} is the plasma characteristic size (observed in the experiment), $v_{TBR} = C_R n_e^2 / (k_B T_e)^{9/2}$ is the three-body recombination rate, E_e is the excess of the ionizing laser frequency above the ionization threshold, $E^* = 3.1 \times 10^{-5} E_I n_e^{1/6} T_e^{1/12}$ is the free electrons energy increase per one recombination act (E_I is the Ca ionization potential), $n_e = N_e / (4/3 \pi R_{eff}^3)$. To study the steady-state regime, the time derivatives in the above equations were set to zero.

Ultracold plasma with a maximum ion density of $2.7 \times 10^6 \text{ cm}^{-3}$, which corresponded to the ions number about 25000, and a minimum electron temperature of approximately 2 K was observed. We estimated maximum coupling strength 0.1 for the electrons and 2.3 for the ions. Our steady-state approach, combined with magnetic plasma confinement, may enable achieving high values of the nonideality parameter in such a system. This nonideal ultracold plasma can be used as a convenient test platform for studying various plasma processes.

References

- [1]. Zelener B. B., et al. Phys. Rev. Lett. 132, 115301(2024)

TWO ELECTRON LOSS MECHANISMS OF ULTRACOLD PLASMA IN CONSTANT HOMOGENEOUS CROSSED ELECTRIC AND MAGNETIC FIELDS

E.V. Vikhrov, B.B.Zelener, B.V. Zelener

*Joint Institute for High Temperatures, Russian Academy of Sciences, Moscow, Russia,
 vikhrov-e@ihed.ras.ru*

We present the results of Xe ultracold plasma expansion simulation in constant homogeneous crossed electric and magnetic fields. The external electric field is applied along X direction and the external magnetic field is applied along Z direction. Other simulation parameters are selected based on the experiment [1]. The simulation results show that the effect of external fields on the plasma leads to two distinct electron escape mechanisms.

The first mechanism is characterized by the formation of an electron cloud outside the plasma, with a spatial distribution similar to that of the electrons remaining within the plasma as shown in Fig. 1(a). This occurs when electrons escape the plasma predominantly due to their relatively high initial kinetic energy, while the contribution of the electric field to this process remains relatively small.

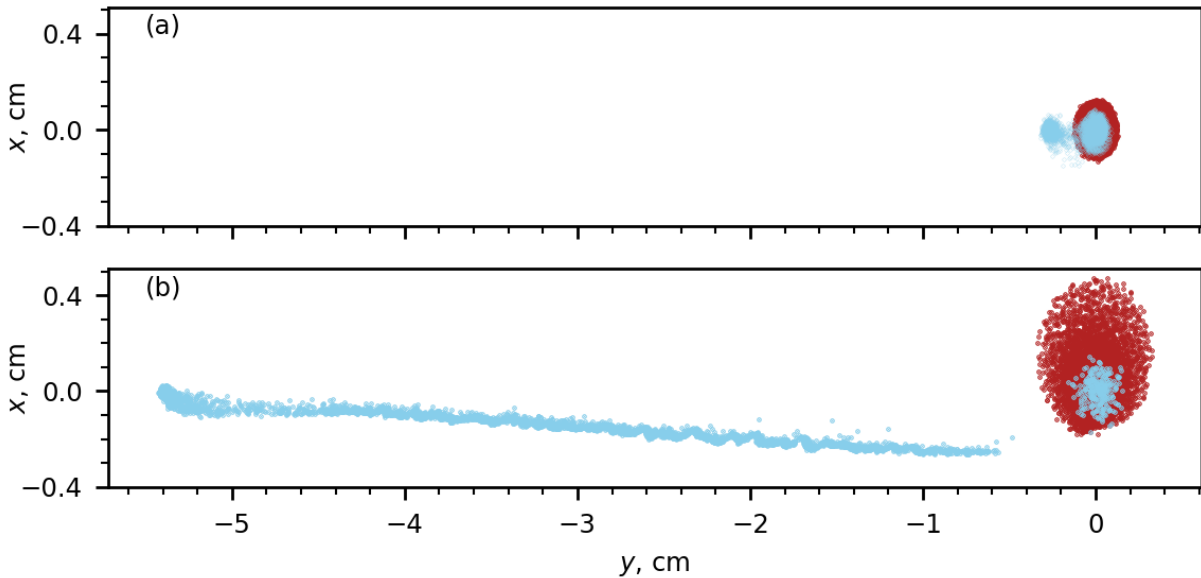


Fig. 1. The projections of ions (red) and electrons (blue) on XY plane for: (a) $T_{e0} = 100\text{ K}$, $n = 10^9\text{ cm}^{-3}$, $B = 10\text{ G}$, $E = 10^{-5}\text{ statV/cm}$, $t = 9\text{ }\mu\text{s}$; (b) $T_{e0} = 10\text{ K}$, $n = 10^{10}\text{ cm}^{-3}$, $B = 20\text{ G}$, $E = 10^{-4}\text{ statV/cm}$, $t = 36\text{ }\mu\text{s}$

The second mechanism is characterized by the formation of an electron beam, as shown in Fig. 1(b). This occurs when electrons are extracted from the plasma predominantly by the external electric field. The beam deforms during its formation due to slip-stream instability [2].

In both cases escaped electron formations drift along $[\vec{E}, \vec{B}]$ direction with constant velocity $V_d = \left| \frac{cE}{B} \right|$.

References

- [1]. X. Zhang, R. Fletcher, and S. Rolston, *Phys. Rev. Letters* **101**, 195002 (2008).
- [2]. W. Knauer, *Jour. of Appl. Physics* **37**, 602 (1966).

CONDUCTOR–INSULATOR CROSSOVER IN ULTRACOLD PLASMAS

Yu.V. Dumin^{1,2}, L.M. Svirskaya^{3,4}

¹*Lomonosov Moscow State University, Moscow, Russia, E-mail: dumin@yahoo.com*

²*Space Research Institute of Russian Academy of Sciences, Moscow, Russia*

³*South Ural State University, Chelyabinsk, Russia*

⁴*South Ural State Humanitarian Pedagogical University, Chelyabinsk, Russia*

A mutual transformation of the ultracold strongly-coupled plasmas into the highly-excited Rydberg gas and *visa versa* was observed in various experiments, both with the atomic beams [1] and magneto-optical traps [2]. These phenomena were commonly described as a sequence of individual interparticle interactions. However, the resulting theoretical curves often appeared too smooth, while the experimental points exhibited a much sharper dependence, reminiscent of a phase transition. So, it was conjectured that “it is possible that the two-body analysis is too naïve” [2], and at the sufficiently low temperature one should expect that interpretation in terms of the collective processes will be more appropriate.

It is the aim of our report to present such a model, which is based on our earlier ideas [3]. Namely, each electron is assumed to move in the potential well formed by the nearest ion (Fig. 1) and sometimes jumps to the neighboring wells due to the multi-particle interactions characterized by the effective “virial” temperature of the entire system [4]. As follows from our recent numerical calculations (Fig. 2), this model exhibits a sharp crossover from the conducting state (plasma) to the insulating one (Rydberg gas) when distance between the particles increases (or the particle number density decreases). The corresponding “critical” value of the interparticle separation normalized to the characteristic size of the Rydberg atom turns out to be $x \approx 3$, which is rather similar to the case of Mott transition in the condensed-matter physics.

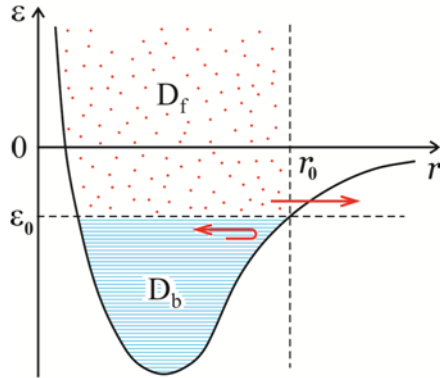


Fig. 1. Phase space of an electron, composed of the regions of bound states D_b and free states D_f .

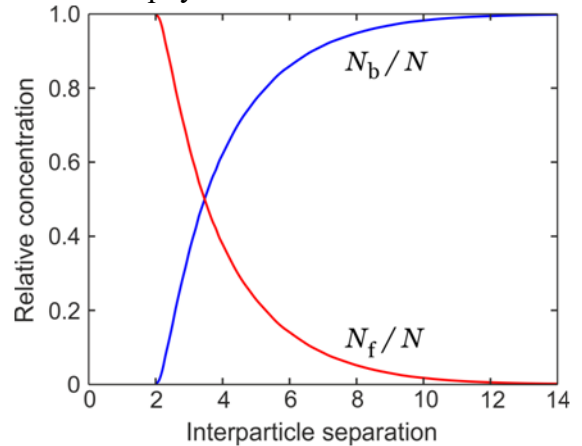


Fig. 2. Relative concentration of the bound and free electrons (N_b/N and N_f/N , respectively) as function of the interparticle separation.

In summary, the undertaken collective description of the ionization–recombination balance should be more appropriate in a certain range of the plasma parameters. It is interesting also that a cascade ionization of Rydberg atoms in the typical atomic beams [1] was predicted to develop at the much greater interatomic separation, $x \approx 15$. Therefore, one can expect that the ionization–recombination processes will exhibit a hysteresis loop.

References

- [1]. Vitrant G., Raimond J.M., Gross M., and Haroche S. *J. Phys. B* **15** L49 (1982).
- [2]. Killian T.C., et al. *Phys. Rev. Lett.* **86** 3759 (2001).
- [3]. Dumin Yu.V. *J. Low Temp. Phys.* **119** 377 (2000).
- [4]. Dumin Yu.V. *Plas. Phys. Rep.* **37** 858 (2011).

**ON THE SCALING OF ANEUTRONIC PROTON – BORON FUSION IN A
NANOSECOND VACUUM DISCHARGE**

Yu. K. Kurilenkov^{1,2*}, A. V. Oginov², S. N. Andreev³, S.Yu. Gus'kov², I.S.Samoylov¹

¹*Joint Institute for High Temperatures RAS, Moscow, Russia, yu.kurilenkov@lebedev.ru*

²*P.N. Lebedev Physical Institute RAS, Moscow, Russia*

³*Moscow Institute of Physics and Technology, Dolgoprudnii, Russia*

The almost aneutronic proton-boron (pB) fusion reaction, $p + 11B \rightarrow \alpha + 8Be^* \rightarrow 3\alpha + 8.7$ MeV, with a yield of only three fast α -particles, is of great fundamental and applied interest, but requires even more extreme states of matter for its implementation than for the nuclear burning of more conventional DD and DT fuels. In addition to the still very far-fetched options for producing "clean" energy based on pB fusion, there is a growing modern need for simple and reliable sources of α -particles for nuclear medicine, materials science, electronics, and other interdisciplinary applications, including aerospace ones. In this regard, in addition to the actively developed laser schemes for pB fusion (see, for example, [1]), it is interesting to implement the pB reaction in a single plasma-confined device, without external laser or proton beam impact on the boron target. Previously, it was shown that in an inertial electrostatic confinement scheme with reverse polarity based on a miniature nanosecond vacuum discharge (NVD) in cylindrical geometry, it is possible to confine and accelerate ions to energies of hundreds of keV in the potential well of the virtual cathode (VC) [2,3]. This allowed for the experimental generation both DD neutrons [2] and the yield of α -particles from the aneutronic proton-boron reaction [3] in the NVD. In this report, we present and discuss new experimental results on the yield of α -particles from the proton-boron reaction in the NVD, and study the scaling of this reaction with changes in the radii of the cylindrical electrodes or the overall size of the anode space [4]. It should be noted that in the oscillating deuteron plasma in the VC field [2], there is a favorable scaling of DD fusion power with a decrease in of VC radius, i.e., the yield of the DD reaction may increase with a decrease in the VC [5]. However, in the case of proton-boron fusion, the oscillation frequencies of ions in the potential well of the VC are significantly different due to the difference in mass and charge between protons and boron ions, and the experiment with a selected set of pairs of advanced electrodes of different diameters reveals a certain trend of increasing the yield of the pB reaction with an increase in the anode radii [4]. This is qualitatively consistent with the results of previous PiC simulations in the KARAT code [6] of the pB reaction yield, which showed an increase with increasing radius [7]. Additionally, the pB reaction yield in the oscillating NVD plasma, obtained independently using an analytical model [8], also appears to be proportional only to the radius of the anode, rather than its volume, as would be the case for a homogeneous plasma. Thus, the scaling of aneutronic pB fusion power with respect to the radius of the anode space is fundamentally differ from DD fusion scaling.

References

- [1]. Scisciò M., Petringa G., et al. *Matter and Radiation at Extremes* **10** 037402 (2025).
- [2]. Kurilenkov Yu.K., Tarakanov V.P., et al. *J. Phys: Conf. Series* **1147** 012103 (2019).
- [3]. Kurilenkov Yu.K., Oginov A.V. et al. *Phys.Rev. E***103** 043208 (2021).
- [4]. Oginov A.V., et al *High Temperature* **63** (6) 793-800 (2025) Supplement.
- [5]. Kurilenkov Yu.K., Tarakanov V.P., Oginov A.V. *Plasma Phys.Rep.* **48** (4) 443-448 (2022),
- [6]. Andreev S.N., Kurilenkov Yu.K. and Oginov A.V. *Mathematics* **11** 4009 (2023).
- [7]. Kurilenkov Yu. K., Andreev S.N. *Front. Phys. (Fusion Plasma Phys.)* **12**:1440040 (2024).
- [9]. Kurilenkov Yu. K. *High Temperature* **63** (6) 674-679 (2025).

POSSIBILITIES OF IMPLEMENTING THE PROTON–BORON-11 NUCLEAR FUSION REACTION IN PULSED SYSTEMS WITH A MAGNETIC FIELD

A.Yu. Chirkov, E.G. Vovkivsky

Bauman Moscow State Technical University, Moscow, Russia, chirkov@bmstu.ru

The proton–boron-11 ($p\text{--}^{11}\text{B}$) reaction is currently at the peak of experimental interest. Significant progress is being made using laser-generated plasma systems. Magnetic structures are formed in laser plasma due to the motion of charged particles. Magnetic structures are generated. Magnetic fields observed in experiments with irradiation of a curved target with a petawatt laser pulse reach levels of >1000 T. At relativistic laser radiation intensities ($>10^{18}$ W/cm²), the transfer of magnetic field energy into the kinetic energy of charged particles is possible due to magnetic reconnection.

In the present work, energy production schemes for $p\text{--}^{11}\text{B}$ plasma are discussed. Schemes based on laser plasma are considered for comparison. Although the laser-based approach appears the most promising, electrophysical pulsed systems have a number of significant advantages. Firstly, this is the comparative simplicity of the process and a single cascade of driver energy conversion into plasma energy. Secondly, this is the high efficiency of energy input into the plasma. Pulsed systems based on the magnetic Field Reversed Configuration (FRC) and Dense Plasma Focus (DPF) are considered. It should be noted that the magnetic fields of these systems allow for an extension of the plasmoid lifetime compared to its purely inertial expansion. The analysis is based on energy balance models [1–4], including taking into account instabilities that cause turbulence [5].

The considered schemes at a moderately high energy level (up to 100 kJ per pulse) should apparently be considered as an initial stage in combination with some subsequent energy input. The obtained parameter estimates for systems based on FRC, DPF/Z-pinch, and laser plasma demonstrate the principal possibilities of their use for implementing the $p\text{--}^{11}\text{B}$ reaction. Within the framework of the indicated approaches, it is possible to obtain a significant energy yield. However, the estimated energy yield does not yet exceed the energy input. Therefore, it is necessary to consider further the extrapolation of the obtained regimes to the higher parameters that exceed the currently achievable level. Non-equilibrium conditions, in which significant acceleration of ions is possible due to their interaction with a non-stationary magnetic field and generated electric fields, were analyzed separately [6]. Under such conditions, the reaction rate can be significantly increased.

References

- [1]. Vovkivsky E.G., Chirkov, A.Yu. *Plasma Phys. Rep.* **51** 21–35 (2025).
- [2]. Chirkov, A.Yu. *Yad. Fiz and Engineering* **4** 1050–1059 (2013).
- [3]. Chirkov A.Yu., Tokarev S.A. *Fusion Science and Technology* **79**, 413–420 (2023).
- [4]. Vovkivsky E.G., Chirkov A.Yu. *Phys. Plasmas* **32** 064701 (2025).
- [5]. Chirkov A.Yu., Khvesyuk V.I. *Physics of Plasmas* **17**, 012105 (2010).
- [6]. Chirkov A.Yu., Morkhova E.A., Frolov A.Yu. *Plasma Phys. Rep.* **48**, 1111–1115 (2022).

ANOMALOUS ELECTRON FLUXES IN A PLASMA WITH ION-ACOUSTIC TURBULENCE AND POSSIBILITY OF CALCULATION OF CURRENT DENSITY IN HOLLOW CATHODES

A.A. Shelkovoy¹, S.A. Uryupin^{1,2}

¹*P.N. Lebedev Physical Institute of the Russian Academy of Sciences, Moscow, Russia*

²*National Research Nuclear University MEPhI, Moscow, Russia*

Hollow cathodes find applications in plasma-surface interaction studies, surface coating and aircraft propulsion systems. It is established that the ion-acoustic instability is the key instability in hollow cathodes, and it causes anomalous resistivity and turbulent heating of the bulk ions. The main contribution to fluxes in nonisothermal plasma in hollow cathodes is made by electrons. According to [2] electron fluxes depend on the ion-acoustic waves distribution over the angles of the wave vector θ_k , which is described by the function $\Psi(\cos \theta_k)$. The expressions for $\Psi(\cos \theta_k)$ obtained earlier are applicable for small or large values of parameter $K = 6\pi|enE - \nabla n\kappa T|r_{Di}^2/mn\omega_{Li}v_s r_{De}^2(1 + \delta)^2$, where e , n , κT , r_{De} , ω_{Le} are the electron charge, density, temperature, Debye radius and Langmuir frequency; r_{Di} and ω_{Li} are the ion Debye radius and Langmuir frequency; v_s is the ion sound speed; E is the electric field strength; δ is the ratio of the damping rate of ion-acoustic waves on hot ions to the damping rate on electrons. However, using data from [3], it was found that in hollow cathodes $K \sim 1$, therefore the expressions for $\Psi(\cos \theta_k)$ obtained earlier can give an error when calculating the electron charge and energy fluxes.

Without imposing any restrictions on the magnitude of the induced scattering of waves by ions, the numerical solution for the function $\Psi(\cos \theta_k)$ is obtained. This solution complements the analytical expressions for $\Psi(\cos \theta_k)$ obtained earlier and is valid for case $K \sim 1$ realized in hollow cathodes. Using this solution, one can calculate the current density in hollow cathodes:

$$j = env_s \left[\frac{3}{2} \beta_1 + \frac{16}{\pi} \beta(1 + \delta) - \frac{24}{\pi} \beta(1 + \delta) \frac{n}{R} \frac{\partial \kappa T}{\partial z} \right], \quad (1)$$

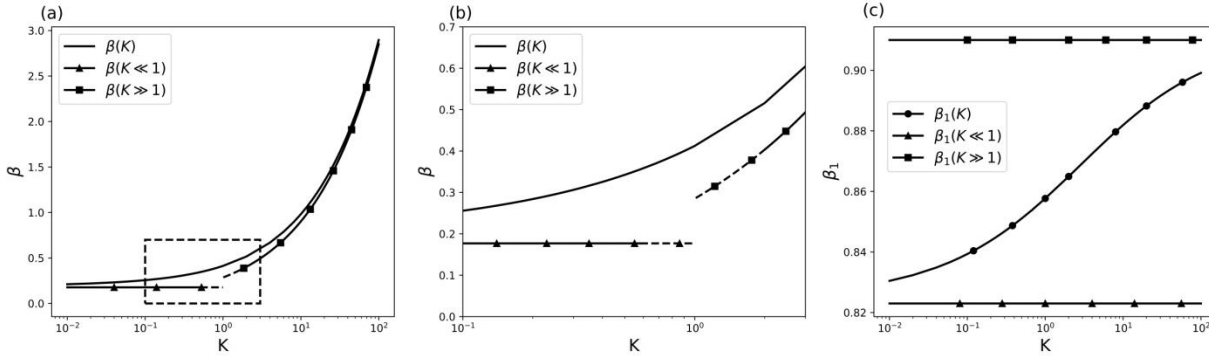


Fig. 1. Dependences of the coefficients β (a), (b), and β_1 (c) on K .

where β and β_1 are coefficients (see Fig. 1 (a) – (c)); The values of all the quantities mentioned above can be obtained using data in [3] except for δ , since δ depends on the temperature of hot ions T_h , for which data in [3] are not presented. Using formula (1) and taking into account that in similar conditions T_h is several times greater than T , at the distance of 1.73 cm from the hollow cathode exit we find $j = 9.9 \div 10.9 \text{ A/cm}^2$. In turn, according to [3], the experimental value of the current density is $j_{exp} = 14.9 \text{ A/cm}^2$. As can be seen, calculation by the formula (1) gives a value of current density close to j_{exp} .

References

- [1]. Shelkovoy A. A., and Uryupin S. A., *Phys. Rev. E* **112** (2) 025210 (2025).
- [2]. Bychenkov V. Yu., Silin V. P and Uryupin S. A., *Phys. Reports* **164** (3) 119-215 (1988).
- [3]. Ortega A. L., Jorns B. A., and Mikellides I. G., *J. Propul. Power* **34** 1026-1038 (2018).

NONLINEAR ION-ACOUSTIC WAVES IN NONISOTHERMAL PLASMA

S.V. Kuznetsov

*Joint Institute for High Temperature of the Russian Academy of Science, Izhorskaya st. 13
Bd.2, Moscow, 125412, Russia, e-mail: svk-IVTAN@yandex.ru*

In one-dimensional geometry, we study the potential nonlinear wave motion of a collisionless, nonisothermal plasma, propagating at a velocity much slower than the thermal velocity of electrons and much faster than the thermal velocity of ions. The study is performed using Sagdeev's formulation [1], which assumes a Boltzmann energy distribution for electrons in the wave's potential well and uses the equations of cold hydrodynamics for ion motion. It is shown that the equations describing the plasma based on Sagdeev's approach allow for motion corresponding to a nonlinear ion-acoustic wave propagating through the plasma at a constant velocity, the value of which is bounded from above by a value exceeding the ion sound speed.

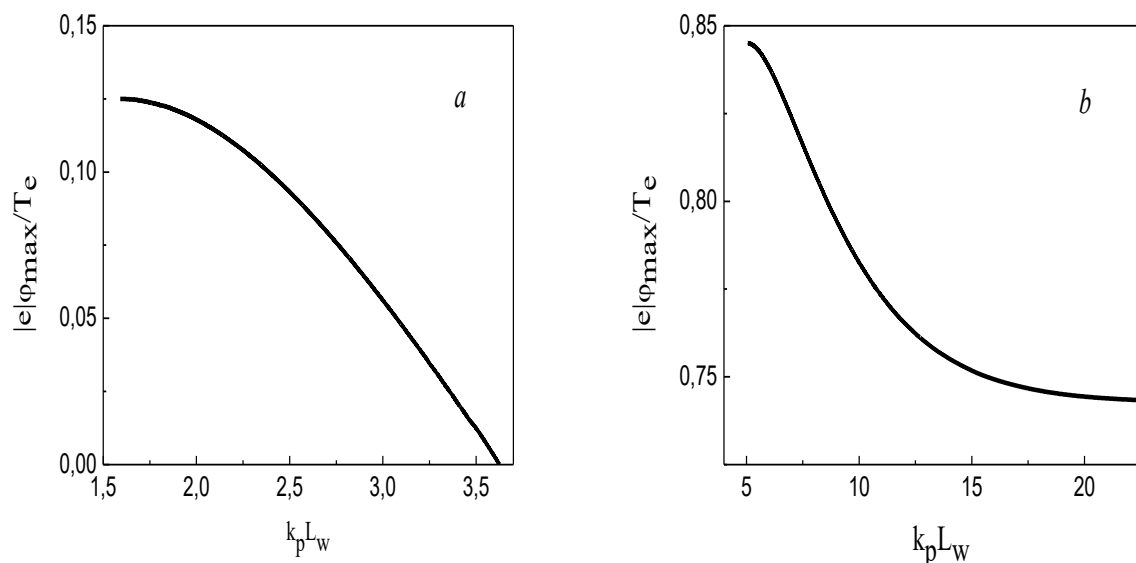


Fig. 1. The amplitude ϕ_{\max} of a nonlinear ion-acoustic wave depending on its wavelength L_w : a) – $V/V_s=0.5$, b) – $V/V_s=1.3$, where V_s - ion sound speed

It has been found that each permissible value of the ion-acoustic wave propagation velocity corresponds to an infinite set of waves differing in amplitude and nonlinear wavelength. For a fixed ion-acoustic wave propagation velocity, the wave amplitude decreases with increasing wavelength (Fig. 1). Moreover, if the wave velocity is less than the speed of sound, then in the limit of its smallest amplitude values, we arrive at waves of infinitely small amplitude, corresponding to the ion-acoustic wave in linear theory. If the velocity of a nonlinear ion-acoustic wave is greater than the speed of ion sound, then in the limit of the smallest possible wave amplitude for a given velocity, we arrive at an ion-acoustic soliton.

References

- [1]. Vedenov A A, Velikhov E. P. Sagdeev R. Z. *Nuclear Fusion* **1** (2) 82-100 (1961).

**TO THE MOST PROBABLE DISTRIBUTIONS OF STRUCTURELESS PARTICLES IN
HIGHER-LEVEL STRUCTURAL UNITS AS APPLIED TO THE PHYSICS OF PHASE
TRANSITIONS**

M.Yu.Romanovsky^{1,2,3}

¹*PE Science and Innovation, Moscow, Russian Federation*

²*ANO National Center for Physics and Mathematics, Sarov, Nizhny Novgorod region,
Russian Federation*

³*Pirogov Russian National Research Medical University, Moscow, Russian Federation*

The combinatorial method is used to study the statistics of accumulation of structureless particles during their movement between structural units of the upper level that differ in the number of these particles. The total number of structureless particles is saved, while the number of top-level structural units can vary widely. When a structureless particle is disconnected from an upper-level structural unit, different energy is consumed each time, and all structureless particles and upper-level structural units are eventually distinguishable, at least for this reason. Before detaching, structureless particles are indistinguishable, and top-level structural units always remain distinguishable.

The distributions of the number of top-level structural units and the number of structureless particles in each of them are determined depending on the energy used on detaching. The developed approach is used for the elementary description of pairs of phase transition processes – melting and sublimation, as well as the transition between ordinary nucleonic matter and quark-gluon plasma in comparison with the transition between quark-gluon plasma and matter of particles with a higher mass (than quarks and gluons). The results are used to estimate the temperature of a more energy-intensive phase transition (for example, sublimation of a substance compared to melting) in comparison with a less energy-intensive one.

LOCALIZED OSCILLATIONS OF A LINEAR PLASMA CRYSTAL

A.M. Ignatov

Prokhorov General Physics Institute of the Russian Academy of Sciences, Moscow, Russia

I consider linear oscillations of a one-dimensional chain of dust grains of unequal masses interacting via nonreciprocal forces. Particle displacements are denoted as $(x_j(t), z_j(t))$ ($-\infty < j < \infty$), and in harmonic approximation $(x_j(t), z_j(t)) = e^{-i\omega t} (x_j, z_j)$ equations of motion are

$$\begin{aligned} (\omega^2 m_j - 2u_{2,0})x_j + u_{2,0}(x_{j-1} + x_{j+1}) + u_{1,1}(z_{j-1} - z_{j+1}) &= 0, \\ (\omega^2 m_j - 2u_{0,2} - \Omega_0^2)z_j + u_{1,1}(x_{j-1} - x_{j+1}) + u_{0,2}(z_{j-1} + z_{j+1}) &= 0. \end{aligned} \quad (1)$$

Here $u_{i,j}$ are force constants equal to the second derivatives of the interparticle potential and m_j is the mass of the j -th grain. A general approach that allows to construct a solution to Eqs. (1) and to get the corresponding eigenfrequencies is proposed.

One example studied in details concerns oscillations of the impurity grain of mass $m_0 = m$ at the center of the infinite grain chain of equal masses $m_j = 1$ ($j \neq 0$). It was found that there exist oscillations localized near the central particle, that is, the displacements of grains decays with growing $|j|$.

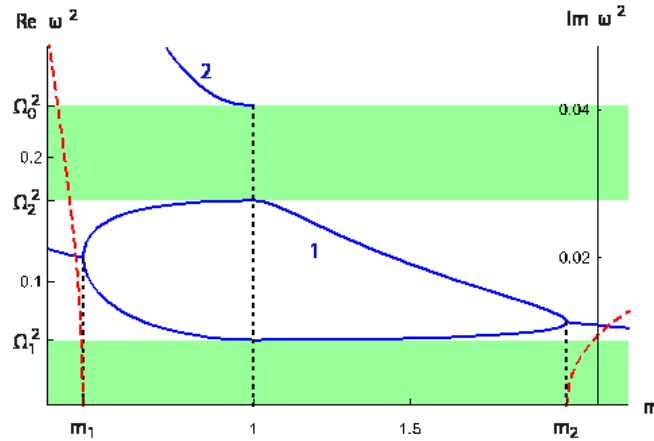


Fig. 1. Eigenfrequencies of the localized oscillations versus the impurity mass. $m_1 \approx 0.46$, $m_2 \approx 2.0$

With the given mass of the impurity m , there exists several types of localized oscillations. Fig.1 shows the dependence of the frequency on the mass of the impurity. Frequency bands where the waves in the homogenous chain of equal masses may propagate are shadowed in the figure. The frequencies of localized oscillations lie in the forbidden gaps either between the optical and acoustic branches (curves 1) or above optical branch (curve 2). With the mass $m \rightarrow 1$ frequency curves are tangent to the horizontal lines. With growing or reducing mass of the impurity ($m = m_{1,2}$ in the figure), the localized oscillations become unstable. In this case, the chain throws out too heavy or too light central particle. Notice that this process is of oscillatory nature and develops due to the nonreciprocal character of the interparticle interactions.

Another example considered is the chain composed of particles with mass m_1 at $j < 0$ and m_2 at $j \geq 0$. It was found that there exist edge oscillations localized near the interface particle which are analogous to surface waves in continuous media. With sufficiently large difference in particle masses edge oscillations also become unstable results in the destruction of the chain.

**MICROPARTICLE SEPARATION BY RECTANGULAR-VOLTAGE PAUL TRAP IN
AIR**

M.S. Dobroklonskaya, L.M. Vasilyak, V.Ya. Pecherkin, V.I. Vladimirov

Joint Institute for High Temperatures of the Russian Academy of Sciences, Moscow, Russia

Numerical and experimental study of charged microparticle trapping in a linear Paul trap with rectangular voltage at atmospheric pressure. Compares trapping stability regions for sinusoidal vs. rectangular waveforms and pulse width influence. Demonstrates size-selective separation of polydisperse particles by adjusting pulse duty cycle.

SELF-ORGANIZATION OF ACTIVE BROWNIAN PARTICLES INTO AN ANISOTROPIC LINEAR STRUCTURE DEPENDING ON EXTERNAL PARAMETERS IN A DC DISCHARGE

A.V. Erilin^{1,2}, E.A. Kononov^{1,2}, R.V. Senoshenko^{1,2}, M. M. Vasiliev¹, O. F. Petrov¹

¹*Joint Institute for High Temperatures of the Russian Academy of Sciences, Moscow, Russia*

²*Moscow Institute of Physics and Technology, Dolgoprudny, Moscow Region, Russia*

For various nonequilibrium systems of microparticles it is possible to observe phenomena of self-organization which is typical for the active Brownian particles. Active Brownian particles are particles capable of accumulating and converting energy obtained from medium into own kinetic energy [1]. These particles can form different structures - from extensive clouds to linear chains in different mediums: liquid, gas and plasma. Dynamic characteristics of particles can be controlled by external parameters, which makes it possible to study the processes of self-organization of particles, in which can include changing morphological properties of the structures they form [2].

Active Brownian particles in a gas-discharge plasma acquire a surface electric charge due to collisions with plasma electrons and ions. As a result, the particles can be trapped in the plasma volume, including the inhomogeneities of the plasma column – stratum. The spatial position of particles inside the stratum can change as a result of the particles interaction with each other through screening Coulomb interaction and ion focus [3]. It leads to structural changing in the system. The investigation of affection of discharge parameters on the morphological characteristics of structures formed by active Brownian particles is an interesting problem.

This study presents the results of an experimental investigation of the processes of self-organization in a system of active Brownian particles into anisotropic linear structures in a DC discharge depending on external parameters. The study was conducted at different experimental conditions: normal (293 K) and cryogenic (1.7 K) temperatures. At cryogenic temperature, active Brownian cerium oxide particles CeO_2 formed a linear anisotropic structure with a length of 6 to 10 grains. It is possible by changing the discharge current from 30 μA to 24 μA and then increasing it in the opposite direction to 29 μA . During the experiment, a change in the morphological characteristics of the particle structure was observed. At normal temperature, cerium oxide particles with an average diameter of 5 microns formed a 10-grain structure. During the experiment, the parameters of the discharge changed: the current through the discharge increased from 0.75 mA to 2.5 mA, then decreased back to 0.75 mA and the pressure from 38 mTorr to 68 mTorr. The particles in the discharge were irradiated by a laser beam with a power density of 100 mW/cm^2 .

From the obtained video data, the trajectories of particles were reconstructed. Mean square displacement, kinetic energies, the average interparticle distance in the structure, as well as their average deviation from the axis of the structure were calculated. In the case of cryogenic temperature, 2D-diagnostics were used, and in the case of normal temperature, 3D-diagnostics were used. The dependences of the structural parameters on the discharge current and buffer gas pressure were investigated. Obtained results were compared for both temperatures.

References

- [1]. Bechinger C., et al. *Rev. Mod. Phys.* **88** 045006. (2016)
- [2]. Fedoseev A.V., et al. *Sci Rep.* **14**(1) 13252 (2024).
- [3]. Melzer A., Schweigert V.A., Piel A. *Physical Review Letters.* **83**(16) 3194–3197 (1999)

DYNAMICS OF ACTIVE BROWNIAN MOTORS IN COMPLEX COLLOIDAL SYSTEM IN VISCOUS MEDIUM

R.V. Senoshenko, E.A. Kononov, M.M. Vasiliev, O.F. Petrov

Joint Institute for High Temperatures of the Russian Academy of Sciences, Moscow, Russia

Investigation of systems of active Brownian motors represents one of the relevant challenges in modern soft matter physics. The active Brownian motion of functional particles in viscous media, characteristic of such systems, resembles the locomotion of microorganisms in low-Reynolds-number dispersion mediums [1] and can be initiated by both chemical and physical methods. In this context, the key principle for the spontaneous movement of particles under conditions where viscous forces dominate is the necessity of spatial symmetry breaking in the system. In biological micro-objects, this asymmetry is provided by the functioning of flagella in bacteria or by intracellular transport along the cytoskeleton. In laboratory synthetic colloidal systems, its role is fulfilled by physicochemical gradients on the particle surfaces.

Alongside the traditional mechanism of particle motion driven by the concentration gradient of components in the surrounding medium and the inhomogeneous distribution of chemical potential in the dispersion medium, the identification of physical mechanisms that sustain such motion over time is of particular scientific interest. Previously mentioned include, for example, asymmetric intradroplet flows in emulsions [1] or the thermophoretic motion of nanoparticles absorbing laser radiation [2]. In the latter case, active particles not only perform directed motion but are also able to generating large-scale vortex flows, which modify their own trajectories and promote collective self-organization [3]. Thus, microdroplets in a complex colloidal system, whose motion is induced by external fields or internal gradients, replicate the fundamental principles of biological locomotion. This fact allows them to be considered promising model objects for studying both the individual dynamics of microorganisms and the patterns of their collective behavior.

This work presents a comprehensive study of an active colloidal system of complex composition, comprising microparticles with partial metal coating (Janus particles) dispersed in a viscous medium and localized within microemulsion droplet. The presence of the metal coating on the Janus particles ensured efficient absorption of laser radiation, which caused their active Brownian motion within the intradroplet volume. In this case, the microemulsion droplet acts as an active Brownian motor [4].

During the experiment, under the constant-intensity laser radiation, the collective dynamics and evolution of an ensemble of Janus particles were recorded. The consequence of the intradroplet motion of the particles was the directed movement of the entire droplet as a whole. It has been demonstrated that the active locomotion of microparticles induces the emergence of large-scale vortex fluid flows inside the oil droplet. The forming flows, in turn, lead to the appearance of inhomogeneous dynamic pressure fields and an uneven redistribution of mass within the droplet. The combination of these factors, including the tendency of particles to localize near the phase interface, creates conditions for the deformation of the interfacial surface, which can ultimately initiate the active movement of the entire droplet as an unified object.

The study was carried out under a grant from the Russian Science Foundation (project № 25-12-00406).

References

- [1]. Tiribocchi A., et al. *Nat. Commun.* **12** (1) 82 (2021).
- [2]. Kononov E.A., Senoshenko R.V., Vasiliev M.M., et al. *Phys. Fluids* **32**(69) 117145 (2024).
- [3]. Senoshenko R.V., et al. *JETP* **167** (4) 594-600 (2025).
- [4]. Hänggi P., Marchesoni F. *Rev. Mod. Phys.* **81** (1) 387–442 (2009).

THE BEHAVIOUR OF SMALL SYSTEMS OF JANUS PARTICLES IN GAS-DISCHARGE PLASMA

X.G. Koss^{1,2}, K.A. Mizeva^{1,2}, D.A. Zamorin^{1,2}, M.M. Vasiliev¹, O.F. Petrov^{1,2}

¹*Joint Institute for High Temperatures of the Russian Academy of Sciences, Moscow, Russia*

²*Moscow Institute of Physics and Technology, Dolgoprudny, Russia*

Colloidal plasma is an object that allows for the visual graphical study of collective phenomena in an ensemble of strongly interacting charged particles [1-5]. The macroscopic structures they form can undergo self-organization and evolution; collective phenomena in a swarm of active Brownian particles during their evolution can demonstrate analogies with conventional phase transitions [6]. Thus, structural transitions in extended and small systems of passive colloidal particles in plasma have been thoroughly studied in recent decades [4, 5]. But the dynamics of mesoscopic systems of active particles in plasma have remained practically unexplored [2, 3]. The questions concerning structural transitions in these systems, energy transformation within them, and their evolution under various external conditions remain open.

In this work, an experiment was conducted to study finite systems of active particles in an RF discharge. A voltage with a frequency of 13.56 MHz was applied to the parabolic electrode; then, melamine-formaldehyde particles, half-coated with molybdenum, were introduced into the discharge. The particles were charged by electron and ion fluxes and levitated above the center of the electrode. They were illuminated by a laser. The laser power was varied from 0.08 W to 1.2 W. The particle motion was recorded using a high-frequency video camera. It has been discovered that the analysis of the particles' dynamics (kinetic energy and localization areas of the particles, fractal dimension of their trajectories) can be indicative of their composition. Specifically, we were able to distinguish different types of particles in the system under study: 1) Janus particles with a shifted center of gravity; 2) particles with less percentage of metal coating.

This work was supported by the Russian Science Foundation (project № 25-12-00406).

References

- [1]. Petrov, O.F., Statsenko, K.B. & Vasiliev, M.M. *Sci Rep* **12**, 8618 (2022).
- [2]. Koss, X.G., Petrov, O.F., Statsenko, K.B. and Vasiliev, M.M. *EPL* **124** (2018).
- [3]. Vasiliev, M. M., Alekseevskayaa, A. A., Koss, K. G., Vasilieva, E. V. and Petrov, O. F.. *High Temp.* **61(6)** 759-763 (2023).
- [4]. Petrov, O.F., Vasiliev, M.M., Tun, Y. *et al. J. Exp. Theor. Phys.* **120**, 327–332 (2015).
- [5]. Ivanov, Y. and Melzer, A. *Physics of plasmas* **12**, 072110 (2005).
- [6]. Klamser, J. U., Kapfer, S. C. & Krauth, W. *Nat. Commun.* **9**, 5045 (2018).

COMPETING MECHANISMS OF DUSTY PLASMA ROTATION IN A MAGNETIC FIELD

V.Yu. Karasev, E.S. Dzlieva, L.A. Novikov, S.I. Pavlov

Saint Petersburg State University, St. Petersburg, Russia, plasmadust@yandex.ru

The dynamics of dusty plasma in a magnetic field are determined by particle fluxes onto the dust grain. These are primarily ion fluxes and entrainment by the discharge gas, which are dominant under certain conditions [1,2]. More subtle force effects exist when the dust subsystem itself is capable of altering plasma conditions, changing the direction and scale of ion and electron fluxes. In this case, the rotation mechanisms not only compete but also overlap, creating differential rotation of the dust structure [3,4].

This paper examines the emergence of additional local vortex motion against the background of the rotation of the dust structure as a whole in a magnetic field up to 400 G. Experimental results of vortex motion in a uniform and non-uniform magnetic field in inert gases with dust particles of significant sizes are presented. The mechanism of the vortex motions observed experimentally is discussed. A possible cause of the additional rotation is the radial flow of ions in the longitudinal magnetic field from a dense region of the dust structure. The ion fluxes passing through the dust structure and the conditions of their formation are estimated from the velocity and geometric size of the vortices.

The work was supported by the Russian Science Foundation, grant № 22-72-10004- II.
<https://rscf.ru/en/project/22-72-10004-II/>

References

- [1]. Konopka U., Samsonov D., Ivlev A.V., Goree J., Morfill G.E. *Phys. Rev. E.*, **61** 1890 (2000).
- [2]. Nedospasov A. V., *Phys. Rev. E* **79**, 036401 (2009).
- [3]. Karasev V.Yu., Dzlieva E.S., Ivanov A.Yu. et al., *Phys. Rev. E* **74**, 066403 (2006).
- [4]. Dzlieva E.S., Dyachkov L.G., Novikov L.A., Pavlov S.I., Karasev V.Yu. *Molecules*, **26**, 3788 (2021)

DUST PARTICLE ROTATION IN PLASMA AROUND ITS OWN AXIS

L.G. Dyachkov¹, E.S. Dзлиeva², L.A. Novikov², S.I. Pavlov², V.Yu. Karasev²

¹*Joint Institute for High Temperatures of Russian Academy of Sciences, Moscow, Russia,
dyachk@mail.ru*

²*Saint-Petersburg State University, Saint-Petersburg, Russia*

The rotation of dust particles around their own axis, which passes through the center of the particle, was discovered at the end of the last century, shortly after the beginning of studies of dusty plasma. It occurs as a result of collisions of plasma particles, mainly ions, with protrusions on the surface of dust particles. Particles with a perfect spherical shape practically do not exist; all have some kind of surface defects. Therefore, they must rotate around their own axis. The angular velocity vector of the different particles has a random direction, which is obviously related to the random shape and nature of the surface defects. The rotation speed does not depend on whether the particle is isolated or part of a dust structure, and should not change when the particle moves, for example, from the discharge axis to its wall. We consider the dust particle rotation mechanism as a result of the particle collision with ions and the transfer of rotational momentum to the particle surface elements. Under various assumptions about the sizes of dust particle surface defects, confirmed by microscopic images of dust particles, it has been shown that their rotation speeds can reach values on the order of 10^3 rad/s, which corresponds to observations of micron-sized particles.

EXPERIMENTAL STUDY OF DUSTY PLASMA FORMATION IN A LOW-PRESSURE CAPACITIVE RF DISCHARGE

M.E. Viktorov¹, S.V. Sintsov¹, D.A. Sergeev¹, I.M. Kraev¹, E.I. Preobrazhensky¹,
A.V. Vodopyanov¹

¹ *Federal Research Center A.V. Gaponov-Grekhov Institute of Applied Physics of the Russian Academy of Sciences, Nizhny Novgorod, Russia, mikhail.viktorov@ipfran.ru*

A new experimental setup for studying dusty plasma dynamics has been created at the IAP RAS. It has been experimentally shown that using acetylene as a carrier gas for carbon atoms in a low-pressure capacitive RF discharge plasma results in the formation of plasma-dust clouds with dust particles smaller than a micrometer. Using the PIV method, the spatial distribution of the dust microparticles velocity illuminated by a flat laser beam formed by the laser knife system has been measured. The average velocity of dust particles in the plasma has been determined. Various modes of dust clouds formation have been studied, including the formation of dust voids and self-excitation of dust plasma waves.

The work has been carried out within the framework of the scientific program of the National Center for Physics and Mathematics in the direction 10 “Experimental Laboratory Astrophysics and Geophysics”.

INFLUENCE OF THE EXTERNAL ELECTROSTATIC POTENTIAL WELL CONFIGURATION ON THE FORM OF THE DUST PARTICLE STRUCTURES

A.V. Fedoseev¹, M.V. Salnikov², M.M. Vasiliev¹, O.F. Petrov¹

¹*Joint Institute for High Temperatures RAS, Izhorskaya str. 13-2, Moscow, Russia*

²*Institute of Termophysics SB RAS, Lavrentyeva Ave. 1, Novosibirsk, Russia*

The effect of the formation of the ordered structures of dust particles in the anisotropic plasma of gas discharges [1] is studied. For this purpose, a 3D multi-block model based on the mean field approximation was developed, which is an extension of the 1D model for dust particle chains developed in the previous stages [2]. The model describes the movement the dust particles and ions under the action of external electric field, electric field (Coulomb) of each charged dust particle, and the field of bulk plasma charge of ions and electrons that screens the charges of dust particles. The gravity and the ion drag forces acting on the dust particles are also taken into account. The influence of the external electrostatic potential well configuration (see Fig. 1 (a) and (b)) on the form of the dust particle structures (i.e., vertical chains, horizontal monolayers or different 3D forms) is investigated. As a result of calculations, self-consistent dusty structure parameters (spatial configuration and dust particles charges) and space distributions of the plasma parameters (bulk charge and electric potential) have been calculated and analyzed for different structures, particle and plasma parameters.

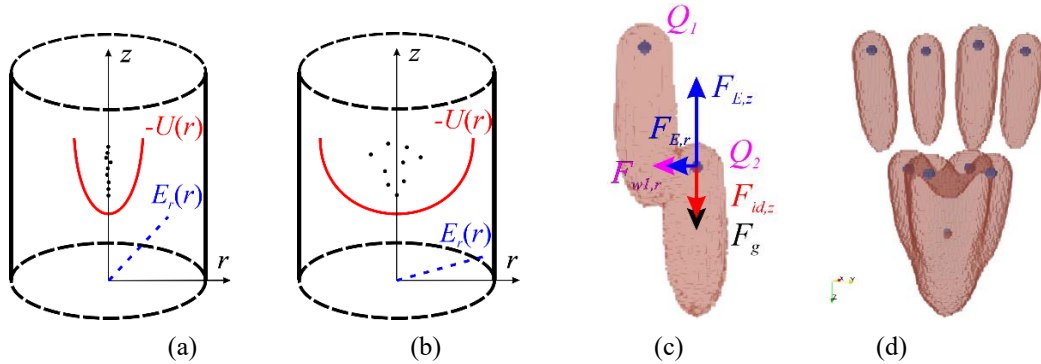


Fig. 1. Schematic configuration of radial electric potential for (a) strong and (b) weak trapping of the dust particles. (c) forces acting on the bottom particle, (d) example of 3D cluster of nine dust particles.

Two series of calculations were performed. First, the configuration of two dust particles aligning vertically due to the effect of both the ion wake behind the top particle ($F_{wl,r}$) and radial confining electric potential ($F_{E,r}$) was investigated (Fig. 1 (c)). It was shown that the force $F_{wl,r}$ acting from the bulk plasma of the ion wake behind the top particle restores the bottom particle right below the top one aligning them into vertical chain even if the confining force of electric field $F_{E,r}$ is close to zero.

The second series of calculations was devoted to the study of the influence of the configuration of confining electrostatic forces on nine dust particles. In Fig. 1 (d) the formed cluster of nine dust particles at moderate radial confinement is presented. It was also demonstrated that the particles align into a vertical chain in strong radial trapping field, and the particles align into a horizontal monolayer in the case of weak radial trapping. The obtained results can be useful in studying the nature of self-organization and in describing the formation of various ordered structures in strongly coupled Coulomb systems.

References

- [1]. Fortov V.E., Khrapak A.G., Khrapak S.A., Molotkov V.I., Petrov, O.F. *Phys. Usp.* **47** 447–492 (2004).
- [2]. Fedoseev A. V., Salnikov M. V., Vasiliev M. M., Petrov O. F. *Phys. Rev. E* **106** 025204 (2022).

DISPERSION OF THE POWDER-GAS INTERFACE BY MICROWAVE RADIATION

R. I. Golyatina¹, S. A. Maiorov²

¹*Prokhorov General Physics Institute of the Russian Academy of Sciences, Moscow, Russia*

²*Joint Institute for High Temperatures of the Russian Academy of Sciences, Moscow, Russia,
E-mail: mayorov_sa@mail.ru*

The problem of the scattering of dust particles from the powder-gas interface at atmospheric pressure $N_a = 2.69 \cdot 10^{19} \text{ cm}^{-3}$ under the influence of microwave radiation from a gyrotron $\nu = 75$ GHz with a radiation intensity of the order $I = 3 \cdot 10^4 \text{ W/cm}^2$ ($E_{max} = 4756 \text{ V/cm}$, $E/N = 17.6 \text{ Td}$) for $\Delta t_{RF} = 10$ ms is considered [1, 2]. Several stages can be distinguished in the evolution of the metal fraction of the powder.

At the first stage, before the metal particles begin to melt, the radiation energy is mainly absorbed by metal granules, and for particles on the surface of the powder, the equation of the balance of their thermal energy can be written as:

$$\frac{4}{3} \pi a^3 \cdot C_p \frac{dT}{dt} = 2\nu \cdot \frac{4}{3} \pi a^3 \cdot \frac{E_{max}^2}{8\pi} - 2\pi a^2 \cdot \sigma_{SB} (T^4 - T_0^4) - 4\pi a^2 \cdot N_a \cdot V_T (T - T_0),$$

where the terms on the right-hand side describe the transformation of the field energy into the thermal energy of the dust particle, radiation losses in the black body radiation approximation, and cooling of the dust particle by gas atoms. For Al, Fe, Cu, Ag, and Pt, the following estimates of the heating time to the melting point were obtained: 21, 73, 50, 33, and 71 ms, respectively. For a black body, the equality of radiation fluxes will be at a surface temperature of 8256 °C, which is an upper estimate for the maximum powder temperature.

In the second stage, after reaching the melting temperature, the radiation energy is spent for some time on the destruction of the lattice of the solid, after which the liquid metal dust particle is heated to the boiling temperature, while the gas in the pores is enriched with metal vapor, lowering the threshold for discharge ignition.

In the third stage, when dust particles are significantly heated due to gas escaping from the powder pores, the gas density in the powder pores decreases and the reduced electric field strength increases. Accordingly, at a certain gas density and metal vapor concentration on the powder surface, a discharge is initiated and the energy input into the near-surface layer increases sharply. Dust particles in the plasma of a gas discharge acquire a significant negative charge, and the forces of Coulomb repulsion cause them to fly away from the surface into the atmosphere. The paper presents the results of numerical modeling and makes estimates for all the listed mechanisms of interaction of powder with radiation.

The work was carried out within the framework of the State Assignment № FFWF-2022-0001 «Study of innovative synthesis of micro- and nanoparticles with controlled composition and structure based on a microwave discharge in gyrotron radiation»

References

- [1]. Skvortsova N. N., et al. *JETP Letters* **109** (7): 452-459 (2019).
- [2]. Skvortsova N. N., et al. *Fusion Science and Technology* **81** (8): 833-847 (2025).
DOI: 10.1080/15361055.2025.2478656

EFFECT OF THE NATURE OF CERIUM-CONTAINING COMPOUNDS ON THE MICROWAVE SYNTHESIS OF LUMINESCENT MATERIALS

N.S. Akhmadullina¹, A.K. Kozak², N.N. Skvortsova², A.S. Sokolov², O.N. Shishilov³

¹*A.A. Baikov Institute of Metallurgy and Material Science of Russian Academy of Sciences, Moscow, Russia, nakhmadullina@mail.ru.*

²*A.M. Prokhorov Institute of General Physics of Russian Academy of Sciences, Moscow, Russia, mukudori@mail.ru*

³*MIREA – Russian Technological University, Institute of Fine Chemical Technology, Moscow, Russia, oshishilov@gmail.com*

For the last decade we developed a new approach for plasma chemical synthesis of micro- and nanodispersed materials. The approach is based on the use of MW discharge, which occurs in the mixtures of metal and dielectric powders when they treated with short (2-8 ms) and high-power (up to 350 kW) pulses of MW irradiation (75 GHz). The experimental setup is described in details in [1]. Particularly, the approach was utilized to prepare luminescent materials based on aluminum oxide and oxynitride doped with rare-earth metals ions including Ce and Eu [2]. Very recently we have studied kinetics of the process resulting from self-non-selfsustained (SNS) microwave discharge in the Al/ γ -Al₂O₃/melamine powder mixtures with an addition of cerium compounds.

The SNS discharge was initiated by MW radiation pulses (75 GHz/ 400 kW/8 ms). Cerium was introduced in the form of CeO₂ (sample **AION:Ce-1**) and Ce(acac)₃·H₂O (**AION:Ce-2**), and by preliminary doping of γ -Al₂O₃ with Ce³⁺ ions (**AION:Ce-3**). Kinetic parameters of the process were determined, microscopic and XRD analyses of the products were conducted, and pulsed cathodoluminescence spectra were recorded. It was shown that the rate of the process and the efficiency of Ce³⁺ ions introduction into the produced Al₅O₆N aluminum oxynitride phase strongly depend on the nature of Ce-containing additive. Figure 1 summarizes key results.

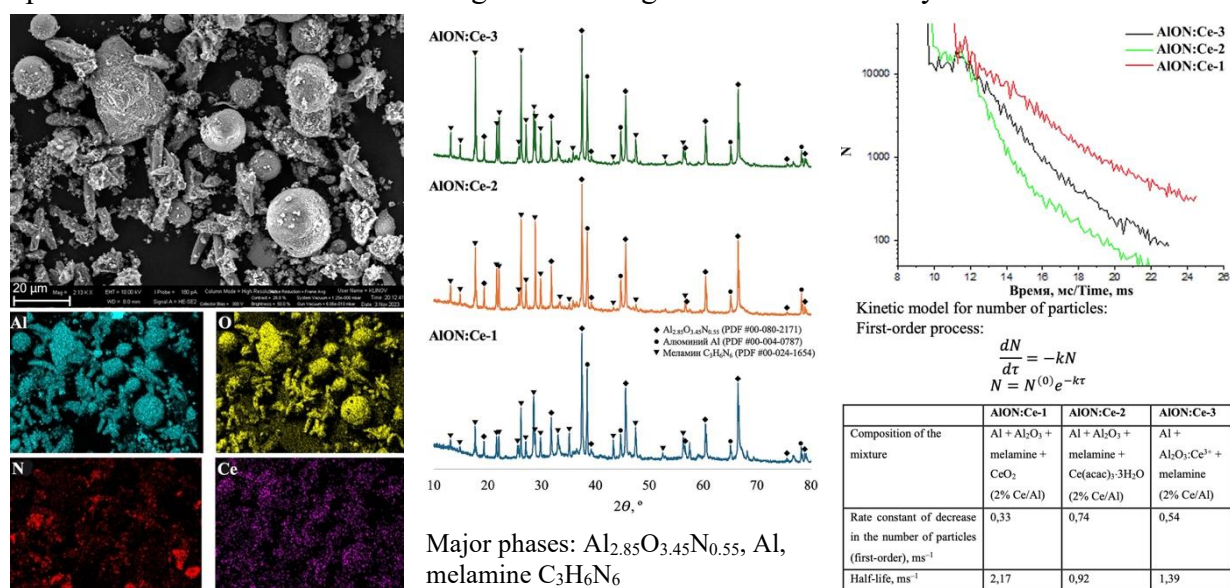


Fig. 1. Left: SEM-image and elemental maps of AION:Ce-1; center: XRD patterns; right: dependence of the number of particles involved in the plasma process (N) on time, kinetic model and its parameters.

The work was carried out within the framework of the State Assignment № FFWF-2022-0001 «Study of innovative synthesis of micro- and nanoparticles with controlled composition and structure based on a microwave discharge in gyrotron radiation».

References

- [1]. Sokolov A.S., et al. *Radiophys. Quantum Electron* **65**: 840–854 (2023).
- [2]. O.N. Shishilov, et al. *Patent RU 2826861 C1* (2024).

DUSTY PLASMA IN THE SOLAR SYSTEM: SPECIFIC DUSTY PLASMA EFFECTS

S.I. Popel, L.M. Zelenyi

*Space Research Institute of the Russian Academy of Sciences, Moscow, Russia,
popel@cosmos.ru*

Dusty plasma is a significantly more complicated system than ordinary dust-free plasma. There are a number of properties specific to dusty plasma that distinguish it from ordinary plasma. Such features include a possibility of the formation of a dusty plasma crystal, fluctuations in the charges of dust particles leading to anomalous dissipation and acceleration of dust particles, the existence of new time scales and new channels for the development of nonlinear interactions. Under natural conditions, dusty plasma in the Solar System exhibits all of these features. This work examines the effects in the Solar System associated with these features. The main emphasis is given to new findings related, in particular, to the influence of the anomalous dissipation on dust particle trajectories, fluctuation acceleration of dust in the vicinity of different cosmic bodies, and a possibility of the formation of a dusty plasma crystal at the comet nucleus. It is shown that for some atmosphereless space bodies (like the Moon or Mercury) dust particles move along periodic trajectories, while under certain conditions the dynamics of dust particles above, for example, the surfaces of comet nuclei can be aperiodic. The anomalous dissipation plays a significant role in justifying the application of the levitating dust particle model describing the dusty plasma above some space bodies. It is demonstrated that in the lunar dusty plasma, fluctuation acceleration of nanoscale and submicron dust particles can lead to a significant increase in their speed. Moreover, sufficiently small nanoscale particles can reach even the speeds exceeding the second astronomic velocity for the Moon, as a result of which such particles can leave the lunar dusty plasma system. Parameters characterizing dusty plasma properties for different comets are shown on phase diagram of Debye systems obtained using numerical simulations, and a possibility of the formation of strongly-coupled plasma states including dusty plasma crystal for these comets is discussed.

The study was supported by the Russian Science Foundation grant № 24-12-00064, <https://rscf.ru/project/24-12-00064/>.

**ON THE POSSIBILITY OF EXISTENCE OF NONLINEAR DUST ACOUSTIC
PERTURBATIONS NEAR COMETS**

Yu.S. Reznichenko, S.I. Popel, A.Yu. Dubinskii

*Space Research Institute of the Russian Academy of Sciences, Moscow, Russia,
dvju@yandex.ru*

Dusty plasma processes near comets are being investigated. The cases of distant and close location of comets relative to the Sun are considered separately. If the comet is located far enough away, dusty plasma formation is possible due to electrostatic processes. In this case dusty plasma processes play a significant role in the dynamics of dust particles. For Halley-type comets, for example, the formation of dusty plasma occurs at a distance from the Sun of at least 2.5-3.5 AU, otherwise the main factor determining the dust particle dynamics will be the effect of a gas stream from the comet's nucleus [1].

The issue of generation and propagation of nonlinear dust acoustic perturbations, such as dust acoustic solitons and nonlinear periodic waves, in the dusty plasma in the vicinity of the comet is discussed. The dependence of the soliton amplitude on the plasma parameters is investigated. It is shown that one of the factors determining the behavior of the soliton is the adiabatic capture of plasma electrons (ions) by the perturbation walls [2, 3]. The possibility of the existence of nonlinear periodic waves with sufficiently large spatial periods in the dusty plasma system near comets is discussed.

The study was supported by the Russian Science Foundation grant № 24-12-00064.

References

- [1]. Popel S. I., Golub' A. P., and Zelenyi L. M. *JETP Lett.* 120 (5) 307-314 (2024).
- [2]. Gurevich A.V. *Sov. Phys. JETP* 26 (3) 575-580 (1968).
- [3]. Reznichenko Yu. S., Izvekova Yu.N., Popel S. I. *Plasma Phys. Rep.* 50 (11) 1428-1437 (2024).

ON DUSTY PLASMAS IN JOVIAN MAGNETOSPHERE

S.I. Kopnin, S.I. Popel

*Space Research Institute of the Russian Academy of Sciences, Moscow, Russia,
kopnin@cosmos.ru*

There are regions in Jovian magnetosphere which are filled by dust particles. Among such regions there are those of Jupiter's rings. Dusty plasmas and their properties are discussed. The results of calculations are given of dust particle charges for different number densities as dependencies on the sizes of dusts under the conditions of different parts of Jovian magnetosphere.

**EXPERIMENTAL INVESTIGATION OF REGOLITH SIMULANT DYNAMICS IN A
FLOW OF CHARGED PLASMA PARTICLES**

I.A. Shashkova, I.A. Kuznetsov, G.V. Koynash, S.I. Popel, G.G. Dolnikov, A.N. Lyash,
M.E. Abdelaal, A.V. Zakharov

*Space Research Institute of the Russian Academy of Sciences, Moscow, Russia,
shi@cosmos.ru*

Recently, significant attention is paid to human exploration of the Moon by construction of scientific bases on its surface. This assumes the necessity to solve the complicated technical problems. One of them is to provide stable functioning of the equipment on the Moon in the presence of nano- and micro-sized regolith particles. They have a negative impact on instrument operations and scientific equipment, as well as an adverse effect on human health. Charged particles of lunar regolith are part of the near-surface dusty plasma that creates special conditions above the lunar surface. The purpose of this study is to investigate experimentally mechanisms of charging of such particles and their movement. We present the results of laboratory experiments using high-speed video recording on the visualization of the dynamics of simulant particles of lunar regolith under the influence of electrons and ions flowing on the simulant particles.

The study was supported by the Russian Science Foundation grant № 24-12-00064, <https://rscf.ru/project/24-12-00064/>.

ON NONLINEAR WAVE STRUCTURES IN ELECTRON-POSITRON-ION DUSTY PLASMAS

Yu.N. Izvekova, S.I. Popel

*Space Research Institute of the Russian Academy of Sciences, Moscow, Russia,
izvekova@cosmos.ru*

Electron-positron-ion dusty plasmas are studied, where charge variation of the dust grain is due to the microscopic electron, positron, and ion currents originating from the potential difference between the plasma and the grain surface. We consider quasistationary nonlinear structures moving with constant speed. Possibility of formation of ion-acoustic solitons and shock waves in electron-positron-ion dusty plasmas is discussed. In particular, we discuss a possibility of the existence of an ion-acoustic shock waves related to anomalous dissipation, which originates from the charging processes. Furthermore, we discuss the influence of the anomalous dissipation on ion-acoustic soliton propagation. We show the difference between the situation in the electron-positron-ion dusty plasmas in the usual dusty plasmas without positrons. In particular, in the electron-positron-ion dusty plasmas the importance of ions can be smaller than in the usual dusty plasmas. Correspondingly, the dissipative processes resulting in damping of the solitons in the electron-positron-ion dusty plasmas can be weaker. The types of space systems where shocks and solitons in electron-positron-ion dusty plasmas can be important are discussed.

This work was partially supported within the framework of Program 10 “Experimental Laboratory of Astrophysics and Geophysics” of the National Center for Physics and Mathematics.

**ON A POSSIBILITY OF DUSTY PLASMA FORMATION IN VENUSIAN
IONOSPHERE**

A.Yu. Dubinsky, S.I. Popel, Yu.S. Reznichenko

Space Research Institute of the Russian Academy of Sciences, Moscow, Russia

Venus continues to be a Solar System object whose study is a priority. The upcoming Venera-D and Venera-Glob missions plan to conduct a comprehensive study of the planet's soil, near-surface, and upper atmosphere. In this regard, analyzing the dusty plasma in Venus's ionosphere is of paramount importance. Several arguments support the existence of dusty plasma on Venus, allowing for preliminary calculations based on a model of dusty plasma structure on Earth.

Despite the extreme conditions on the surface of Venus, the atmospheric pressure and temperature at the altitude of 50-65 km are almost identical to those on Earth's surface. This makes the upper atmosphere of Venus the most Earth-like in our Solar System. This concerns also the ionosphere of Venus which is located at the altitudes of 120-300 km. We present the plasma parameters characterizing the ionosphere of Venus and discuss possible ways of dusty plasma formation there such as cosmic dust, condensation of gases constituting the ionosphere, dust transport from lower altitudes. Possible parameters of dusty plasmas in the ionosphere of Venus are discussed.

**DUST ION-ACOUSTIC WAVES FROM THE INTERACTION OF A COMET'S TAIL
WITH THE PLASMA OF THE ZODIACAL SOLAR CLOUD**

T.I. Morozova, S.I. Popel

*Space Research Institute of the Russian Academy of Sciences, Moscow, Russia,
timoroz@yandex.ru*

The interaction of a comet's tail with the plasma of a zodiacal solar cloud is examined.

The possibility of exciting dust ion-acoustic waves is demonstrated. Dispersion relations for these waves are determined.

Wave processes occurring under the interaction of the comet tail with dusty plasma of zodiacal light are studied. Dust ion-acoustic waves are shown to be excited due to the development of a linear hydrodynamic instability. This results in the excitation of ion-acoustic turbulence in these regions.

The turbulence level is estimated, and consequences of an appearance of dust ion-acoustic turbulence are discussed.

GENERATION OF ELLIPTICALLY POLARIZED RADIATION BY GAS MEDIA IN TWO-COLOR LASER FIELDS

S.Yu. Stremoukhov^{1,2}

¹*Moscow State University, Leninskie Gory str., bld. 1, Moscow, 119991, Russia,*

²*National Research Center “Kurchatov Institute”, Academician Kurchatov sqr., bld. 1, Moscow, 123182, Russia sustrem@gmail.com*

High-harmonic generation in gaseous media interacting with intense laser fields is one mechanism for obtaining coherent short-wavelength radiation [1]. Such radiation, possessing elliptical polarization, opens up opportunities for studying the magnetic and polarization-sensitive properties of matter [2]. At the same time, the nonlinearity of the radiation generation process dictates the need to develop methods for controlling the polarization properties of generated high-order harmonics. Moreover, such methods must take into account the peculiarities of the nonlinear optical response of the medium at both the microscopic (atomic) and macroscopic (propagation effects) levels of description of such interaction, including under conditions of phase and quasi-phase matching [3].

Here we present the results of our research on the generation of coherent elliptically polarized radiation in gaseous media through interaction with two-color laser fields, composed of the fundamental and second harmonic of a laser source. This work examines the cases of both linearly and circularly polarized components within these fields. Furthermore, we propose techniques for controlling the polarization state of the resulting radiation. For this study, we have used the interference model presented in [4] and non-perturbative theory of the single-atom response calculation discussed in [5].

This research was supported by the RSF (Project No. 24-22-00188).

References

- [1]. Popmintchev T. et al. *Science* **336**, 1287–1291 (2012).
- [2]. G. Lambert, et al. *Nature Communications*, **6**:6167 (2015).
- [3]. Hareli L., Shoulga G., Bahabad A., *J. Phys. B At. Mol. Opt. Phys.* **53** 233001 (2020).
- [4]. Stremoukhov, S. Andreev, A. *Laser Phys.* **28** 035403 (2018).
- [5]. Stremoukhov, S. et al. *Phys. Rev. A* **94** 013855 (2016).

LASER INDUCED DYNAMICS OF THE CONTINUUM STATE ELECTRONS AND SUBSEQUENT HARMONIC GENERATION IN SOLIDS

K.V. Lvov^{1,2}, S.Yu. Stremoukhov^{1,2}

¹*Lomonosov Moscow State University, Moscow, Russia*

²*National Research Center "Kurchatov Institute", Moscow, Russia*

A nonperturbative approach [1] to describing the properties of short-wavelength radiation generated by gaseous media, in particular high-order harmonics, has been successfully applied for many years to analyze the polarization and spectral features of such radiation [2-3], as well as to search for new methods of phase and quasi-phase matching of high-order harmonics [4-5]. The calculations require taking into account a large number of bound and continuum electron states in an atom, as well as summation over numerous matrix elements of the momentum operator and the transition operator between computational bases. Due to its computational complexity, the applicability of this approach to the problem of laser radiation propagation in a medium is very difficult, since it requires calculating the current density and nonlinear polarization at each point of the spatial computational grid and at each instant in time.

At the same time, due to their computational simplicity, single rate equation (SRE) and multiple rate equation (MRE) models for continuum electron dynamics [6], in which the continuous spectrum of states is replaced by discrete equidistant levels separated by the energy of the laser photon, have become widely used. These models are typically used to simulate the propagation of intense laser radiation in condensed matter. Additional refinements related to the time delay of impact ionization, caused by the need for electron to reach a critical energy for impact ionization, as well as those related to the dependence of the single-photon absorption rate on the electron energy, are incorporated into the extended (EMRE) model [7]. These refinements made it possible to correctly describe the occurrence of micromodifications in the silicon volume by single femtosecond mid-infrared laser pulses [8]. Moreover, in addition to the energetic impact of laser radiation on matter, coherent radiation is generated during its propagation.

This paper proposes a combination of two approaches: the EMRE continuum electron model for calculating the dynamics of the population amplitudes of continuum states and a nonperturbative approach for calculating the current density and spectrum of the generated coherent radiation. According to the EMRE model, a characteristic feature of the population amplitude dynamics is the upward energy movement of carriers due to the absorption of laser photons and the downward energy movement of carriers due to impact ionization. The generation of a microscopic current (and, consequently, a radiation field) accompanying this population movement can be calculated using the principles of a nonperturbative theoretical approach [1]. Analysis of the spectrum of the generated radiation demonstrated the presence of harmonics of the fundamental frequency of the laser radiation.

These studies are the first step toward developing a theory for the generation of coherent radiation in condensed media interacting with intense laser fields.

References

- [1]. Andreev A.V., Stremoukhov S.Y., Shoutova O.A. *Eur. Phys. J. D* **66**, 16 (2012).
- [2]. Ganeev R.A., Boltaev G.S., Stremoukhov S.Y. et al. *Eur. Phys. J. D* **74**, 199 (2020).
- [3]. Stremoukhov S.Y., Andreev A.V., Vodungbo B. et al. *Phys. Rev. A* **94**, 013855 (2016).
- [4]. Stremoukhov S. *J. Opt. Soc. Am. B* **39**, 1203 (2022).
- [5]. Stremoukhov S.Yu., Andreev A.V. *Laser Physics*, **28**, 035403 (2018).
- [6]. Rethfeld B. *Phys. Rev. Lett.* **92**, 187401 (2004).
- [7]. Lvov K.V., Potemkin F.V., Stremoukhov S.Yu. et al. *Mat. Tod. Comm.* **35**, 105594 (2023).
- [8]. Mareev E.I., Pushkin A.V., Migal E.A. et al. *Scientific reports* **12**, 7517 (2022).

HARMONICS GENERATION FROM RELATIVISTIC LASER STRUCTURED PLASMA

A.A. Andreev^{1,2}, K.Yu. Platonov³, M.V. Sedov^{4,5}, I.M. Ustinov⁵

¹*Saint Petersburg State University, Saint Petersburg, Russia*

²*Ioffe Physico-Technical Institute, Saint Petersburg, Russia*

³*Saint-Petersburg State Polytechnic University, Polytechnicheskaya str. 29, 2195251, St. Petersburg, Russia;*

⁴*Joint Institute for High Temperatures of the Russian Academy of Sciences (JIHT RAS), Izhorskaya str. 13 Bd.2, 125412 Moscow, Russia;*

⁵*National Research Nuclear University MEPhI (Moscow Engineering Physics Institute), Kashirskoe Shosse 31, 115409 Moscow, Russia;*

Harmonic generation was one of the first nonlinear optical phenomena observed shortly after the invention of the lasers. The study of harmonic generation processes is of considerable scientific and practical interest. For example, harmonic generation of intense laser radiation is a method for producing attosecond and even zeptosecond pulses, as it provides the necessary spectral width of the generated radiation [1].

This paper examines the optimization of conditions for generation of laser harmonics from submicron high-density plasma clusters irradiated by laser pulses lasting tens of femtoseconds and with (sub)relativistic intensities. Relativistic intensities were considered in our work [2]. Numerical simulations were performed using the EPOCH code [3], a modern package for simulating the interaction of laser radiation with matter using the Particle-in-Cell (PIC) method, taking into account field and collisional ionization. In particular, figure 1 shows the conversion efficiency into the 2nd and 5th harmonics as the function of the cluster diameter.

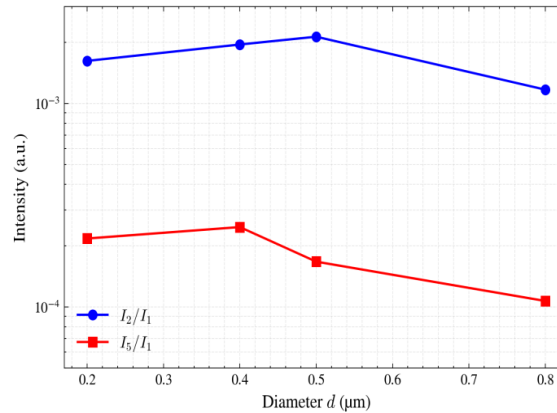


Fig. 1. Dependence of the energy conversion efficiency into the 2nd and 5th harmonics on the Si cluster diameter.

As a result of the calculations, the angular characteristics of the scattered radiation and the energy conversion efficiency of the incident laser radiation into the energy of the second and higher harmonics were determined, depending on the cluster diameter and the pre-plasma density scale length, induced by the laser pre-pulse.

References

- [1]. Pfeifer T., Spielmann C., Gerber G. *Rep. Prog. Phys.* **69** (2) 443-505 (2006).
- [2]. Andreev A.A., Platonov K.Yu., Sedov M.V. *Bulletin of the Lebedev Physics Institute.* **52S327-S339**(2025).
- [3]. Arber T.D. et. al. *Plasma Physics and Controlled Fusion.* **57**(11) 113001 (2015).

REFRACTIVE INDEX ULTRAFAST ANISOTROPY IN GASEOUS MEDIA INDUCED BY ULTRA-SHORT LASER PULSES

K.A. Galyuk, A.A. Ushakov, P.A. Chizhov

*Prokhorov General Physics Institute of the Russian Academy of Sciences, Moscow, Russia,
karina272001@yandex.ru*

The propagation of high-intensity femtosecond laser pulses through a gas induces anisotropy of the refractive index of the medium and leads to plasma formation. Dynamic balance of the nonlinear phenomena of Kerr self-focusing and plasma defocusing results in the formation of a filament (a thin, extended luminous channel). The filament acts as a source of ultrabroadband electromagnetic pulses in ranges from radio waves to the ultraviolet [1-3]. Filamentation is a threshold process dependent on the critical power of self-focusing of the laser radiation. Changes in the properties of a gaseous medium—such as pressure, molecular composition, and atomic composition—lead to alterations in the critical power, filament length, and generation efficiency of secondary radiation. Investigating how filament parameters vary with different medium characteristics is essential for developing a highly efficient, laser-plasma-based supercontinuum source.

In this paper, the anisotropy of the refractive index of gaseous media (air, argon, nitrogen, and carbon dioxide) is studied at various pressures ranging from 1 to 5.5 atm in the presence of high-power laser radiation. The source of laser radiation was a multi-gigawatt Ti:Sapphire femtosecond laser system with pulse energy of 2.7 mJ, a repetition rate of 1 kHz, a duration of 40 fs, a central wavelength of 800 nm, and a beam diameter of 12 mm at the e^{-2} level. We studied the refractive index anisotropy and electron concentration in the pre-focal region using the pump-probe method [4]. The laser beam was split into two parts: a pump beam and a probe beam, such that the propagation axes of these beams were mutually perpendicular in their intersection region. The pump pulse was focused into a gas cell containing different gases at various pressures, thus forming a filament. The probe pulse (~1% of the original radiation) was directed transversely to cross the path of the pump pulse and interacted with it at different time delays.

The induced anisotropy of the gas refractive index results in depolarization of the probe pulse [5]. We recorded the change in the spatial intensity distribution in the cross-section of the probe beam after it passed through the interaction region with the pump beam. The degree of depolarization of the probe radiation increases with gas pressure. The obtained results allow for the non-invasive assessment of local laser radiation intensity at various gas pressures.

References

- [1]. Mitrofanov A.V., et al. *Opt. Lett.* **46** (5) 1081–1084 (2021).
- [2]. Matsubara E., Nagai M., and Ashida M. *Appl. Phys. Lett.* **101** (1) 011105 (2012).
- [3]. Zhang X.-C., and Xu J. *Springer. New York: Springer* (2010).
- [4]. Lorient V., Hertz E., Lavorel B., Faucher O. *J. Chem. Phys.* **132** 184303 (2010).
- [5]. Ushakov A., Chizhov P., Bukin V., Dolmatov T., and Garnov S. *Appl. Opt.* **62** 8000–8006 (2023).

THE ROLE OF AIS IN THE MULTIPHOTON IONIZATION PROCESSES

S.N. Yudin¹, M.M. Popova^{1,2}, A.N. Grum-Grzhimailo¹, E.V. Gryzlova¹

¹*Skobeltsyn Institute of Nuclear Physics, Lomonosov Moscow State University, Moscow, Russia*

²*Gaponov-Grekhov Institute of Applied Physics of the RAS, Nizhny Novgorod, Russia*

Multiphoton spectroscopy has been a versatile and powerful tool for probing atomic structure. It enables the probing of such continuum structures as the Cooper minimum in ionization from excited states, dipole-forbidden autoionizing states (AIS), and many others [1]. Of particular interest is the fact that some properties, such as the Fano profile index [2], are determined not by the AIS alone, but also by the state from which the AIS is excited and even by the field polarization [3].

The present report is inspired by recent progress in observation of high harmonic generation (HHG) in the vicinity of the $3d^9 4s^2 4p$ AIS of Ga^+ ion [4,5]. Here we developed an approach based on a solution of the time-dependent Schrödinger equation in a limited basis of discrete states of the unperturbed ion [6]. The advantage of this approach is that a high quality spectroscopic model can be developed and implemented. Using MCHF we calculated energies and dipole matrix elements for transitions within a large group (46) of discrete states of Ga^+ ; in addition, we calculated dipole transition amplitude from the ground and the excited states into 20 continuum channels and several autoionization matrix elements. Then the system of equations on the coefficients of wave function series was found for the two different electromagnetic pulses.

First, we applied the approach to single photon ionization of Ga^+ in the vicinity of the AIS under consideration (Fig. 1a) and checked the sensitivity of the AIS profile to their relative configuration interaction. Having tested the method, we then applied it to seven-photon ionization in the conditions relevant for [4]: intensity 1.6 TW/cm^2 , wavelength 397 nm, pulse duration 128 opt. cycles (30 fs) (Fig. 1b).

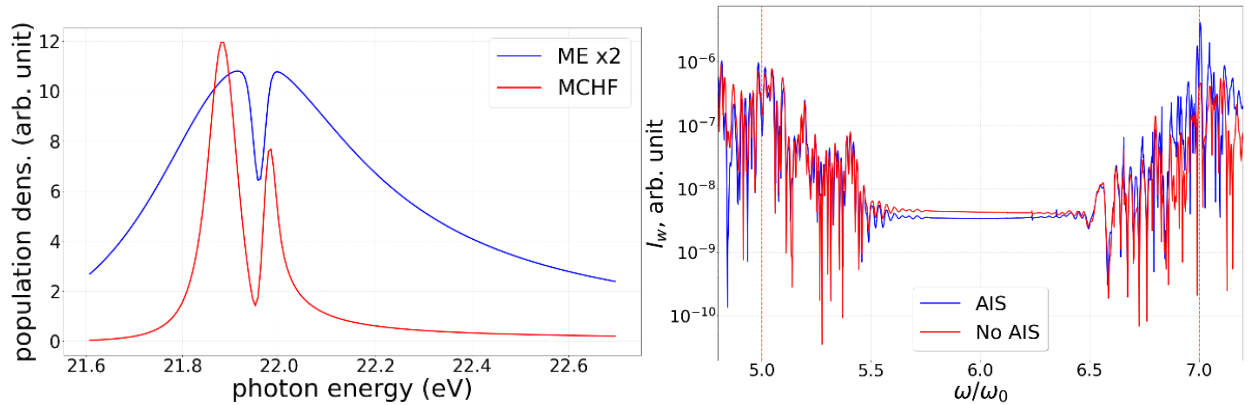


Fig. 1. (a) The photoionization profile of the $3d^9 4s^2 4p$ AIS of Ga^+ ion; (b) 7th photon ionization of Ga^+ ion with and without accounting for AIS, see text for the details

The results reveal a significant enhancement, by nearly two orders of magnitude, in the radiation of the seventh harmonic at the corresponding energy compared to the same calculation for the continuum structure.

References

- [1]. Mainfray G. and Manus C. *Rep. Prog. Phys.* **54**, 1333-1372 (1991).
- [2]. Fano U. and Cooper J. W. *Phys. Rev. A* **137**, 1364 (1965).
- [3]. Popova M.M. *et al Atoms* 10(4), 102 (2022).
- [4]. Ganeev R.A. *Opt. Express* **32** (24), 43571–43585 (2024).
- [5]. Strelkov V. *Phys. Rev. Lett.* **104**, 123901 (2010).
- [6]. Magunov A.I., Strelkov V.V. and Yudin S.N. *Phys. Wave Phen.* **31**(6), 418–426 (2023).

COMPTON IONIZATION OF HYDROGEN BEAM BY TWISTED PHOTONS WITH USE OF THE COLTRIMS DETECTOR

Yu.V.Popov^{1,2}, K.A.Kouzakov³, K.A.Bornikov³

¹*Skobeltsyn Institute of Nuclear Physics, Lomonosov Moscow State University, 119991, Moscow, Leninskiye gory, 1, Russia, popov@srd.sinp.msu.ru*

²*Bogoliubov Laboratory of Theoretical Physics, Joint Institute for Nuclear Research, 141980, Dubna, Russia*

³*Faculty of Physics, Lomonosov Moscow State University, 119991, Moscow, Leninskiye gory, 1, Russia*

Cold-Target Recoil-Ion Momentum Spectroscopy (COLTRIMS) is currently the most advanced tool for detailed study of the processes of Compton ionization of atoms [1]. We have performed a theoretical analysis of the capabilities of this method as applied to Compton ionization of an atom by a twisted x-ray photon. Our analysis uses the nonstationary formalism of quantum scattering theory, which, unlike the generally accepted stationary formalism, allows one to take into account the specifics of real initial states (wave packets) of a photon and an atom. We have shown that the energy and angular distribution of ionized electrons measured in coincidence with recoil ions does not depend on the angular momentum projection of the twisted photon on the z-axis, but depends on its opening angle θ_k , which is one of the main twisted-photon characteristics [2].

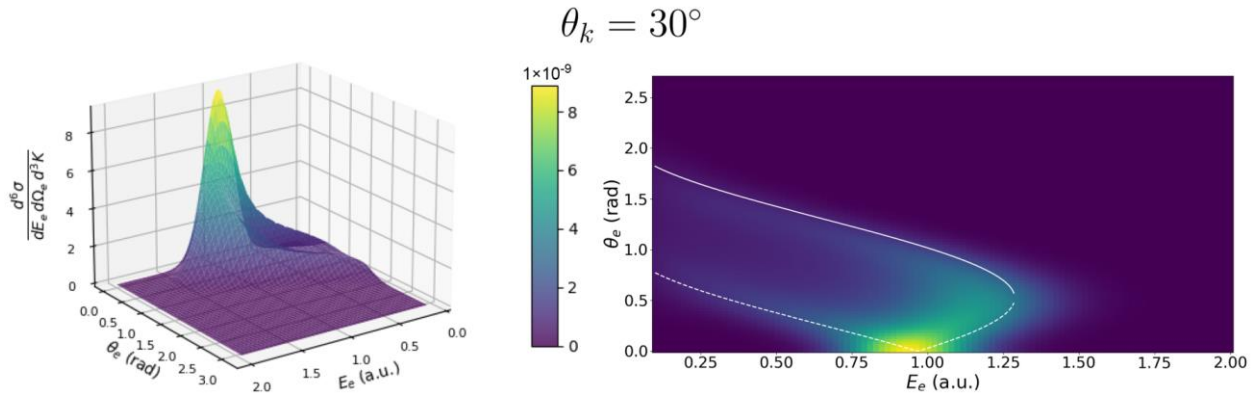


Fig. 1. The fully differential cross section for a fixed final ion momentum $\mathbf{K}=\mathbf{K}_H$, where \mathbf{K}_H is the average momentum of atoms in the hydrogen atomic beam, versus the electron energy and its scattering angle (left panel). The intensity distribution corresponding to the graph on the left is shown in the right panel. The initial photon energy is $\omega = 3$ keV

As an illustration, in Fig. 1 the differential cross section is displayed for a fixed opening angle of twisted photons. The intensity distribution can be qualitatively explained on the basis of the Klein–Nishina formula for photon scattering on a free electron: the ionized electron is preferably emitted in the forward direction that corresponds to the photon scattering in the backward direction.

References

- [1]. Haubenreißer D. M. et al., *Phys. Rev. Lett.* **135** (3) 033203 (2025).
- [2]. Bornikov K. A., Kouzakov K.A., Popov Yu. V. *Phys.Rev. A* **112**(2) 022812 (2025).

**METAMATERIALS AND OPTOACOUSTICS, LASER-INDUCED
DEFORMATION OF SOLIDS, BERYLLIUM OPTICS AND FINE FOCUSING
OF HARD X-RAYS FROM XFEL**

N.A. Inogamov

L.D. Landau Institute for Theoretical Physics of Russian Academy of Sciences

The weak femtosecond (fs) optical excitation regime is considered [1, 2]. Remarkably, the metamaterial we have created functions for the first time as an optoacoustic transducer, in addition to its conventional role in extraordinary optical transmission [1, 2].

The slow (subsonic) heating (without melting) of a solid target by a nanosecond pulse is investigated. Descriptions are provided for (a) grain boundary creep in crystallites [3,4] and (b) thermo-elastoplastic effects in an isotropic solid.

A method for the optimal utilization of a hard X-ray (9 keV) femtosecond pulse to fabricate ultra-long channels of submicron diameter is described [5].

References

- [1]. Petrov et. al. *Zh. Exp. Theor. Phys.* 2025. Vol. 167, № 5. P. 645-671
- [2]. Dyshlyuk et. al, *Pis'ma v Zhurnal Eksperimental'noi i Teoreticheskoi Fiziki* 2026. Vol. 123, №. 3
- [3]. Nelasov et. al. *Zh. Exp. Theor. Phys.* 2025. Vol. 167, № 6. P. 782-797.
- [4]. Rogalin et. al. *Fizika Tverdogo Tela* 2025. Vol. 67, № 12
- [5]. Makarov et. al. *Nature Communications* 2025. Vol. 16, 11504

X-RAY GENERATION IN A MICROCLUSTER MEDIUM IRRADIATED BY AN ULTRASHORT LASER PULSE

D.A. Gozhev^{1,2}, S. G. Bochkarev^{1,2}, O. E. Vais^{1,2}, M. G. Lobok^{1,2}, V. Yu. Bychenkov^{1,2}

¹*Lebedev Physical Institute, Russian Academy of Sciences, Moscow, Russia*

²*Center for Fundamental and Applied Research, Dukhov All-Russian Research Institute of Automation, Rosatom, Moscow, Russia*

One of the widely used types of nano- and microstructured targets for laser heating and charged particle acceleration is cluster targets. Such targets, formed by the supersonic expansion of a gas jet, rapidly recover their initial parameters after each laser shot and can be used for high-repetition-rate laser systems. It is well known that gas clustering under the interaction with an intense laser pulse can significantly enhance the yield and average energy of charged particles [1], promote neutron generation in deuterated cluster media [2], and increase the yield of X-ray and gamma radiation.

In this work, using comprehensive 3D Particle-in-Cell (PIC)-GEANT4 simulations, together with analytical estimates, were performed to investigate the interaction of large submicron clusters composed of heavy atoms with relativistically intense laser radiation ($\geq 10^{18}$ W/cm²). The primary objective was to study the dependence of X-ray emission yield on cluster size and laser intensity.

The simulations demonstrate that bremsstrahlung radiation provides the dominant contribution to the emitted X-ray spectrum, exceeding the synchrotron component associated with stochastic electron motion in complex laser–plasma fields. It is shown that irradiation of submicron cluster media leads to the formation of a pronounced plateau in the high-energy region of the electron spectrum, which is responsible for the enhanced bremsstrahlung emission.

The study reveals a weak increase in the laser-to-bremsstrahlung energy conversion efficiency for photon energies above 100 keV with increasing laser intensity at fixed pulse energy. At a laser intensity of 3×10^{19} W/cm², the conversion efficiency reaches approximately 10^{-4} . In addition, it is found that increasing the laser intensity enhances the yield of the hardest photons. Thus, at a fixed laser pulse energy, one may either increase the laser intensity to obtain higher-energy photons or reduce the intensity to generate a larger number of photons with moderate energies.

This research was carried out with partial support from the scientific program of the National Center for Physics and Mathematics (project “Physics of High Energy Densities. Stage 2023–2025”).

References

- [1]. Gozhev D.A., Bochkarev S. G., and Bychenkov, V. Y. *JETP Letters*, 114(4), 200-207(2021).
- [2]. Gozhev D. A., Bochkarev S. G., Lobok M. G., Brantov A. V., Bychenkov V. Y. *Phys. Plasmas* V. 31. P. 073103 (2024)

FEATURES OF THE CREATION AND CONTROL OF SUBWAVELENGTH MICROSTRUCTURES IN THE PROCESS OF DIRECT LASER WRITING IN THE VOLUME OF TRANSPARENT DIELECTRICS

A.V. Bogatskaya^{1,2}, E.A. Volkova³, M.P. Verteletskaya^{1,2}, A.M. Popov^{1,2}

¹*Department of Physics, Lomonosov Moscow State University, Moscow, Russia, annabogatskaya@gmail.com*

²*Lebedev Physical Institute, Russian Academy of Sciences, Moscow Russia*

³*Skobeltsyn Institute of Nuclear Physics, Lomonosov Moscow State University, Moscow, Russia*

In this study we conduct 3D self-consistent numerical simulations of an intense focused femtosecond laser pulse ($\lambda_0 = 1030$ nm, 100 fs duration) propagating through fused silica, coupled with the evolution of laser-induced solid-state plasma. The model combines a second-order wave equation in cylindrical geometry with a carrier density rate equation, employing the full Keldysh solid-state ionization formalism alongside the Drude model for electron impact ionization [1]. It was shown that placing a high-reflectivity dielectric or silver mirror at the back surface of the fused silica sample (near the focal plane) produces a standing-wave interference pattern between the incident and reflected beams. This substantially modifies the laser field distribution and the resulting in a qualitatively different plasma self-organization pattern compared to the free-propagation case. The simulations indicate that varying the relative position of the mirror and the focal plane provides flexible control over the interference topology and thus over the spatial profile of the induced plasma tracks. Simulations indicate that the presence of the mirror can approximately double the energy deposited in the bulk when offset between the mirror and the focal plane is ~ 5 mkm (Fig.1).

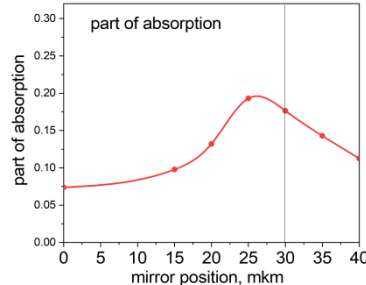


Fig. 1. The part of absorbed energy in the bulk of fused silica depending on the mirror position. The position of focal plane is 30 mkm.

The results show that at pulse durations of ~ 100 fs and longer, electron impact ionization becomes dominant over multiphoton ionization. Because avalanche growth is exponential while multiphoton production scales linearly with time, including impact ionization in the simulations increases the peak electron density by several times and substantially extends the longitudinal extent of the hot-plasma zone. The authors attribute effective material modification and the accumulation-regime formation of subwavelength birefringent microtracks to this elongated high-density region.

The proposed approach is seen as a promising route toward reproducible, controllable fabrication of volumetric birefringent nanostructures with diverse topologies for applications in optical polarizing elements, waveguides, photonic crystals, and data-storage devices.

This work was supported by Russian Science Foundation (grant no. 22-72-10076-P).

References

- [1]. Bogatskaya, A. V., Volkova, E. A., Popov, A. M. *Applied Physics A* **131** 79 (2025)

EFFECT OF LASER ENERGY DENSITY ON ABLATION EFFICIENCY OF ZINC SULFIDE NANOPARTICLES

A.V. Kharkova, D.A. Kochuev, A.A. Voznesenskaya, D.N. Bukharov

Vladimir State University named after A.G. and N.G. Stoletovs, Vladimir, Russia,
alenaenergie@gmail.com

Exposure of a material surface to laser radiation with an energy density exceeding the ablation threshold results in particle formation [1–3]. The resulting particle characteristics and ablation efficiency depend directly on the exposure conditions. Even when ultrashort laser pulses are used, it is difficult to completely eliminate thermal effects, owing to relaxation processes in the ablated material and the formation of a laser-induced plasma plume in the irradiated region.

This paper presents the results of an experiment investigating the effect of laser energy density on particle yield. A laser system with a pulse duration of 280 fs, a repetition rate of 10 kHz, and a wavelength of 1030 nm was used. Polycrystalline zinc sulfide served as the target material, and ablation was carried out in an argon atmosphere. When the laser fluence exceeded the ablation threshold ($\leq 0.3 \text{ J/cm}^2$), nanoparticle ejection was observed without optical breakdown of the surrounding medium or significant plasma formation, thereby minimizing the influence of the laser-induced plume on the ablation products. The energy density (fluence) was varied from 0.3 to 3.4 J/cm^2 . At the highest fluence (3.4 J/cm^2), optical breakdown occurred, leading to the formation of a pronounced laser-induced plasma plume in the interaction region, which reduced ablation efficiency. This plume promoted coalescence and aggregation of the ablated nanoparticles.

In the fluence range of $1.0\text{--}1.2 \text{ J/cm}^2$, thermal effects associated with plasma formation were effectively suppressed, resulting in enhanced ablation efficiency. Ablation performance as a function of laser fluence was evaluated based on the mass loss of the sample before and after irradiation (fig. 1).

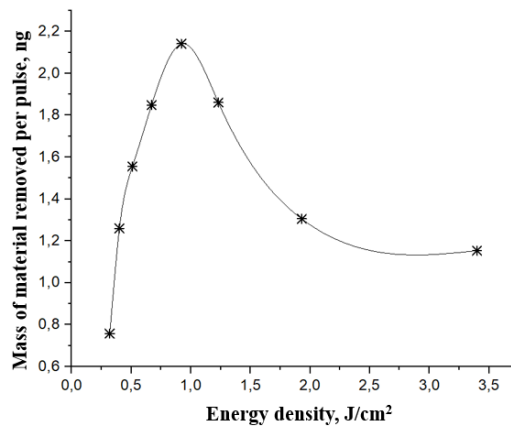


Fig. 1. Dependence of the mass removed per pulse on the energy density of laser radiation during zinc sulfide ablation

Increasing the laser fluence from the ablation threshold to $1.0\text{--}1.2 \text{ J/cm}^2$ leads to an increase in the mass of material removed. Further increases in fluence result in a significant decrease in the ablation yield. The formation of a laser-induced plasma plume dramatically reduces ablation efficiency – by an average of 100% in some regimes.

The study was supported by a grant from the Russian Science Foundation № 25-22-20075.

References

- [1]. Ganash E. A. *Laser Physics Letters* **20** (1) 013001 (2022).
- [2]. Chen L., et al. *Opto-Electronic Science* **1** (5) 210007-1 (2022).
- [3]. Alheshibri M., et al. *Optics & Laser Technology* **155** 108443(2022).

TIME DELAY OF REFLECTED AND TRANSMITTED LASER PULSE AT LASER ACTION ON A DENSE PLASMA SLAB

A.A. Frolov

*P.N. Lebedev Physical Institute RAS, 53, Leninskiy Prospekt, Moscow, 119991, Russia,
frolova@lebedev.ru*

This article considers the oblique incidence of as-polarized unfocused laser pulse on the boundary of the supercritical plasma slab [1]. The boundary value problem is solved and the distribution of the electric field of laser radiation in the whole space is found in the form of Fourier integrals over frequencies. The time delay of the reflected signal is calculated and its dependence on the thickness of the plasma slab and the angle of the laser radiation incidence is studied. It is shown that the time delay of the reflected signal at the small angles of laser radiation incidence increases and reaches the plateau with increasing thickness of the plasma slab. At the grazing angles of the laser pulse incidence, the time delay of the reflected signal increases with increasing slab thickness, reaches the maximum, decreases, and only then does it saturate. The dependence of the reflected signal time delay on the angle of the laser pulse incidence is considered, and it is shown that it is maximum for the thick slab at the normal incidence, and for the thin slab at incidence at the grazing angles.

The field of the laser pulse transmitted through the plasma slab is considered, its intensity and time delay are calculated, and their dependence on the thickness of the plasma slab, electron density, and angle of incidence of laser radiation are studied. It is shown that the time delay of the transmitted signal coincides in value with the delay of the reflected pulse. It is found that when the time delay of the transmitted signal tends to saturate, its intensity is so negligibly small that it makes no sense to talk about the penetration of the laser pulse through the slab, since under these conditions the effect of almost total reflection of the incident laser radiation takes place. It is established that the time delay of the signal transmitted through the overdense plasma decreases with increasing electron concentration.

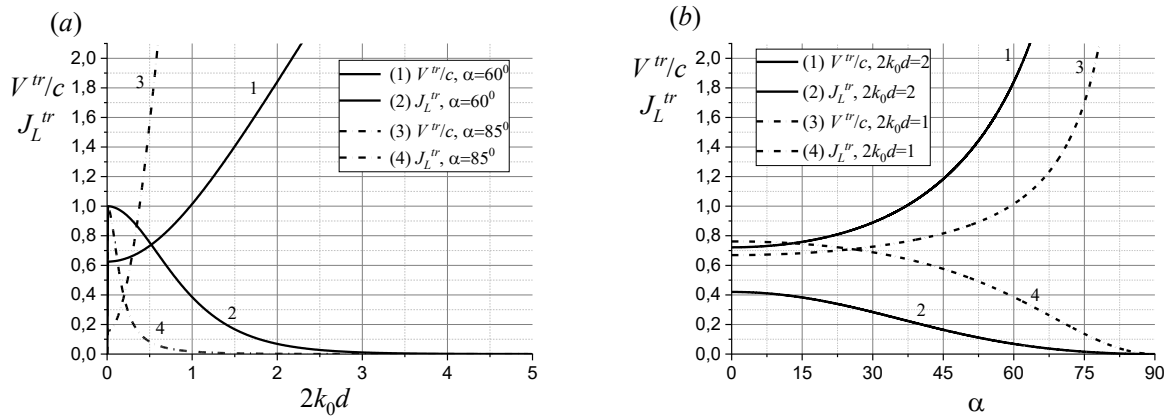


Fig. 1. The speed of the laser pulse energy tunneling V^tr through the slab of near-critical plasma (a) as a function of the slab thickness $2d$ for different angles of incidence α , (b) as a function of the angle of incidence for different thickness of the plasma slab, where c is speed of light, k_0 and J_L^tr are wave number and normalized intensity of transmitted laser radiation.

The Hartman effect [2] is discussed and the possibility of superluminal tunneling of the laser pulse is considered. The tunneling speed of the laser pulse energy through the plasma slab is calculated, and it is shown that at the large angles of incidence it can exceed the speed of light in a vacuum, and this is due to the short time delay of the transmitted signal (See Fig. 1).

References

- [1]. Frolov A.A. *Phys. Plasmas* **31** (10) 103107 (1-10) (2024).
- [2]. Hartman T. *E.J. Appl. Phys.* **33** (12), 3427-3433 (1962).

SCALABLE QUANTUM NEUROMORPHIC ARCHITECTURES BASED ON QUANTUM MEMRISTORS

A.S. Frolova^{1,2}, S.Yu. Stremoukhov^{1,2}, P.A. Forsh^{1,2}, I.A. Kovalishin¹, D.M. Rusakov¹,
K.Yu. Khabarova², N.N. Kolachevsky^{2,3}

¹*Faculty of Physics, Lomonosov Moscow State University, Leninskie Gory, 1/2, Moscow, 119991, Russia, frolova.as17@physics.msu.ru (A.S. Frolova)*

²*P.N. Lebedev Physical Institute of the Russian Academy of Science, Leninskiy Prospekt, 53, Moscow, 119991, Russia*

³*Russian Quantum Center, Skolkovo, Moscow, 143025, Russia*

Quantum memristors (QMs) have emerged as promising building blocks for neuromorphic quantum computing, offering the potential to combine the memory and nonlinear dynamics of classical memristors with quantum advantages such as high-dimensional state spaces and entanglement. Proposed realizations include various physical platforms such as superconducting circuits [1,2], quantum photonics [3-5], ion traps [6] and light-matter [7]. An experimental realization has been achieved in [5], where the authors have also demonstrated a numerical quantum advantage, comparing the performance of QMs versus classical memristors in an image recognition task.

In this work, we propose and numerically validate a novel approach to define three coupled QMs on a single trapped ¹⁷¹Yb⁺ ion, enabling the operation of any two as a coupled pair at a given time. This architecture significantly reduces the number of ions required for complex neural architectures, paving the way for scalable multilayer quantum perceptrons.

Through numerical simulations of the coupled system, we demonstrate that coupling preserves the memristive hysteresis behavior and enables signal transfer between QMs. Robustness analysis confirms that the hysteresis behavior remains stable under realistic experimental fluctuations in Rabi frequencies and pulse timing, with modern laser systems providing the necessary precision. We further evaluate the performance of QM-based models in a handwritten digit classification task using the MNIST dataset. Our results show that coupled QMs achieve recognition accuracies of 91–92%, matching the performance of ‘ideal’ memristors and uncoupled QMs. These findings validate the feasibility of coupled QMs for scalable, hardware-efficient quantum neural architectures and highlight their potential for advancing quantum-inspired machine learning.

This study was supported by the Russian Science Foundation grant 24-12-00415, <https://rscf.ru/project/24-12-00415/>.

References

- [1]. Pfeiffer P., Egusquiza I. L., Di Ventra M., et al. *Sci. Rep.* **6** (1) 29507 (2016).
- [2]. Salmilehto J., Deppe F., Di Ventra M., et al. *Sci. Rep.* **7** (1) 42044 (2017).
- [3]. Sanz M., Lamata L., Solano E. *APL Photonics* **3** (8) 080801 (2018).
- [4]. Gonzalez-Raya T., Lukens J. M., Céleri L. C., et al. *Materials* **13** (4) 864 (2020).
- [5]. Spagnolo M., Morris J., Piacentini S., et al. *Nat. Photonics* **16** (4) 318–323 (2022).
- [6]. Stremoukhov S.Yu., Forsh P.A., Khabarova K.Yu., Kolachevsky N.N. *Entropy* **25** (8) 1134 (2023).
- [7]. Norambuena A., Torres F., Di Ventra M., et al. *Phys. Rev. Appl.* **17** (2) 024056 (2022).

**ANALYTICAL ANALYSIS OF A QUANTUM MEMRISTOR ON AN ULTRACOLD
¹⁷¹YB⁺ ION**

I. A. Kovalishin¹, S. Yu. Stremoukhov^{1,2,3}, P. A. Forsh^{1,2}, K. Yu. Khabarova²,
N. N. Kolachevsky^{2,4}

¹*Faculty of Physics, Moscow State University, Moscow, 119991 Russia*

²*Lebedev Physical Institute, Russian Academy of Sciences, Moscow, 119991 Russia*

³*National Research Center Kurchatov Institute, Moscow, 123182 Russia*

⁴*Russian Quantum Center, Moscow, 121205 Russia*

A quantum memristor is a quantum system with a dynamic internal state and hysteretic input-output characteristics, capable of performing operations with quantum information [1]. We study a three-level quantum memristor implemented on a single ultracold ¹⁷¹Yb ion confined in a Paul trap, where the input and output signals are determined by the populations of the energy levels, and the system is controlled by two resonant laser pulses with Gaussian envelopes [2].

We focus on the experimentally relevant regime where the two resonant pulses are significantly separated in time, so that during each pulse the other field envelope is negligible. Under these conditions, we derive explicit closed-form analytical expressions for the population dynamics and the memristor's input (x) and output (y) signals. The resulting dependences are expressed via the error-function integrals of Gaussian envelopes. The obtained analytical dependences for x and y are benchmarked against direct numerical integration of the original equations and show good agreement; for representative parameters used in the paper the reported relative standard deviation is below 0.03%.

Within the memristor formalism, we introduce a control parameter (denoted as the reflection-coefficient analog R) and a feedback model with a sliding integration window, similar to photonic platform [3]. We demonstrate that the output-input hysteresis y(x) exhibits strong dependence on the window parameter T, which is essential for tuning the memristor response and implementing neuromorphic computing devices on the ion platform. We also compare the separated-pulses regime to the previously studied simultaneous-pulses configuration and observe that hysteresis persists, while the output variation range can change [4].

The developed analytical approach provides a consistent method for determining input and output signals, simplifying both experimental verification and the analytical simulation of ion-based quantum memristors for neuromorphic applications.

This work was supported by the Russian Science Foundation (project no. 24-12-00415).

References

- [1]. Chua L. O. *IEEE Trans. Circuit Theory***18**, 507 (1971).
- [2]. Stremoukhov S., Forsh P., Khabarova K., Kolachevsky N. *Entropy* **25**, 1134 (2023).
- [3]. Spagnolo M. et al. *Nat. Photonics***16**, 318 (2022).
- [4]. Kovalishin I. A. et al., *JETP Letters*, **122 (12)**, 862–866 (2025).

LASER AND BEAM PLASMA PARTICLE-IN-CELL SIMULATION IN A RELATIVISTIC REFERENCE FRAME

A.G. Zhidkov

National Research Nuclear University MEPhI, Moscow, Russia

Developing of new coherent radiation sources requires deeper numerical analysis of physical processes, which can be done only via kinetic simulations. Particle-in-cell (PIC) method here is the ultimate method for that. However, in view of high spatial resolution, problems with long-length targets are frequently out of ability of PIC method. The advantages of space-time dilation allow the simulation of complex physical systems for long distances (up to meters) in Cartesian PIC using even a single workstation extending class of solvable problems. This makes clear request for PIC simulation in relativistic reference frames (RRF) [1, 2]. The non-intuitive aspects of working in a RRF (e.g., Gaussian beam elongation, field transformation, relativistic Doppler) make simulations non-trivial. Due to the intrinsic features of the Lorentz transformation, an instant t' in the RRF can result in a time window of Δt in the laboratory reference frame (LRF), therefore, making the interpretation of the code raw results non-trivial in several instances. An example of importance of the approach is demonstrated for an electron beam inside an undulator with plasma as an optical element. Adding plasma as an optical element into tens of meters undulators leaves no way for avoiding PIC simulations in RRF. Developing of plasma-based undulators as cheap, compact sources of coherent radiation also needs in PIC simulations in RRF. Despite of several groups proposed usefulness of this technique (see [1, 2] and references there) still there are many problems have yet to be solved.

Advantage of PIC simulation in RRF long-length propagation of laser pulses or charge particle beams in plasma or/and undulator is shortening of plasma (undulator) length L as $L/2\gamma_R$ where γ_R is relativistic factor of RRF. It is great feature of RRF. However, any system has backward scattered radiation. This radiation has shortened wavelength compare to LRF: $\lambda/2\gamma_R$. In Fig.1 a density wake after an electron beam in a low-density plasma which is $\lambda_{pl} * 2\gamma_R$ before wave breaking and very peaky after the wave breaking. To explore all the system one has to apply special resolution as $\lambda/2\gamma_R$ that can discard advantage of RRF. Poor resolution can result in numerical instability even if the scattering signals are weak. Another problem concerning to propagation of laser pulses is the change of plasma “optical density” in RRF. All these problems are discussed.

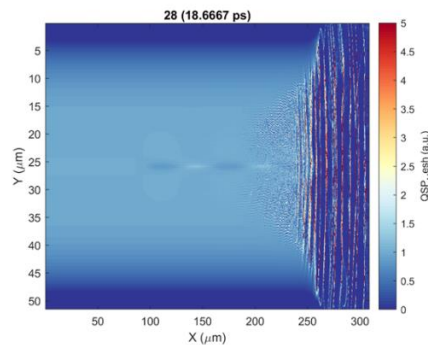


Fig. 1. Density wake after a relativistic electron beam in low density plasma ($4 \times 10^{16} \text{ cm}^{-3}$) in RRF with $\gamma_R=10$

References

- [1]. R. Lehe, M. Kirchen, B. B. Godfrey, A. R. Maier, J.-L. Vay, *Physical Review E* **94**, 053305 (2016)
- [2]. D. O.Espinos, A. Zhidkov, A. Rondepierre, M. Tawada, M. Masuzawa, *Physical Review Accelerators and Beams*, **28**, 060702 (2025)

PROPAGATION OF A MONOENERGETIC BEAM OF RELATIVISTIC ELECTRONS IN VACUUM

D.E. Iankhotov^{1,2}, S.V. Kuznetsov¹, N.E. Andreev^{1,2}

¹*Joint Institute for High Temperatures, Russian Academy of Sciences, Moscow, Russia, E-mail: iankhotov.de@phystech.edu*

²*Moscow Institute of Physics and Technology (State University), Moscow, Russia*

The generation of high-current, highly focused relativistic electron beams has become possible thanks to the use of low-density polymer foams, which enable the generation of relativistic electrons by the interaction of an intense laser pulse with plasma at an electron density close to the critical value (n_e near 10^{21} cm⁻³ at a laser wavelength of 1 μ m). High absorption of the relativistically intense laser pulse in plasma with a density close to the critical value and efficient direct laser acceleration (DLA) of electrons in the plasma channel lead to the efficient conversion of laser energy into relativistic electron beam energy.

In high-current beams, typical of the conditions of the analyzed experiments, the transverse motion of electrons can only be described within the framework of a relativistic approach. The solution of the corresponding equations shows that the electron trajectories in the beam asymptotically approach a dependence in which the angle of inclination of the electron trajectory to the beam axis is determined solely by the initial electron energy, whereas when describing low-current beams using nonrelativistic equations, the beam dynamics are determined by both its energy and charge.

For the parameters considered, analysis shows that the electrostatic repulsion of relativistic beam electrons plays an insignificant role during their transport in the vacuum chamber. However, with increasing laser pulse energy and a proportional increase in the current carried by the electrons, the influence of the beam's electrostatic and magnetic self-action on its propagation in the vacuum chamber increases. Furthermore, with increasing beam charge, relativistic effects can influence the change in the electron concentration in the radial direction.

This paper considers an analytical model for the propagation in a vacuum of a monoenergetic homogeneous beam of relativistic electrons with an infinite longitudinal length and a finite radius of the initial distribution. The model parameters were selected from experimental work on the PHELIX laser facility [1]. The PIC modeling results for this problem formulation revealed qualitative differences from experiment: a monotonic increase in concentration with increasing beam radius was detected, which does not correspond to the experimental maximum on the axis demonstrated in the experiment. The increase in concentration toward the beam edges is due to a feature of relativistic mechanics, which postulates a limit on the speed of light. This phenomenon is considered in an analytical paper [2] using the infinitely long beam model.

By refining the initial model—removing the infinite length and considering Gaussian initial concentrations—new PIC modeling data were obtained, yielding a maximum concentration on the beam axis, which qualitatively matches experiment.

References

- [1]. Tavana P., Bukharskii N., Gyrdymov M. et. al. *Front. Phys.* 2023. Vol. 11. Art. 1178967
- [2]. Iankhotov D.E., Kuznetsov S.V., Andreev N.E. *Vestnik JIHT RAS.* 2025. V. 18. P. 32–36.

ION WEIBEL INSTABILITY DIRECTLY OBSERVED IN FEMTOSECOND LASER-PLASMA EXPANSION

A.V. Korzhimanov, R.S. Zemskov, S.E. Perevalov, A.V. Kotov, A.A. Murzanev, A.I. Korytin, K.F. Burdonov, V.N. Ginzburg, A.A. Kochetkov, S.E. Stukachev, I.V. Yakovlev, I.A. Shaikin, A.A. Kuzmin, A.A. Nechaev, V.I. Kocharovskiy, A.A. Soloviev, A.A. Shaykin, A.N. Stepanov, M.V. Starodubtsev, E.A. Khazanov

A. V. Gaponov-Grekhov Institute of Applied Physics of the Russian Academy of Sciences, Nizhny Novgorod, Russia

We present experimental results demonstrating the formation of long-lived, large-scale current filaments in a plasma generated by irradiating a solid target with a high-intensity femtosecond laser pulse (2×10^{18} W/cm²). Direct optical diagnostics, including shadowgraphy and polarimetry, reveal filaments oriented perpendicular to the target surface, extending hundreds of microns in length with a characteristic transverse spacing of 50–90 μm. Remarkably, these structures persist for up to 20 ns, significantly exceeding the typical sub-nanosecond lifetimes associated with electron-driven kinetic instabilities [1]. Simultaneous interferometric measurements show a correlated modulation in plasma density at the level of ~ 10 %, and polarimetric data indicate the presence of strong, self-generated magnetic fields on the order of 50–100 T within the filaments.

The observed filament characteristics, particularly their scale length and long lifetime, point to an ion-driven Weibel instability. The key evidence is that the filament spacing is consistent with the ion inertial length, and is orders of magnitude larger than the electron skin depth. The dynamics, including the sustained modulation up to tens of nanoseconds, are incompatible with the short-lived filaments of electron Weibel instability but are well-explained by ion Weibel instability.

The formation of these filaments is explained by a multi-stage model. First, the laser prepulse creates an extended pre-plasma. The main pulse then generates a population of fast electrons, which in turn produce strong, large-scale "fountain" magnetic fields (~ 70 T) [2]. These fields collimate the subsequent ablation flow from the target surface. This results in a supersonic plasma stream, composed of ions with a directed velocity significantly exceeding their thermal speed, expanding into a cooler, stationary pre-plasma. This configuration—counter-streaming plasma flows with a large directed velocity difference—provides the conditions for the development of the ion Weibel filamentation instability. Linear theory analysis, using parameters consistent with the experiment, yields a dominant wavelength of ~ 100 μm and a growth time of ~ 150 ps, in agreement with the observed filament scale and their early appearance.

This work provides a clear laboratory demonstration of a long-lived, ion-driven Weibel instability, directly linking its observation to a well-defined model of plasma ablation and flow. The results highlight the critical role of the ion component in sustaining magnetic field structures on nanosecond timescales. These findings have direct implications for understanding plasma dynamics in high-energy-density physics, particularly for inertial confinement fusion where such filaments can affect fast electron transport [3]. Moreover, the experimental platform offers a valuable analog for studying collisionless shock formation, magnetic field amplification, and turbulent processes in astrophysical plasmas, such as in stellar coronae and supernova remnants [4].

References

- [1]. Kocharovskiy V. V., Nechaev A. A., Garasev M. A. *Rev. Mod. Plasma Phys.* **8** 17 (2024).
- [2]. Sarri G. et al. *Physical Review Letters* **109** 205002 (2012).
- [3]. Wen H. et al. *Plasma Physics and Controlled Fusion* **61** 044007 (2019).
- [4]. Bulanov S. V. et al. *Plasma Physics Reports* **41** 1 (2015).

**ENHANCEMENT OF QUASI-STATIONARY MAGNETIC FIELDS BY
ORDERS OF MAGNITUDE VIA OPTIMIZATION OF THE PLASMA
TRANSVERSE DENSITY PROFILE IN THE REGIME OF RELATIVISTIC
SELF-CHANNELING**

V.A. Kuleshova¹, A.V. Korzhimanov²

¹*Faculty of Physics and Sarov branch, Lomonosov Moscow State University, Moscow, Russia, ya.vitalia31-01@yandex.ru*

²*Gaponov-Grekhov Institute of Applied Physics of the Russian Academy of Sciences, Nizhny Novgorod, Russian Federation*

This work investigates a novel approach to enhancing quasi-stationary magnetic fields generated via the inverse Faraday effect during the self-channeling of circularly polarized laser radiation at relativistic intensity. We generalize a previously established method [1] for constructing self-consistent, stationary, axisymmetric laser-plasma structures to the case of transversely inhomogeneous plasma density distributions. To circumvent discontinuous solutions encountered in prior work [2], we introduce a small regularization parameter with the physical meaning of temperature. This method describes filaments formed during the relativistic self-focusing of circularly polarized radiation [3,4]. Numerical modeling showed that the presence of a narrow, optimally parameterized density peak overcomes the saturation effect of the magnetic field observed in homogeneous plasma following complete channel cavitation. The peak ensures a high concentration of electrons within the region of strong laser field, leading to an increase in the induced currents. As a result, the generated axial magnetic field increases by more than an order of magnitude compared to the homogeneous case and becomes comparable in magnitude to the magnetic field of the laser wave. This opens a path toward achieving teragauss-level quasi-stationary fields at laser intensities of $\sim 10^{26}$ W/cm².

References

- [1]. Kim, A. et al. *Phys. Rev. Lett.* **89**, 095003 (2002).
- [2]. M. D. Feit, et al *Phys. Rev. E* (1998)
- [3]. Kim, A. et al. *Phys. Rev. E* **65**, 036416 (2002).
- [4]. A.V. Korzhimanov and A.V. Kim *Eur. Phys. J. D* **55**, 287–292 (2009)

LASER-DRIVEN AUTORESONANT ACCELERATION OF THERMAL ELECTRONS IN MAGNETIZED PLASMA CHANNELS

Iu.K. Gagarin¹, Ph.A. Korneev^{1,2}

¹*National Research Nuclear University MEPhI, Moscow, Russia, ikgagarin@yandex.ru*

²*Lebedev Physical Institute of the Russian Academy of Sciences, Moscow, Russia*

Rapid progress in development of laser facilities paved the way to several important fields of laser-plasma research. Particularly, charged particle acceleration schemes considering relativistic laser pulses as drivers became a promising alternative to conventional accelerators. Reaching ultrarelativistic energies of accelerated electrons stimulates further investigation of laser-based acceleration schemes, for example, such beams can be used as a secondary source of gamma radiation relevant for diagnostic purposes in medicine.

There are two basic approaches of laser acceleration referred to the mechanism of electron energy gain. The energy can be either transferred from an electric field induced in plasma with a laser or directly from the laser pulse. One of prospective schemes considering direct energy transfer is the autoresonant laser acceleration (ALA), which uses the specific resonance (autoresonance) occurring in a magnetic field aligned with the laser propagation direction. The condition for this resonance in the optical domain of the driver laser radiation requires the magnetic field amplitude of the order of 10 kT. Although creation of the magnetic field with an amplitude of this level is complicated, it may be feasible with the contemporary laser facilities [1].

The autoresonance can accelerate an electron to high energies in case of a particle interacting with a plane electromagnetic wave in a static uniform magnetic field [2-4]. However, in real conditions various inhomogeneities can break the resonance and sufficiently lower the energy of the accelerated electron [5]. To investigate the feasibility of the effective production of ultrarelativistic electron bunches in the ALA scheme numerical simulations were performed. The introduced nonidealities included an inhomogeneity of laser electromagnetic fields, occurring due to the focusing, a nonuniformity of the profile of the magnetic field and electromagnetic fields in plasma, induced by plasma collective effects.

One set of simulations was performed in the 2-dimensional (2D) geometry considering a solenoidal magnetic field. The target was chosen to be a rectangle with a density of 10^{16} cm⁻³. Electrons were initially cold, the laser pulse had a Gaussian temporal profile. Results of this set of simulations show that an ultrarelativistic electron bunch can be created in the ALA scheme with the use of a relativistic laser pulse even within a nonideal geometry. The bunch had a total charge of the order of 100 nC, which can be increased by increasing the laser intensity.

The other set of simulations was performed in the 3-dimensional geometry (3D) for the same laser parameters. The target had a cylindrical shape with the same length and a smaller transverse size, the density was of the order of 10^{19} cm⁻³. In this set of simulations electrons were hot at the initial stage. Simulations results in this case also demonstrate that an effective creation of an ultrarelativistic electron bunch is possible and effective in the ALA scheme with the use of a relativistic laser pulse.

References

- [1]. Korneev Ph., Tikhonchuk V. and d'Humières E. *New Journal of Physics* **19** (3) 033023 (2017).
- [2]. Kolomenskii A A. and Lebedev A.N. *JETP***17** (1) 179-184 (1963).
- [3]. Roberts C.S. and Buchsbaum S.J. *Phys. Rev.***135** (2A) A381-A389 (1964).
- [4]. Salamin Y. I., Faisal F. H. M. and Keitel C. H. *Phys. Rev.* **A62** 053809 (2000).
- [5]. Gagarin Iu. and Korneev Ph. *Phys. Rev. E*(2026).

ON SCALINGS OF ACCELERATION OF ELECTRONS AND GENERATION OF SHORT WAVELENGTH RADIATION IN LASER PLASMA AND SOLID TARGETS

M.E. Veysman, I.R. Umarov, N.E. Andreev

*Joint Institute for High Temperatures of the Russian Academy of Sciences, Moscow, Russia,
e-mail: bme@ihed.ras.ru*

We propose simple models for estimating the energy, spatial-angular, and spectral characteristics of electrons accelerated in long-scale laser plasmas [1, 2], as well as high-energy secondary photons generated in laser plasmas by the betatron mechanism [3] and in solid-state converters by bremsstrahlung [4]. Particularly, using these models one can estimate the number of super-ponderomotive electrons generated in near critical density plasma by direct laser acceleration mechanism, their characteristic temperature, critical frequency of betatron radiation of these electrons, total number of betatron photons and number of these photons generated per energy interval of 0.1% of bandwidth, total number and spectre of bremsstrahlung photons generated in converter metallic foil, effective temperature of the spectrum and brightness of bremsstrahlung gamma ray source and dependence of these characteristics on converter target thickness and material.

These models can be used for preliminary evaluation and optimization of the parameters of laser-accelerated electrons and their radiation in plasmas and solid-state converters. Preliminary (before the launch of respective simulations or experiments) estimate of the parameters of laser generated sources of X and gamma - ray radiation can be helpful for their optimization for applications like radiography of ultrafast process in matter at extreme states (like X-ray imaging of D-Ti inertial confinement fusion capsules) [5], generation of electron-positron pairs for experiments on laboratory astrophysics [6], generation of laser-induced nuclear reactions at quanta energies in the region of giant dipole resonance (several MeV – tens MeV) with generation of neutrons and isotopes, which can be used in medical applications [7].

References

- [1]. Veysman M.E., Popov V.S., Umarov I.R. and Andreev N.E. *Bulletin of the Lebedev Physics Institute* **52**(4), 462-473 (2025).
- [2]. Veysman M.E., Umarov I.R. and Andreev N.E., *Matter and radiation at extremes*, to be submitted (2026).
- [3]. Veysman M.E., *Physics of Plasmas* **31**, 103112 (2024).
- [4]. Veysman M.E., Umarov I.R. and Andreev N.E., *Plasma Physics and Controlled Fusion*, submitted.
- [5]. J. Kozioziemski et. al., *J. of App. Phys.* **97**, 063103 (2005).
- [6]. M. R. Stoneking, T. S. Pedersen, P. Helander et. al., *J. of Plasma Physics* **86**, 155860601 (2020).
- [7]. Z. Ma, H. Lan, W. Liu, et al., *Matter and Radiation at Extremes* **4**, 064401 (2019).

ROLE OF PLASMA WAVES IN RESCATTERING PROCESSES IN INTENSE LASER FIELDS

V. V. Strelkov¹, S. A. Bondarenko^{1,2}, I. V. Smetanin¹

¹*P.N. Lebedev Physical Institute of the Russian Academy of Sciences, Moscow, Russia;*

e-mail: v.strelkov@lebedev.ru

²*National Research Nuclear University MEPhI, Moscow, Russia*

Rescattering of the photoelectron at its parent ion underlies a number of phenomena in intense laser field interaction with matter, such as high harmonic generation, attosecond pulse production, nonsequential double ionization, and others [1]. These processes are unavoidably accompanied by the medium photoionization. The interaction of the laser pulse with the photoionization-induced plasma excites wake field plasma waves. We study theoretically the effect of the electric field of the plasma wave on the rescattering processes.

We show that the plasma wave field can compensate for the magnetic drift of the rescattering electron [2]. In the 1D approximation we derive analytical equations describing the amplitude of the plasma wave as a function of the laser pulse intensity, frequency, and duration, as well as of the plasma density. Using this result, we find conditions in which the field of the plasma wave can compensate for the rescattering electron's magnetic drift, which otherwise dramatically suppresses the rescattering efficiency in intense low-frequency laser fields [3], see the Figure. Thus, the efficiency of such rescattering processes as nonsequential double ionization or recollisional excitation can be improved under proper plasma density, providing this compensation. For the cut-off high harmonics, the required plasma density is relatively high, which might prevent the increase of the overall generation efficiency. However, for the plateau harmonics the required plasma density is closer to its typical experimental values; thus, the efficiency increase due to the compensation of the magnetic drift is feasible.

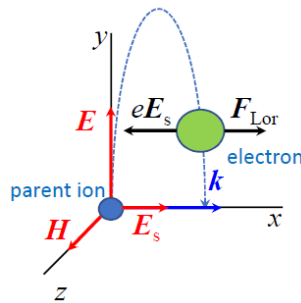


Fig. The fields of the electromagnetic wave E and H , its wavevector k , and the electric field of the plasma wave E_s . The dotted curve shows the electron's trajectory before rescattering. The Lorentz force F_{Lor} accelerates the electron in the pulse propagation direction, and the electric field of the plasma wave accelerates it in the opposite one.

Moreover, the presence of the plasma-wave field leads to new lines in the spectrum emitted due to the XUV free-induction decay (XFID). Numerically solving the time-dependent Schrödinger equation for an atom emitting XUV due to free-induction decay, we simulate the XFID process in the presence of the plasma wave. We show that this field leads to the appearance of the satellite lines near the allowed transition frequencies and also to the appearance of pairs of new lines shifted by \pm plasma frequency from the forbidden transition frequencies. Observation of these lines allows the detection of the forbidden transition frequencies, thus providing new perspectives for XFID spectroscopy.

References

- [1]. Ryabikin M. Yu., Emelin M. Yu., Strelkov V. V., *Phys. Usp.* **66** 360 (2023).
- [2]. Strelkov V. V., Bondarenko S. A., Smetanin I. V., *Phys. Rev. A* **112** 053101(2025).
- [3]. Taranukhin V. D., *Laser Phys.* **10**, 330 (2000).

TOWARDS GENERATING ELECTRON-POSITRON AVALANCHE PRE-CURSORS AT MULTI-PETAWATT LASER FACILITIES

A.A. Mironov

Center for Theoretical Physics (CPHT), CNRS, Ecole Polytechnique, Institut Polytechnique de Paris, Palaiseau, France, mironov.hep@gmail.com

Prolific avalanche-type electron-positron-photon cascades generated by ultra-high-intensity lasers are a bright theoretical prediction of strong-field QED yet to be tested experimentally, see [1] for a recent review. In this process, a focused laser field of a certain configuration accelerates injected electrons to ultra-relativistic energies at a sub-cycle time scale. Such electrons emit hard photons via the non-linear inverse Compton process, which can create secondary electron-positron pairs (non-linear Breit-Wheeler process). As the process is repeated, the cascade multiplicity grows exponentially. Among the promising field configurations that could trigger such cascades are standing waves formed by two counter-propagating laser pulses of intensity $>10^{24}$ W/cm².

The state-of-the-art value of 10^{23} W/cm² [2] is just one order of magnitude below the threshold necessary for triggering avalanche-type cascades. As next-generation facilities will be commissioned, this fundamental process will likely become observable. In this context, to plan future experiments, it is already necessary to consider setups beyond simplified toy models by using more realistic field configurations and targets for the injection of the electrons in the focus.

In this talk, we will consider such realistic scenarios based on our recent work [3]. We consider QED avalanches (or, more precisely, their precursors) triggered in the mutual focus of two counter-propagating femtosecond laser pulses of near-threshold intensity $\sim 10^{24}$ W/cm². First, we will compare the injection of initial electrons in the field by using various targets: a noble gas, plasma, and foil. Second, we will discuss the effect of the possible laser field configuration imperfections: tilting of the laser beams (required to avoid damaging the optics by back-propagation), misalignment of the beams, and the mistiming of the pulse arrival at the target. We will demonstrate that the cascade can be effectively triggered even in non-ideal conditions. Finally, we will discuss how avalanche-type cascades can be identified near the threshold by studying the final particle distributions.

References

- [1]. A. Mercuri-Baron, A.A. Mironov, C. Riconda, A. Grassi, M. Grech, *Phys. Rev. X* **15** (1), 011062, (2025).
- [2]. J. W. Yoon, Y. G. Kim, et al, *Optica* **8**, 630 (2021).
- [3]. A.A. Mironov, S.S. Bulanov, et al, *Phys. of Plasmas* **32**(9), p. 093302 (2025).

MEASURING ULTRA-STRONG FIELDS VIA PAIR PRODUCTION IN LASER PLASMA

A.A. Andreev¹, I.A. Aleksandrov²

¹*Saint Petersburg State University, Saint Petersburg, Russia, alexanderandreev72@yahoo.com*

²*Ioffe Physical Technical Institute, Saint Petersburg, Russia*

Rapid progress in high-power laser technology has intensified interest in testing quantum electrodynamics (QED) in extremely strong electromagnetic fields. Peak intensities around 10^{23} W/cm² have already been demonstrated, and forthcoming facilities are expected to surpass 10^{24} W/cm². A central experimental difficulty is determining the true peak intensity reached in the tiny focal region, where indirect estimates can be affected by uncertainties in pulse shape, focal spot structure, and shot-to-shot fluctuations. In this context, a natural alternative is to use a QED signal generated by the laser itself: in ultra-strong fields, electrons emit energetic photons, some of which convert into electron-positron pairs. Since pair production turns on in a threshold-like manner, the number of positrons provides a sensitive indicator of the laser intensity.

In this talk, we summarize our recent results on positron-based intensity diagnostics across several realistic laser-matter scenarios. In laser-foil interactions, we found that positrons are emitted within a relatively narrow angular region, which helps isolate the signal and enables an in situ diagnostic approach for petawatt-class experiments [1]. In a complementary scheme, we considered supplying seed electrons either directly (a dilute electron gas) or via ionization of a neutral xenon (Xe) gas. The laser accelerates these electrons, leading to photon emission and subsequent pair creation; by measuring the positron yield and using one-to-one correspondences between yield and intensity established for specific geometries, the peak intensity can be inferred with good precision [2]. We analyzed both a single focused pulse and a configuration with two counter-propagating pulses, demonstrating a broad operating window extending up to very high intensities [2].

We also discuss two effects that extend the reach and reliability of the method. First, at extreme intensities, positron production can become more prolific through QED cascades, where newly created particles generate additional photons and pairs. Our simulations show that near the threshold, cascade contributions remain modest, leaving a sizable region in which positron counting is straightforward and particularly accurate [3]. Moreover, changing the geometry of the setup shifts the effective threshold, allowing the diagnostic sensitivity to be optimized for a given intensity range [3]. Second, we review how an additional magnetic field can enhance positron production in Xe targets. Magnetic fields comparable in scale to the laser field can arise in relevant high-energy-density conditions and can substantially increase the positron yield by altering particle motion in a way that favors the underlying QED processes, strengthening the measurable signal and broadening practical applicability [4].

Overall, these results support an efficient route to measuring peak laser intensity—from currently accessible conditions to super-intense regimes—using positron yields in experimentally feasible configurations [1–4].

References

- [1]. LécZ Zs., Andreev A.A., *Laser Phys. Lett.* **17**, 056101 (2020).
- [2]. Aleksandrov I.A., Andreev A.A., *Phys. Rev. A* **104**, 052801 (2021).
- [3]. Aleksandrov I.A., Andreev A.A., *Phys. Rev. A* **110**, 013111 (2024).
- [4]. Aleksandrov I.A., Andreev A.A., *Phys. Rev. A* **112**, 043122 (2025).

ACCELERATION/DECELERATION OF ATOMS BY CIRCULARLY POLARIZED LASER PULSES

V.S. Melezhik

*Joint Institute for Nuclear Research, Dubna, Moscow Region, Russia,
 melezhik@theor.jinr.ru*

We discuss the m-photon resonance mechanism proposed in our recent work [1]

$$H_{n=1} + m(\hbar\omega) \rightarrow H_{n'}, \quad m(\hbar\omega) = 1/(2n) - 1/(2n')$$

for twisting atoms by a circularly polarized laser pulse with the transfer of photon helicity to them. It is shown that when interacting with a circularly right-polarized electromagnetic pulse, the atom accelerates/ decelerates and twists - it acquires an orbital momentum with a projection $L_z = m\hbar$ on the direction of its motion (see Fig. 1). The proposed method of twisting atoms opens up new possibilities here compared to traditional methods using fork-shaped diffraction gratings developed for elementary particles (photons and electrons), but requiring significant modifications for twisting composite particles (protons, neutrons and atoms). In this regard, it should be noted that, despite the almost thirty-year history of experimental studies of twisted photons and electrons, obtaining twisted atoms represents a difficult experimental task. So far, only one experiment has been carried out in which twisted helium atoms were obtained using a specially designed diffraction grating [2].

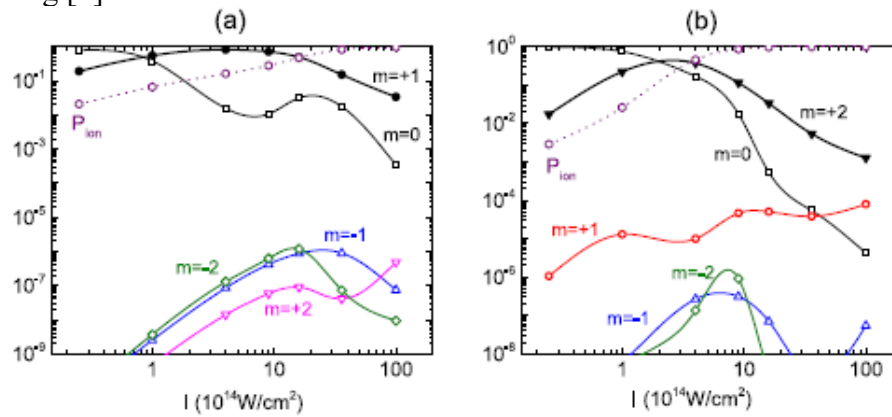


Fig. 1. Calculated dependences on the intensity (I) and laser frequency (ω) of the populations $P_m(I, \omega)$ of states with a fixed value $m\hbar$ of the projection of the orbital momentum of the hydrogen atom on the direction of propagation of the laser pulse after the interaction of the atom with circularly right-handed polarized laser radiation of duration 8 fs.

The calculation was performed for two resonant frequencies $\omega = 0.48$ a.u. (a) and 0.24 a.u. (b) [1]. The calculated probabilities of the competing ionization process of the atom $P_{ion}(I, \omega)$ are also given.

References

- [1]. Melezhik V.S., Shadmehri S. *J. Chem. Phys.* **162**, 174304 (2025).
- [2]. Luski A. et.al. *Science* **373**, 1105 (2021).

RELATIVISTIC TUNNEL IONIZATION OF HIGHLY CHARGED IONS BY LASER RADIATION OF EXTREME INTENSITY

D.D. Baranov, S.V. Popruzhenko

*National Research Nuclear University MEPhI (Moscow Engineering Physics Institute),
Moscow, Russia, ejineAMS@gmail.com*

The production of laser pulses with multi-petawatt power opens up broad prospects for studying the fundamental effects of the interaction of electromagnetic fields of extreme intensity with matter and vacuum [1,2]. The possibility of observing nonlinear phenomena of classical and quantum electrodynamics during such interaction is determined mainly by the peak radiation intensity achieved at the center of the laser focus. Currently, according to [3], the maximum intensity value is at the level of 10^{23} W/cm^2 . With the expected transition of power to the sub-exawatt regime in the next decade [4], intensities of the order of 10^{25} W/cm^2 can be achieved. In fields of such intensity, deep ionization of multi-electron atoms will be observed, leading to the formation of ions with a charge of $Z = 50$ and more. At high intensities of laser radiation in the infrared wavelength range, the dynamics of atomic ionization is close to tunneling in a constant field [5]. The relativistic theory of tunnel ionization in an ultra-strong electromagnetic field was developed in detail in [6], where it was assumed that the electric and magnetic field vectors are perpendicular, but can be different in magnitude. The case of parallel fields was also considered. However, obtaining ultra-high intensities is possible only with very tight focusing of the laser beam, at the level of the diffraction limit. In this case, the fields at the focus are not orthogonal and unequal in magnitude. To describe the relativistic ionization of deep atomic levels in such fields, the results obtained in [5, 6] require generalization.

In this paper, we present a generalization of semiclassical formulas for the relativistic ionization rate of an atomic level in a constant electromagnetic field [6] to the case where the spatial configuration of this field is arbitrary. The calculations utilize the imaginary time method [5], determining electron trajectories with appropriate initial conditions. Furthermore, using perturbation theory, the Coulomb correction due to the interaction of the electron with the atomic core is determined, and the spin factor averaged over the projection of the electron spin onto the direction of the external magnetic field is found. The obtained formulas are used to calculate the ionization probability of the hydrogen-like ion Rn^{85+} by a laser pulse with a duration of $T = 30 \text{ fs}$ and a peak intensity of $3.6 \times 10^{25} \text{ W/cm}^2$. The results demonstrate probability suppression with increasing magnetic and electric field strength ratio H/E , with the exception of the case of parallel fields, which is associated with the elongation of the subbarrier trajectory.

The obtained equations make it possible to find the formation rate of highly charged ions in an ultra-strong, tightly focused laser field and the photoelectron momentum distribution. The results allow us to estimate the contribution of relativistic effects to subbarrier dynamics and are of interest for the diagnostics of high-power laser beams and laser plasma physics.

References

- [1]. Popruzhenko S. V., Fedotov A. M. *Uspekhi Fizicheskikh Nauk* **193** (5): 491-527 (2023).
- [2]. Fedotov A. M., et al. *Physics Reports* **1010**: 1-138 (2023).
- [3]. Yoon J. W., et al. *Optica* **8** (5): 630-635 (2021).
- [4]. Bashinov A. V., et al. *The European Physical Journal Special Topics* **223** (6): 1105-1112 (2014).
- [5]. Popov V. S. *Uspekhi Fizicheskikh Nauk* **174** (9): 921-951 (2004).
- [6]. Mur V. D., Karnakov B. M., and Popov V. S. *Journal of Experimental and Theoretical Physics* **87** (3): 433-444 (1998).

RADIATION OF RELATIVISTIC ELECTRONS CREATED IN TUNNEL IONIZATION OF ATOMIC GASES BY LASER BEAMS OF EXTREME INTENSITY

N.V. Makarenko¹, S.V. Popruzhenko^{1,2}

¹*National Research Nuclear University MEPhI, Kashirskoeshosse 31, 115409, Moscow, Russia*

²*Institute of Applied Physics RAS, Ulyanova 46, 603950, Nizhny Novgorod, Russia*

Recent development of the new generation of femtosecond laser sources with peak power in the interval 1-10 petawatts (PW) has opened a way to systematic laboratory studies of laser-matter interactions at intensities 10^{22} W/cm² and higher. The field strength and its distribution inside the laser focus are key characteristics that determine the probabilities of nonlinear effects of classical and quantum electrodynamics, so that reliable diagnostics of such extremely strong electromagnetic fields is a key technology for upcoming experiments.

One of the proposed methods for measuring the peak laser intensity is based on the observation of tunneling ionization of heavy atoms [1]. In this contribution, we consider the process directly connected with ionization: electrons liberated from ions through tunnel ionization will be accelerated by the same electromagnetic field, which caused the ionization process, and emit radiation predominantly in the direction of the laser pulse propagation. The spectral-angular distribution of this radiation depends both on the peak intensity of the laser and on its distribution inside the focus, which provides an additional tool for analyzing the structure of the electromagnetic field. However, radiation of relativistic particles in the field of an external electromagnetic wave is strongly suppressed during co-propagating motion [2], as a result, even in a laser focus with a peak intensity of $\approx 10^{22}$ W/cm², the tunnel-injected electrons emit, before leaving the strong field region, only several high-frequency photons. A relatively weak counter-propagating probe pulse is needed to enhance the signal and make it useful for analysis of the focal volume field distribution.

The initial conditions for the classical trajectories of photoelectrons are determined by the instants of ionization, which are randomly set for an ensemble of 10^2 argon Ar⁸⁺ ions distributed in a laser focus. The rate of tunnel ionization is calculated using the Perelomov-Popov-Terentyev formula [3]. The electrons are accelerated by the main laser pulse to Lorentz-factors $\gamma \sim 10^2 - 10^3$ and collide with a counter-propagating weakly focused probe pulse of intensity 10^{18} W/cm². The wavelength of both pulses is 1 μ m. The main pulse is a Gaussian beam with the waist radius $w_0 = 3 \mu$ m. To calculate the spectral-angular distribution of radiation in a weakly focused probe pulse, we used the plane wave approximation and adapted the results of [4].

Our results show that the angular distribution of radiation has the form of a cone with the angle depending on the intensity of the main laser beam. The wave vectors of the emitted photons are concentrated in a small range of angles near the cone surface, which is a consequence of the specific form of photoelectron trajectories, which all start with zero velocity inside the laser focus and leave the strong field region mainly through its front surface. The total radiated energy and its spectral distribution appear sensitive to the peak intensity of the main beam. Results presented in this contribution are based on our recent publication [5].

This work was supported by the Russian Science Foundation through Grant No.25-22-00308 and the Basis foundation.

References

- [1]. Ciappina M., Popruzhenko S., et al., *Phys. Rev.* **A99**, 043405 (2019).
- [2]. Landau L. D., Lifshits E. M., *Theoretical Physics. Field Theory*, *M. Nauka* (1988).
- [3]. Popov V. S., *Phys. Usp.* **47**, 855 (2004).
- [4]. Sarachik E. and Schappert G., *Phys. Rev.* **D1**, 2738 (1970).
- [5]. Makarenko N. V., Popruzhenko S. V., *arXiv:2602.04835* (2026).

PLASMA SPECTRUM SIMULATION: INFLUENCE OF EQUILIBRIUM PLASMA COMPOSITION AND LOWERING OF IONIZATION POTENTIALS

M. Kuzmanović, M. Ristić, N. Krstevski

Faculty of Physical Chemistry, University of Belgrade, Studentski Trg 12-16, Belgrade, Serbia, miroslav@ffh.bg.ac.rs

Software applications for simulating spectrum of a plasma, for a given composition, pressure, and temperature, are a very useful tool in optical spectroscopy. One widely used application is the NIST LIBS Database written by Kramida et al [1]. An important drawback of the NIST LIBS application is that, in addition to the initial composition, it has temperature (T) and electron number density (Ne) as independent inputs. However, for a given initial composition and T, Ne is not an independent variable, but has exactly one possible value [2]. Another drawback is not taking the ionization potentials lowering (IPL) into account [3] when calculating partition functions [4,5]. As can be seen in Figure 1.a), the value of IPL is not negligible in the temperature range of interest for LIBS (Laser Induced Breakdown Spectroscopy). The influence of IPL on the value of the partition function for some elements cannot be neglected either, Figure 1. b). IPL and its influence on partition functions must be taken into account when calculating plasma composition, in plasma diagnostics and calibration-free methods. We have developed an application that has all the functionality of the NIST LIBS Database, with the exception that the application itself calculates the equilibrium plasma composition, including Ne, then the reduction of the ionization potential and the influence of IPL on the values of the partition functions.

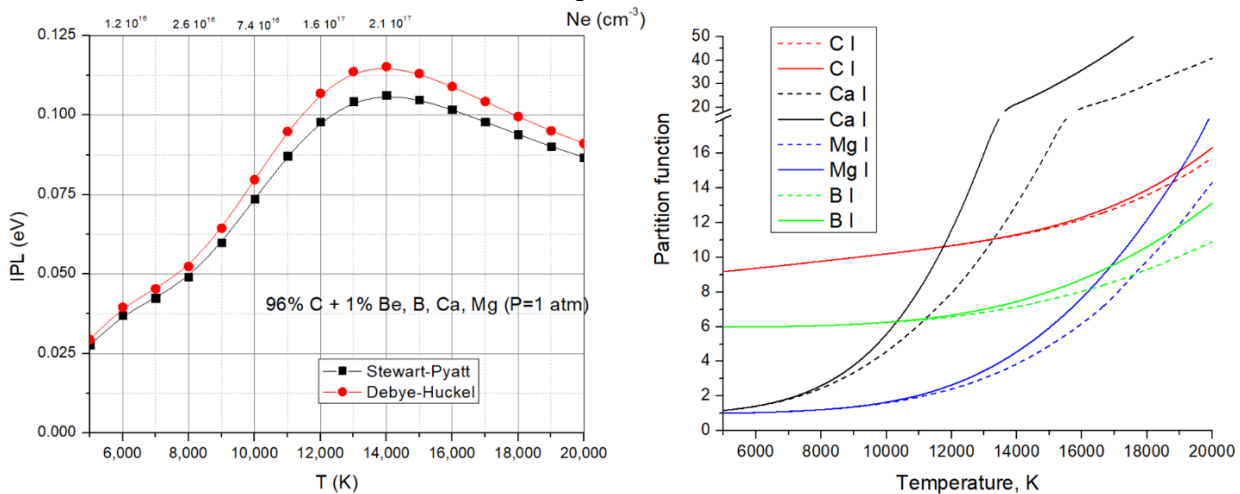


Fig. 1. a) Lowering of ionization energy for graphite plasma with impurities for two LIP models b) Influence LIP on partition functions for several elements (solid line – no LIP, dashed line – with LIP)

References

- [1]. Kramida A., Ralchenko Y., Reader J., and NIST ASD Team, NIST Atomic Spectra Database (version 5.12), National Institute of Standards and Technology, Gaithersburg, MD (2024).
- [2]. Семенова ОП, Изв. вузов. Физика. **1** (1958) 95
- [3]. Ciricosta O., Vinko SM., Chung HK., Jackson C., Lee RW., Preston TR., Rackstraw DS., Wark JS. *Phys. Plasmas* **23** 022707 (2016).
- [4]. Ristić M., Krstevski N., Ranković D., Marković M., Šajić A., and Kuzmanović M. *Plasma Phys. Control. Fusion* **66** 125014 (2024).
- [5]. Alimohamadi P., Ferland G.J. *Publ. Astron. Soc. Pac.* **134**:073001 (2022).

EXPERIMENTAL INVESTIGATION OF ⁸³KR ISOMERIC STATES POPULATION IN FEMTOSECOND LASER PLASMA

S.N. Ryazantsev, S.S. Makarov, I.Yu. Skobelev

*National Research Nuclear University MEPhI (Moscow Engineering Physics Institute),
Moscow, Russia, SNRyazantsev@mephi.ru*

*Joint Institute for High Temperatures of the Russian Academy of Sciences (JIHT RAS),
Moscow, Russia, ryazantsev@ihed.ras.ru*

Currently, krypton is usually irradiated with a beam of accelerated protons to obtain the nuclear isomer ^{83m}Kr. The nuclear reaction produces the radioactive isotope rubidium-83, which has a half-life of about 86 days and decays by electron capture into the krypton nuclear isomer states. The report is devoted to the results of experiments on the implementation of an alternative method for obtaining this isomer: the interaction of a relativistic-intensity laser pulse with a gas cluster jet of krypton. Pioneering work in this direction is [1], which demonstrates that irradiation with a femtosecond laser pulse of petawatt power ($E = 3.6$ J, $\tau = 30$ fs, $I = 1E19$ W/cm²) of a krypton gas cluster flow leads to the population (via the Coulomb excitation mechanism) of the ^{83m}Kr₂ isomeric state with an energy of 41.6 keV with an efficiency of 5.04E14 particles/second. This value is significantly higher than the values characteristic of classical methods. It is extremely important in the context of implementing the concept of γ -lasers, as well as for studying the mechanisms of nuclear excitation in general.

The methodology used to conduct the experiment that yielded this result involves collecting laser-irradiated gas containing nuclear isomers into a separate volume using a pumping system with a nitrogen trap. This approach is possible due to the long half-life ($T_{1/2} = 1.86$ hours) of the ^{83m}Kr₂ state and allows the radiation emitted from the trap to be unambiguously associated with the decay of the investigated state. On the other hand, this approach is not applicable for determining the efficiency of population of the short-lived ($T_{1/2} = 156.94$ ns) ^{83m}Kr₁ state. In this regard, the radiation associated with the decay of this state must be recorded directly from the interaction region. The report discusses the results of experiments in which a crystal spectrometer with a spherically curved α -quartz crystal was used as a dispersing element for this purpose. Based on the analysis of the recorded data, it is demonstrated that during a single interaction of a laser pulse ($E = 2$ J, $\tau = 25$ fs, $I \sim 1E20$ W/cm²) with a gas cluster flow from the focusing region, $\sim 8.3E8$ photons with an energy of ~ 9.4 keV are emitted. Assuming that the registered signal is the result of the radioactive decay of the ^{83m}Kr₁ state and considering the internal conversion coefficient $\alpha = 20$ [2], such a number of photons can be observed if $\sim 1E10$ nuclei of the ⁸³Kr isotope were transferred to this state in the interaction region. This result is in good agreement with the estimates of the population of the ^{83m}Kr₁ state given in [1].

References

- [1]. Jie Feng, Wenzhao Wang, Changbo Fu et al. *Phys. Rev. Lett.* **128**: 052501 (2022).
- [2]. Kolk B., Pleiter F., Heeringa W., *Nucl. Phys. A.* **194**(3): 614-624 (1972).

CALCULATION OF THE GENERATION OF KR NUCLEAR ISOMERS IN THE INTERACTION OF HIGH-POWER LASER PULSES WITH A GAS CLUSTER JET

M.V. Sedov^{1,2}, I.Yu. Scobelev^{1,2}

¹*Joint Institute for High Temperatures of the Russian Academy of Sciences (JIHT RAS),
Izhorskaya st. 13 Bd.2, 125412 Moscow, Russia;*

²*National Research Nuclear University MEPhI (Moscow Engineering Physics Institute),
Kashirskoe Shosse 31, 115409 Moscow, Russia;*

Nuclear isomers are metastable (lifetime ≥ 0.1 ms) excited states of the atomic nucleus. Isomeric states are typically observed when a low-lying excited state near the ground state of the nucleus differs significantly from the ground state in spin. Nuclear isomers are currently being actively studied within the framework of nuclear astrophysics. They are also considered promising for use in nuclear batteries, nuclear lasers, and nuclear clocks.

In this paper, we consider the nuclear isomer ^{83m}Kr . It is widely used for the precise calibration of various detectors. In particular, it has served for several decades as a calibration source in experiments to determine the mass of neutrinos. The production of nuclear isomers using high-power laser radiation is currently being studied intensively, both experimentally and theoretically. It was shown in [1] that Coulomb excitation (QE) is the main mechanism for the excitation of Kr nuclear isomers by laser-accelerated electrons.

To study the interaction of femtosecond laser pulse with gas-cluster jet we used 3d particle-in-cell code EPOCH [2]. The simulation parameters were the following: a femtosecond laser pulse was focused into a Kr gas-cluster jet. In simulations we used single cluster approximation. The results for one cluster were then scaled to the entire focal volume. We calculated the number of nuclear isomers in two stages. In the first, using the results from PIC calculation and the $\sigma E\lambda$ cross-section from [3], we can calculate the number of isomers produced by irradiating a single cluster with an intense femtosecond laser pulse. Then, to study the further evolution of the electron distribution function and the generation of nuclear isomers we have written a simple program that calculates how electrons lose energy when passing through a gas-cluster jet. We considered a rather low-density gas jet, so particle scattering could be neglected in the first approximation. We used the principle of continuous deceleration. The calculation results were verified by comparison with known experimental data. These results will be used to plan future experiments to study the behavior of krypton nuclear isomers when irradiated with intense laser radiation.

References

- [1]. J. Feng, W. Wang, C. Fu, L. Chen, J. Tan, Y. Li, J. Wang, Y. Li, G. Zhang, Y. Ma, et al., ‘Femtosecond Pumping of Nuclear Isomeric States by the Coulomb Collision of Ions with Quivering Electrons’, *Phys. Rev. Lett.*, vol. 128, no. 5, p. 052501, Jan. 2022,
- [2]. T. D. Arber, K. Bennett, C. S. Brady, A. Lawrence-Douglas, M. G. Ramsay, N. J. Sircombe, P. Gillies, R. G. Evans, H. Schmitz, A. R. Bell, et al., ‘Contemporary particle-in-cell approach to laser-plasma modelling’, *Plasma Phys. Control. Fusion*, vol. 57, no. 11, p. 113001, Nov. 2015
- [3]. J. Feng, J. Qi, H. Zhang, S. Chen, M. Zhu, X. Hu, H. Xu, C. Fu, X. Wang, L. Chen, et al., ‘Laser-based approach to measure small nuclear cross sections in plasma’, *Proc. Natl. Acad. Sci.*, vol. 121, no. 47, Nov. 2024

**OBSERVATION AND INTERPRETATION OF X-RAY EMISSION SPECTRA OF
LASER PLASMA OF KRYPTON CLUSTERS**

R.K. Kulikov^{1,2}, S.S. Makarov^{1,2}, S.N. Ryazantsev^{1,2}, I.Yu. Skobelev^{1,2}

¹*National Research Nuclear University MEPhI, Moscow, Russia*

²*Joint Institute for High Temperatures of the Russian Academy of Sciences, Moscow, Russia*

The analysis of the time-integrated spectra of krypton plasma from cluster targets containing lines of the Ne-like Kr XXVII ion is presented. Based on a simple model of plasma expansion, detailed time-dependent kinetic calculations were performed and the plasma parameters corresponding to quasi-stationary expansion were determined.

DIAGNOSTICS OF PREPLASMA PROFILES WITH REFLECTION SPECTRA OF A RELATIVISTICALLY-INTENSE FEMTOSECOND LASER PULSE

A.R. Poletaeva¹, N.D. Bukharskii^{1,2}, Ph.A. Korneev^{1,2}, I.P. Tsygvintsev³

¹*National Research Nuclear University MEPhI, Moscow, Russia, e-mail: anro.poletaeva@gmail.com*

²*P. N. Lebedev Physical Institute, Moscow, Russia*

³*KIAM RAS, Moscow, Russia*

In ultra-high-intensity (petawatt-level) laser facilities, the concepts of the prepulse and contrast are critical parameters that determine the outcome of experiments on laser-matter interaction. A prepulse is a part of laser radiation with moderate intensity and a characteristic duration up to a few nanoseconds that arrives at the target before the main relativistically intense ultrashort laser pulse. The preplasma generated as a result of the prepulse action on the target defines the subsequent physics as it significantly influences the interaction of the femtosecond high-intensity laser pulse with the target. Therefore, it is important to account for this effect when planning and analyzing the experiments [1].

In this work, a possibility of the characterization of the preplasma profile is considered on the basis of the analysis of the spectral properties of a reflected relativistically-intense fs laser pulse. As this profile is formed with the prepulse action on the target, the contrast (the ratio of the peak intensity of the main pulse to the intensity of the prepulse $C = I_{\text{prepulse}} / I_{\text{peak}}$) may be estimated on the next step. The generated harmonics of the fs laser pulse at the fundamental laser frequency result from the strongly nonlinear interaction near the target surface, where the preplasma is formed. To demonstrate the method, hydrodynamic and kinetic simulations were performed for a laser pulse irradiating a metal target at a 45-degree angle, with a peak intensity of the main pulse of $5 \cdot 10^{21}$ W/cm², 32 fs (FWHM) and the wavelength $\lambda = 805$ nm, the interaction parameters were similar to that used in Ref. [2].

Three-dimensional numerical simulations of the nanosecond-duration prepulse interacting with the target were conducted using the 3DLINER radiation-hydrodynamics code [3] for several values of C in the range ($10^{-11} \dots 3 \cdot 10^{-9}$). Thermodynamical parameters as functions of density and temperature were calculated via the FEOS code [4, 5]. The thermal radiation transport coefficients were calculated using the collisional-radiative model by the THERMOS code [6]. The results from these hydrodynamic calculations were used as input for the kinetic simulations.

Kinetic simulations of the interaction of the main pulse with the target and the formed preplasma were carried out using the PIC code Smilei [7] in Cartesian 2D geometry. To determine an amount of the reflected energy at different harmonics, at each time step electromagnetic field values were recorded at the boundaries of the simulation domain through which the radiation exited. Based on this data, the Fourier analysis of the reflected spectrum was performed.

As a result of the numerical simulations, angular distributions of the target spectral reflectivity in dependence on the parameter C in the considered range were calculated. The most robust dependences with respect to the simulation and interaction parameters were obtained for the back-reflection at the fundamental frequency. It is mostly defined by the shape of the cavity formed in the target by the prepulse, which reflects and focuses incident laser radiation. With the analysis of reflectivity at other frequencies (2ω , 3ω), the contrast value estimations may be refined, providing a possibility for a qualitative assessment of the preplasma parameters and a contrast in realistic experimental conditions.

References

- [1]. Ivanov K. A., Shulyapov S. A., Gorlova D. A., Mordvintsev I. M., Tsybalov I. N., and Savel'ev A. B. *Quantum Electronics* 51 (9) 768-794 (2021).
- [2]. Kiriyama H., Pirozhkov A. S., Nishiuchi M., Fukuda Y., Ogura K., Sagisaka A., et al. *Optics Letters* 43 (11) 2595-2598 (2018).
- [3]. Krukovskiy A. Yu., Novikov V. G., and Tsygvintsev I. P. *Mathematical Models and Computer Simulations* 9 (1) 48-59 (2017).
- [4]. Faik S., Tauschwitz A., and Iosilevskiy I. *Computer Physics Communications* 227 117-125 (2018).
- [5]. Kemp A. J. and Meyer-ter-Vehn J. *Nuc. Instr. and Methods in Physics Research* 415 (3) 674-676 (1998).
- [6]. Vichev I. Y., Solomyannaya A. D., Grushin A. S., and Kim D. A. *High Energy Density Physics* 33 100713 (2019).
- [7]. Derouillat J., Beck A., Perez F., et al. *Computer Physics Communications* 222 351-373 (2018).

PLASMODYNAMIC ESTIMATION OF A MULTILAYER TARGET UNDER THE INFLUENCE OF EXTERNAL WIDE BAND RADIATION

V.V. Kuzenov, A.G. Polyanskiy, S.V. Ryzhkov

Bauman Moscow State Technical University (BMSTU), Moscow Russia, artgpol@mail.ru

The paper investigates the currents of an intensely radiating plasma accumulating on the geometric axis in the presence of heat and mass transfer, electromagnetic fields and nuclear reactions exposed to external wide band radiation [1-5]. A pulsed radiation source is a system of conical cavities located in a solid high-density material. Each conical cavity (exposed to external laser radiation) is filled with deuterium gas or its mixture with tritium. The gas is held by a flat thin-walled or convex shell. In the process of interacting with a concentrated stream of energy (laser beams), the shell moves inside the cavity at supersonic speed, compressing and heating the mixture. Plasma compression in conical part of a pulsed radiation source can lead to the formation of intense wide band radiation directed along its axis of symmetry [6-11].

Simulation has been performed that take into account a wide range of physical effects and plasmodynamic parameters of a multilayer cylindrical target when exposed to wide band radiation. The main stages of target compression are analyzed and it is shown that the temperature of the central part of the target can reach $T > 250$ millionK. At certain points in time, the qualitative behavior of electron and ion temperatures in the transition region near the shock wave front is described. The number of neutrons per unit length at the time of exposure termination is calculated.

This research has been supported by the Ministry of the Science and Higher Education of the Russian Federation (Russian Minobrnauki), Project No. FSN-2024-0022.

References

- [1]. Chirkov A. Yu., Ryzhkov S. V. *Physics of Atomic Nuclei* 81, 1432-1440 (2018), doi: 10.1134/S1063778818100058
- [2]. Kuzenov V. V., Varaksin A. Yu., Ryzhkov S. V. *Symmetry* 16, 1200 (2024), doi: 10.3390/sym16091200.
- [3]. Polyanskiy A. G., Ryzhkov S. V. *AIP Conference Proceedings* 3177, 060005 (2025), doi: 10.1063/5.0295139.
- [4]. Kuzenov V. V., Ryzhkov S. V., Polyanskiy A.G. *Applied Sciences*, 15 (20), 11155 (2025), doi: 10.3390/app152011155.
- [5]. Kuzenov V. V., Ryzhkov S. V. *Fusion Science and Technology* 81, 789-799 (2025). doi: 10.1080/15361055.2025.2512616.
- [6]. Kuzenov V. V., Ryzhkov S. V., Varaksin A. Yu. *Journal of Computational and Applied Mathematics* 451: 116098 (2024).
- [7]. Varaksin A. Yu., Ryzhkov S. V. *Mathematics* 11: 3293 (2023).
- [8]. Kuzenov V. V., Ryzhkov S. V. *Technical Physics* (2025), doi: 10.1134/S1063784225700392.
- [9]. Varaksin A. Yu., Ryzhkov S. V. *Aerospace* 12: 894 (2025).
- [10]. Kuzenov V. V., Varaksin A. Yu., Ryzhkov S. V. *Symmetry* 16: 1200 (2024).
- [11]. Polyanskiy A.G. *Heat Transfer Research*, 56, 73-89 (2025).

**THE IMPACTING LASER RADIATION DIFFRACTION INFLUENCE ON
PHOTOEMISSION OF ELECTRONS FROM A METAL NEEDLE**

A.V. Borovskiy ¹, A.L. Galkin ²

¹*Baikal State University, 664003 Irkutsk, Lenin st., 11. Russia andrei-borovskii@mail.ru*

²*Prokhorov General Physics Institute, Russian Academy of Sciences, 119991 Moscow, Vavilov st., 38, Russia galkin@kapella.gpi.ru*

For the problem of generating ultrashort electron pulses using an emitter in the form of a sharp metal tip irradiated by femtosecond laser radiation, the influence of diffraction is investigated in relation to experiments [1,2].

In a model of plane wave diffraction by a two-dimensional wedge tip [3], the position of the incident wave intensity maxima on the tip surface is determined and the spatial distribution of the total (incident and reflected) TE (Fig. 1) and TH waves is constructed.

The nonrelativistic motion of a test electron in a diffraction field under the action of a ponderomotive force and taking into account an applied voltage is considered.

The emergence of high- and low-energy parts of the electron spectrum and the saturation of the emitted charge by the laser pulse energy is discussed.

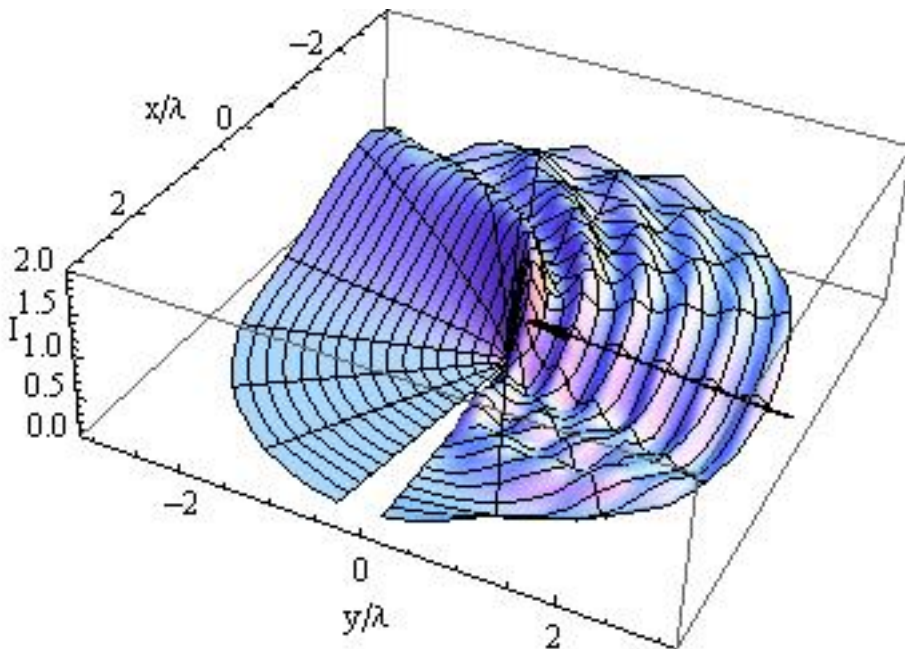


Fig. 1. Two-dimensional distribution of relative intensity in the TE wave

References

- [1]. Abramovsky N. A., et al. High Temperature, 58(6) 938-941 (2020).
- [2]. Ovchinnikov A.V., et al. High Temperature, 60(1) 16-19 (2023).
- [3]. Borovskiy A. V., Galkin A. L., Selected Problems of Laser Physics. Vacuum
- [4]. Acceleration of Electrons. Focusing by a Parabolic Mirror. Diffraction on a Wedge as a
- [5]. Problem of Subwavelength Physics, Palmarium Acad. Publ., Saarbrucken, Deutschland 267(2016).

CONTROL OF ELECTROMAGNETIC CHARACTERISTICS OF SEMICONDUCTOR AND NANOCOMPOSITE STRUCTURES USING PLASMAS OF THEIR OWN FREE CHARGE CARRIERS

V. Yu. Timoshenko^{1,2}

¹*Lomonosov Moscow State University, Faculty of Physics, Leninskie Gory 1, Bldg.2, 119991 Moscow, Russia*

²*Lebedev Physical Institute of the Russian Academy of Sciences., Leninskiy Prospekt 53, 119991 Moscow, Russia*

Nanostructured semiconductors, plasmonic metals and semiconductor/metal nanocomposites are extensively studied for numerous applications in industrial technologies and biomedicine. Semiconductor nanostructures from silicon (Si) are especially interesting for biomedical purposes because they are biocompatible, biodegradable and can be easily prepared by electrochemical and laser-plasma assisted methods [1,2]. On the one hand, nanocrystalline Si nanoparticles (NPs) and nanowires (NWs) exhibit efficient photoluminescence (PL), Raman scattering and optical nonlinearities, which can be used themselves for photonics and bioimaging by means of the linear and nonlinear optics [2,3]. On the other hand, the optical properties of Si-based NWs, porous films and other nanostructures are controlled by mobile free charge carriers (electrons and holes) that opens up new promising opportunities for the development of ultrafast optical devices as switches and modulators for processing electromagnetic signals in Si-based photonics [4]. Moreover, Si-NPs and nanocomposite Si/gold-NPs can act as efficient light absorbers in the visible and near-infrared spectral regions that determines their high potential for photohyperthermia applications in biomedicine [5,6].

Sensor properties of Si-based NW structures can be significantly improved by plasmonic metal NPs, which are deposited on their surfaces. Arrays of Si NWs decorated with gold (Au) NPs [7] and zinc oxide (ZnO) nanorods (NRs) with deposited silver (Ag) NPs [8] have been successfully tested for ultrasensitive molecular recognition by means of the surface-enhanced Raman scattering (SERS). Numerical simulations of the light scattering in ZnO-NRs/Ag-NPs structures reveal the role of the wedge-like morphology of ZnO-NRs in the 3D electromagnetic enhancement of the SERS signal up to $3 \cdot 10^8$ for the optimized nanostructure morphology and desired analyte concentration [8]. The electric field of a light wave in an array of Si NWs with attached Au-NPs is found to be significantly enhanced because of the combined contribution of the enhancement of the local electric fields due to Mie scattering on Si NWs and the localized surface plasmon resonance in Au-NPs [9].

Thus, the high SERS activity of hybrid semiconductor/plasmonic metal nanostructures combined with the simplicity and flexibility of preparation methods open new prospects for their applications in molecular sensorics and photonics.

References

- [1]. Timoshenko V. Yu. In “*Handbook of Porous Silicon*”, Springer, 2018, 1461-1469.
- [2]. Kabishan A. V., Timoshenko V. Yu. *Nanomedicine* **11**, 2247-2250 (2016).
- [3]. Kharin A. Yu. et al. *Adv. Opt. Mat.* **7**, 1801728 (2019).
- [4]. Deng Y. et al. *Appl. Phys. A* **130**, 809 (2024).
- [5]. Oleshchenko V. A. et al. *Appl. Surf. Sci.* **516**, 145661 (2020).
- [6]. Kondakova A. V. et al. *Nanoscale* **18**, 3181-3193 (2026).
- [7]. Ikramova S. B. et al. *Int. J. Mol. Sci.* **23**, 259 (2022).
- [8]. Kapitanova O. O. et al 2025 *Nanotechnology* **36** 375702 (2025).
- [9]. Kornilova A. V. et al. *Bull. Lebedev Phys. Inst.* **52**, S726–S734 (2025).

EFFECT OF FREE CHARGE CARRIER PLASMA IN ANISOTROPIC SILICON NANOSTRUCTURES ON THEIR OPTICAL PROPERTIES

Y. Deng, A.V. Ikonnikov, V. Yu. Timoshenko

Faculty of Physics, Lomonosov Moscow State University, Leninskie Gory, Moscow 119991, Russian Federation, yingying.d@outlook.com

It is well known that porous silicon (PSi) can exhibit strong optical birefringence due to the shape anisotropy of its nanostructures, resulting in different refractive indices for orthogonal linear polarizations. Owing to this property, PSi has attracted considerable interest for photonic applications such as optical filters, detectors, and sensors [1–3]. Beyond geometrical anisotropy, the optical anisotropy of PSi is strongly affected by mobile free charge carriers (FC) in silicon (Si) crystallites. Their concentration can be widely tuned by doping, molecular adsorption, or photoexcitation, enabling active control of optical anisotropy via FC plasma effects. This work investigates the combined influence of shape anisotropy and FC plasma on the optical properties of anisotropic PSi nanostructures.

PSi layers are modeled as a composite medium composed of anisotropic crystalline Si ellipsoids separated by voids (Fig. 1). The complex permittivity is calculated using the Bruggeman effective medium approximation incorporating FC effects via the Drude model [4]. The simulations show that multipath interference and FC absorption are essential for accurately describing reflectance and transmittance. Increasing the FC concentration in Si nanocrystals to $(1 \div 5) \times 10^{19} \text{ cm}^{-3}$ results in a pronounced enhancement of polarization-dependent transmittance and reflectance, indicating increased birefringence and linear dichroism. The simulated transmittance spectra and birefringence are in good agreement with experimental infrared measurements on anisotropic PSi films fabricated by electrochemical etching of heavily boron-doped (110)-oriented crystalline Si substrates.

In conclusion, FC plasma plays a decisive role in tailoring the optical anisotropy of PSi nanostructures. The combination of shape anisotropy and controlled carrier concentration enables engineering of birefringence and dichroism over a wide infrared spectral range, offering promising opportunities for Si-based infrared photonic devices.

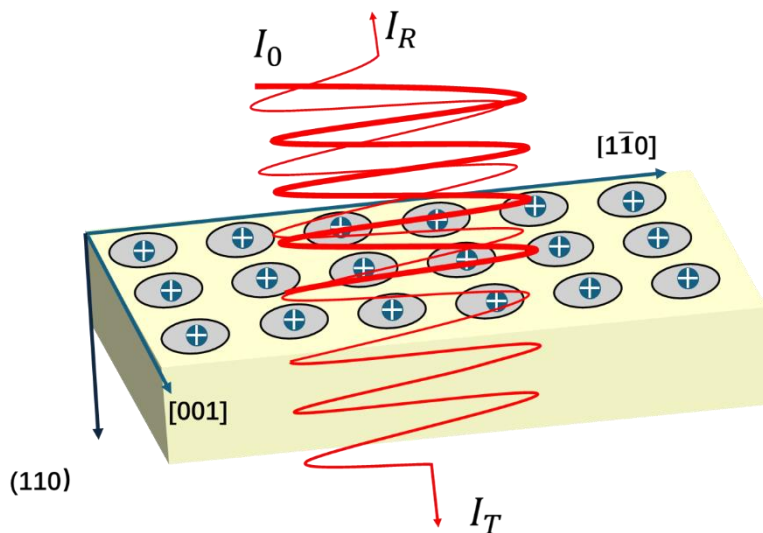


Fig. 1. Schematics of analyzed structure.

References

- [1]. Baets R., Rahim A. *Opt. Mater. Express* **13** (12), 3439-3444 (2023).
- [2]. Shekhar S., et al. *Nat. Commun.* **15** (1), 751 (2024).
- [3]. Quack N., et al. *Microsyst. Nanoeng.* **9** (1), 27 (2023).
- [4]. Sekerbayev K.S., et al. *Semicond.* **51** (8), 1047–1051 (2017).

FIELD EMISSION OF ELECTRONS FROM DISPERSED HYBRID DIAMOND-GRAPHITE FILM STRUCTURES

R.K. Yafarov

Saratov branch of the Kotelnikov Institute of Radioengineering and Electronics of Russian Academy of Sciences; Saratov, Russian Federation

Hybrid diamond-graphite film composites were obtained using microwave plasma in the range of ethanol vapor pressures between the synthesis of graphite and polycrystalline diamond films at a temperature of 300 °C, bias on the substrate holder of 300 V and various durations of the deposition processes [1]. It was found that with an increase in the specific surface resistances (ρ), the activation energies of the conductivities increase with a small range of resistances, in which they slightly decrease and amount to about 0.05 eV, the heights and sizes of the bases of the microprotrusions, as well as the aspect ratios, undergo the most significant changes. The increase in the maximum field currents is more than one order of magnitude and occurs with a decrease in the aspect ratio (Fig. 1).

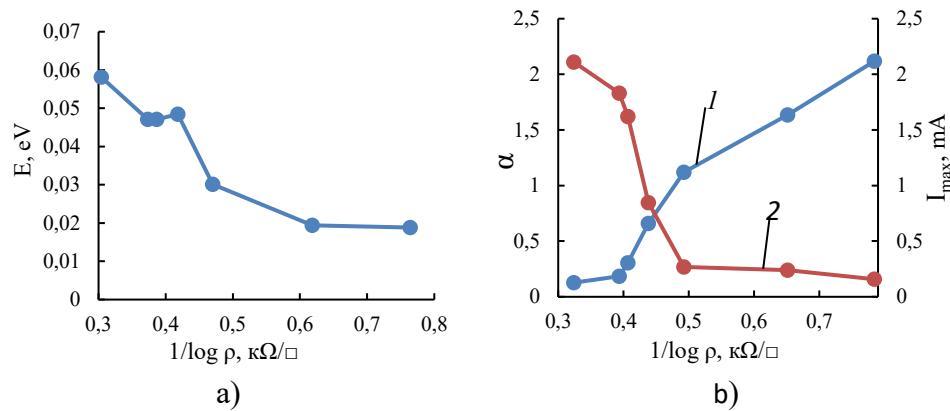


Fig. 1. Dependences of conductivity activation energies (a), aspect ratios (1), and maximum field currents (2) (b) on the specific surface resistances of dispersed diamond-graphite structures.

Estimates show that the decrease in conductivity activation energy, which occurs with increasing ρ , begins at rough surface microprotrusion heights of approximately 10 nm, where, due to size quantization, the transverse component of the zero-point energy of electrons is 0.05 eV [2]. This corresponds with good accuracy to the conductivity activation energy of hybrid diamond-graphite structures in the range of surface resistances where it does not increase.

Diamond-graphite structures obtained with short deposition times are numerous self-organized two-dimensional chains of islands—nuclei or individual microcrystallites—with a certain average size r . When an electric field is applied to such systems, the relative positions of the Fermi levels of adjacent islands shift, and the heights and widths of potential barriers at the boundaries decrease. An increase in the electron self-energy due to size quantization in dispersed film structures leads to an increase in the thermionic component of the field current. With increasing anode voltage, the transparency coefficient for electron tunneling at the solid-vacuum interface increases, despite the lower kinetic energy of electrons in the solid. Consequently, the ranges of permissible pulsed electric field strengths and maximum field currents increase significantly.

References

- [1]. Yafarov R.K. Physics of Microwave Vacuum-Plasma Nanotechnologies. Moscow: Fizmatlit, 2009. 216 p.
- [2]. Dragunov V.P., Neizvestny I.G., Gridchin V.A. Fundamentals of Nanoelectronics. Moscow: Fizmatkniga, 2006. 496 p.

FEATURES OF AVALANCHE AND FIELD IONIZATION IN THE VOLUME OF TRANSPARENT DIELECTRICS IN PROCESS OF DIRECT LASER WRITING BY ULTRASHORT LASER PULSES

M.P. Verteletskaya^{1,2}, A.V. Bogatskaya^{1,2}, A.M. Popov^{1,2}

¹*Lomonosov Moscow State University, Faculty of Physics, Moscow, Russia*

²*P.N. Lebedev Physical Institute of the Russian Academy of Sciences, Moscow, Russia*

The micro- and nanostructuring of transparent dielectrics is a rapidly advancing area of research, driven by its significant potential in photonics and communication technologies. One of the promising materials used for laser micromodification is fused silica [1]. Interaction of laser radiation with plasma formed in the dielectric volume is a crucial mechanism underlying microstructuring technologies by powerful femtosecond pulses. For femtosecond laser exposure plasma formation occurs in the dielectric conduction band mostly due to the crystal lattice atoms photoionization [2]. This process is usually characterized by Keldysh's theory of photoionization [3-5].

Formulas derived by Keldysh in [5] describe photoionization of a single atom and atoms of a crystal lattice by a linear harmonic field. In the recent paper [6] a comparison of ionization probabilities obtained for a single atom and a solid crystal lattice was conducted. It was shown that at moderate intensities the probability dynamics are similar, allowing the ionization of a wide-bandgap dielectric to be described in the single-atom approximation taking into account the replacement of the electron mass with the effective mass and the ionization potential with the band gap. However, as the intensity of the incident radiation increases (tunneling regime), the band structure of the solid becomes significant, leading to differences in the ionization dynamics. In this study we focus on investigating the contributions of multiphoton and avalanche ionization for different durations of the writing laser pulse. As is known from a number of studies [7], the role of avalanche ionization becomes significant at pulse durations more than 100 fs. Preliminary analysis has shown that at terawatt laser intensities and more, the quiver energy of an electron in laser field becomes comparable to the energy of ionization, which calls into question the applicability of accounting for avalanche ionization within the Drude model, which is widely used in the literature. Here we propose alternative models to correctly account avalanche ionization process.

Thus, a more detailed insight into the physics of the interaction of high-power laser radiation with matter and the initial stage of the formation of electron-hole plasma in the conduction band is necessary for further experimental progress in controlled laser writing in the volume of transparent dielectrics.

The work was supported by the Russian Science Foundation (grant № 22-72-10076-II).

References

- [1]. Shimotsuma Y., Hirao K., Qiu J. R., Kazansky P. G. *Mod. Phys. Lett. B.* **91** 225-228 (2005).
- [2]. Bogatskaya A.V., Gulina Yu. S., Pupasov A. A., Volkova E. A., Popov A. M. Kudryashov S. I., *Pis'ma v JETP* **122** (8) 484-494 (2025).
- [3]. Keldysh L. V., *Sov. Phys. JETP* **20** (5) 1307-1314 (1965).
- [4]. Perelomov A. M., Popov V. S., Terent'ev M. V., *Sov. Phys. JETP* **23** (5) 924-934 (1966).
- [5]. Perelomov A. M., Popov V. S., Terent'ev M. V., *Sov. Phys. JETP* **24** (1) 207-217 (1967).
- [6]. Bogatskaya A.V., Verteletskaya M.P., Gulina Yu.S., Popov A.M., Rupasov A.E., *Quantum Electronics* **55** (11) 749-754 (2025).
- [7]. Rajeev P. P., Gertsvolf M., Corkum P. B., Rayner D. M., *Phys. Rev. Lett.* **102** 083001 (2009).

CORRELATION EFFECTS IN INDUCED BINARY DIPOLAR SYSTEMS IN A DOUBLE-PLATE GEOMETRY

E. Allahyarov^{1,2,3,4}, H. Lowen²

¹*Theoretical Department, OIVTRAN, Moscow, Russia*

²*Soft Matter Theory II, Heinrich-Heine University of Dusseldorf, Germany*

³*Department of Physics, Case Western Reserve University, Cleveland OH, USA*

⁴*Recognition Science Institute, Austin TX, USA.*

Previous studies have demonstrated that one-component and binary systems of polarizable spheres in two-dimensional geometries can undergo fluid-fluid phase separation under strong external fields applied perpendicular to the planar surface. This demixing phenomenon is associated with dipole reversal of a subset of induced dipoles, occurring predominantly at packing fractions above 0.1. Molecular dynamics (MD) simulations revealed that particles with reversed dipoles cluster together, forming a dense phase with dipole moments oriented antiparallel to the applied field, dispersed within a dilute phase of normally oriented dipoles aligned with the field. Similar behavior has been observed in binary systems. The present study investigates the effect of extending the 2D geometry to a quasi-3D configuration by introducing a second parallel plate at distance A above the first, with both plates containing induced dipoles. Contrary to the vertical alignment of inverted clusters expected from simple energy minimization arguments, our simulations reveal a distinct scenario: the positions of clusters on neighboring plates exhibit strong spatial anticorrelation, creating a zigzag-like morphology. This ordering is weakly dependent on the interplate separation A . Notably, cluster size increases with A , indicating that morphology can be externally controlled through both field strength and geometric parameters. Positional correlations were also detected among normally oriented dipoles on different plates. These findings have significant implications for sensor applications and metamaterial design.

EXCITATION OF TERAHERTZ SURFACE PLASMONS AT THE INTERFACE BETWEEN JOSEPHSON SANDWICH AND DIELECTRIC

A.S. Malishevskii, S.A. Uryupin

P.N. Lebedev Physical Institute of the Russian Academy of Sciences, Moscow, Russia,
malish@lebedev.ru

Previously, Cherenkov radiation from a Josephson vortex in a sandwich into an external dielectric was studied at a vortex velocity greater than the speed of light in the dielectric c_m . Here, other conditions are considered, when the vortex velocity in the sandwich is less than the speed of light in the dielectric, and it is shown that the vortex excites terahertz surface plasmons.

Along the surface of a superconducting layer with a thickness of $2L$ surrounded by a dielectric (Figure 1), plasmons can propagate with a frequency $\omega^2(k) = c_m^2 k^2 [1 - \lambda^2 k^2 \tanh^2(L/\lambda)]$, where λ is the London penetration depth of the magnetic field [1].

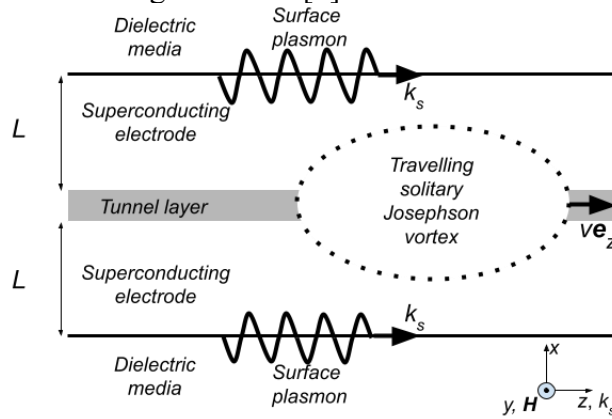


Fig. 1. A Josephson sandwich surrounded by a dielectric. The solitary vortex travels with velocity v . Surface waves excited by the vortex are depicted on the lateral surfaces of the sandwich

If there is a thin layer inside the superconductor (shown in grey in Figure 1) through which Josephson tunneling can occur, then an equation describing the excitation of a surface plasmon can be written [2]:

$$[\partial_{tt} - c_m^2 \partial_{zz} - c_m^2 \lambda^2 \tanh^2(L/\lambda) \partial_{zzzz}] H_s = [\phi_0 \lambda c_m^2 \sinh(L/\lambda) / 2\pi \cosh^2(L/\lambda)] \varphi_{zzzzz}.$$

Here, H_s is the magnetic field at the surface of superconducting electrodes, ϕ_0 is the magnetic flux quantum, and φ is the Josephson phase difference of the superconducting order parameter at the tunnel layer.

If the right-hand side of this equation is the phase difference of a solitary Josephson vortex travelling in an extended sandwich embedded in a dielectric, then an exact solution to this equation has been found. It has been shown that the magnetic field created by the vortex at the boundaries of the sandwich corresponds to a surface plasmon travelling at the interface between the superconducting electrodes of the sandwich and the dielectric medium. The wave vector of such a plasmon is determined by the relation $\omega(k_s) = vk_s$ and depends on the velocity of the vortex as $\propto (c_m - v)^{1/2}$. The frequency of the generated surface plasmon falls in the terahertz range.

The field of the surface plasmon is mainly localized in the external dielectric, in a region of width which is large compared to the London penetration depth. For typical sandwiches it has been shown that the power of the surface wave can be tens of milliwatts. This method of surface plasmon generation can be implemented in ‘conventional’ niobium-based junctions at helium temperatures, where the London length is $\sim 0.1 \mu\text{m}$, and the Josephson length is $\sim 10 \mu\text{m}$, which corresponds to a relatively low critical Josephson current density of $\sim 1.3 \text{ kA/cm}^2$.

References

- [1]. Economou E. N. *Phys. Rev.* **182** (2) 539-554 (1969).
- [2]. Malishevskii A. S. and Uryupin S. A. *Phys. Lett. A* **540** 130389 (2025).

PLASMONIC INTERBAND HYBRIDIZATION IN HGTE QUANTUM WELLS

Yu.B. Vasilyev

Ioffe Institute, Sankt-Petersburg, Russian Federation, yu.vasilyev@mail.ioffe.ru

We present a model describing the mechanism of polariton generation under electrical pumping and explaining the emergence of electroluminescence in the case of unipolar current excitation of two-dimensional plasmons in HgTe quantum wells. It is well known that, due to inelastic quantum tunneling, electrons can tunnel through a finite potential barrier while simultaneously exciting plasmons [1]. In a two-dimensional electron gas, plasmons can be excited by various means, including electrical current flowing through structures with inhomogeneities [2].

We propose that, in narrow-band-gap HgTe quantum wells, plasmonic modes can be directly excited by electrons during inelastic interband (Zener) tunneling in an external electric field. Electroluminescence originating from plasmonic tunneling transitions arises as a consequence of polariton formation and involves the following processes (Fig. 1): (1) elastic tunneling of electrons from the filled valence band to available states in the conduction band, including transitions from the H_1 and H_2 valence-band subbands; (2) inelastic tunneling of electrons accompanied by plasmon generation; (3) coupling of plasmons with interband transitions, resulting in polariton formation and subsequent optical emission. Polaritons form at a specific bias voltage V , at which the energy eV corresponds to the interband transition energy E_1-H_2 . The applied bias also determines the plasmon energy E_{pl} generated during inelastic interband tunneling. As a result, the energies E_1-H_2 and E_{pl} become approximately equal, as illustrated in Fig. 1, thereby fulfilling the condition for efficient plasmon–interband hybridization.

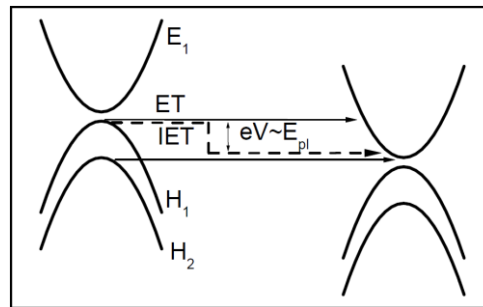


Fig. 1. Schematic picture of the inelastic tunneling process with plasmon excitation (broken line) in narrow-gap quantum wells. Straight horizontal lines represent elastic tunneling.

The feasibility of the proposed plasmon hybridization mechanism is supported by electroluminescence spectra obtained from HgTe/CdHgTe quantum wells [3]. The spectra exhibit two distinct emission peaks, which can be attributed to two polariton modes arising from the coupling between a dipole plasmon mode excited via inelastic electron tunneling and an interband transition. This interaction can be modeled using a Drude–Lorentz formalism, where the interband transition is treated as a Lorentz oscillator coupled to a dipole plasmon mode. From the emission spectra, both the plasmon energy and the Rabi splitting can be extracted. These results are of particular importance in the context of ongoing discussions on possible mechanisms for achieving plasmon lasing in such semiconductor structures [4,5].

References

- [1]. Tang J., et al. *ACS nano* **18** (4) 2541-2551 (2024).
- [2]. Muravev V. M., and Kukushkin I. V.. *Physics-Uspechi* **63** (10) 975-993 (2020).
- [3]. Vasilyev Yu. B., et al. *46th IRMMW-THz*: 1-1 IEEE (2021).
- [4]. Kapralov K., et al. *Journal of Physics: Condensed Matter* **32** (6) 065301 (2020).
- [5]. Aleshkin V. Ya., et al. *Journal of Optics* **23** (11) 11501 (2021).

QUANTUM FLUCTUATIONS OF THE NUMBER OF CURRENT CARRIERS AND ELECTRIC CHARGE IN QUASI-ONE-DIMENSIONAL SYSTEMS IN THE POLAR CRYSTAL MODEL

L.M. Svirskaya^{1,2}

¹*South Ural State Humanitarian and Pedagogical University, Chelyabinsk, Russia*

²*South Ural State University, Chelyabinsk, Russia, svirskayalm@mail.ru*

Fluctuations in the number of current carriers and the electric charge at a crystal lattice site are considered within the framework of the polar model of the Shubin-Vonsovsky crystal [1] in the Hubbard approximation [2] with the Hamiltonian

$$\hat{H} = \sum_{g_1, g_2, \sigma} t_{g_1 g_2} \hat{c}_{g_1 \sigma}^+ \hat{c}_{g_2 \sigma} + U \sum_g \hat{n}_{g \uparrow} \hat{n}_{g \downarrow}, \quad (1)$$

which takes into account the processes of transfer ($t_{g_1 g_2}$) of electrons between the sites of the crystal lattice and the intra-atomic Coulomb repulsion (U) of two electrons with opposite spin projections (“couples”).

The kinetic energy Hamiltonian does not commute with the operator sU , where s is the operator of the number of couples, $s = \sum_g \hat{n}_{g \uparrow} \hat{n}_{g \downarrow}$, therefore the number of couples is not an integral of motion. The change in the average number of couples \bar{s} with increasing U is determined by fluctuations in their number in the stationary state. According to the general properties of the generalized differential susceptibility [3], in the ground state

$$\frac{\partial \bar{s}}{\partial U} \Big|_0 \leq 2 \frac{(\Delta s)_0^2}{E_1 - E_0}. \quad (2)$$

An increase in U has opposite effects on the change in the number of couples in the ground and excited states.

In a state described by a test wave function

$$\Psi = \prod_g \left[\alpha_g c_{g \downarrow}^+ + \beta_g c_{g \uparrow}^+ + \gamma_g c_{g \downarrow}^+ c_{g \uparrow}^+ + \delta_g \right] |0\rangle, \quad (3)$$

where $|\alpha_g|^2$, $|\beta_g|^2$, $|\gamma_g|^2$, $|\delta_g|^2$ – the probabilities of finding an electron with a negative spin projection, a positive spin projection, a couple, or a hole in a crystal lattice site, fluctuations in the number of couples Δs_g and the electric charge Δq_g at site g increase with increasing $|t|$ and decrease with increasing U . Relative root-mean-square fluctuation of the number of couples

$$\frac{\Delta s}{\bar{s}} = \frac{1}{\sqrt{N}} \sqrt{\left(3 + \frac{U}{4t}\right) / \left(1 - \frac{U}{4t}\right)} \quad (4)$$

tends to infinity, which corresponds to the disappearance of ionized states (metal-dielectric phase transition). Under the condition $U \ll 4|t|$ the limit transition to the model of a gas of non-interacting electrons is performed and the dependence $\Delta s / \bar{s} \sim 1 / \sqrt{N}$ is preserved (N is the number of crystal lattice sites), which has a statistical origin.

The coherence of state (3) allows us to consider collective excitations whose wave functions are orthogonal to (3). These specifically solid-state collective excitations with zero average electric charge of a crystal lattice site ($\langle \tilde{q}_g \rangle = 0$, $\Delta \tilde{q}_g = |e| \sqrt{2 \langle \hat{s}_g \rangle}$), determined by the integrals U and t , can propagate through the crystal along with plasmons. The corresponding quasiparticles can be excited both externally (by electrons, electromagnetic radiation, neutrons, etc.) and virtually during various interactions in a solid body.

References

- [1]. Shubin S.P., Vonsovsky S.V. *Sov Phys.* **7** 292-328 (1935).
- [2]. Hubbard J. *Proc. Roy. Soc. A* **276** 238-257 (1963).
- [3]. Svirsky M.S., Svirskaya L.M., Vonsovsky S.V. *JETP* **81** 1(7) 255-262 (1981).

DIAGNOSTICS OF ATMOSPHERIC PLASMAS USING ATOMIC EMISSION LINE PROFILES

B. Obradović¹, G. Sretenović¹, N. Cvetanović², S. Ivković¹, V. Kovačević¹, I. Krstić¹
and M. Kuraica¹

¹*University of Belgrade, Faculty of Physics, Stud. Trg 12, 11001 Belgrade, Serbia*

²*University of Belgrade, Faculty of Transport and Traffic Engineering, Vojvode Stepe 305, 11000 Belgrade, Serbia*

Optical emission spectroscopy (OES) continues to serve as a cornerstone diagnostic method for studying electrical gas discharges across diverse operating regimes. By examining the alterations in atomic spectral line profiles—caused by distinct physical broadening processes—key plasma properties such as gas temperature, electron density, and electric field strength can be derived. These broadening mechanisms are frequently interconnected, and their relative significance is highly dependent on discharge conditions. For instance, in low-pressure plasmas, resolving Doppler broadening—which stems from the thermal motion of emitters—allows accurate gas temperature measurements, whereas in atmospheric-pressure low-temperature discharges, Doppler effects are usually insignificant compared to dominant pressure broadening. In particular, evaluating resonant and van der Waals broadening contributions not only yields gas temperature data but also helps in assessing partial pressures of perturbing species.

At high charged-particle densities, microscopic electric fields produce Stark broadening, a phenomenon employed for diagnosing electron number density and temperature. Macroscopic electric fields—such as those found in cathode fall regions of glow discharges or inside streamer heads—lead to Stark splitting, spectral line shifts, and occasionally the emergence of normally forbidden transitions that become allowed under strong fields. These spectral changes enable the quantification of local electric field intensities.

This lecture examines the use of spectral line profile analysis for diagnosing various atmospheric-pressure discharges, such as dielectric barrier discharges [1], RF discharges [2], freely expanding plasma jets, jets interacting with solid surfaces, pulsed discharges with liquid electrodes [3], and pulsed discharges within liquid media [4]. Illustrative experimental case studies are discussed, along with practical guidelines for applying these diagnostic approaches. As an example, the Balmer H_α and H_β lines were utilized to measure the average electron density (N_e) in an underwater discharge plasma [4]. Notably, several experiments reviewed here reveal different forms of Stark line shifts in atmospheric-pressure plasmas. A key distinction is highlighted between Stark shifts induced by the microscopic field of surrounding charged particles and those resulting from macroscopic electric fields present in plasma sheath regions.

References

- [1]. N. Cvetanovic N. et al. *Plasma Sources Sci. Technol.* **27** 025002 (2018).
- [2]. Wang L. et al. *Plasma Sources Sci. Technol.* **28** 055010 (2019).
- [3]. Sretenović G. B. et al. *Plasma Sources Sci. Technol.* **34** 055013(2025).
- [4]. Krcma et al. *Plasma Sources Sci. Technol.* **27** 065001 (2018).

**ELECTRICAL BEHAVIOUR OF SUB-ATMOSPHERIC ALTERNATING CURRENT
PLASMA FOR CARBON DIOXIDE CONVERSION TO ALTERNATIVE FUEL
PRODUCTION**

Pratyay Chattopadhyay, Satyananda Kar

*Atmospheric Plasma Research Laboratory, Department of Energy Science and Engineering,
Indian Institute of Technology Delhi, Hauz Khas, New Delhi, India*

Carbon Capture and Utilization (CCU) is vital for mitigating climate change, with the conversion of CO₂ to carbon monoxide (CO) serving as a critical step for producing sustainable fuels like syngas and methanol. While traditional methods like thermal catalysis are limited by high costs and harsh operating conditions, plasma technology offers a viable alternative by utilizing electron-driven processes under milder environments. This study investigates a sub-atmospheric alternating current (AC) plasma system for direct CO₂ and Argon mixed CO₂ dissociation. By analyzing electrical characteristics through Optical Emission Spectrum analysis, Lissajous figures and optimizing pressure, the setup achieves a stable discharge and generates ~2723.01 PPM (calculated) of CO. This approach highlights the potential of AC plasma as a scalable, renewable-compatible solution for effective emission management.

**CONTROL OF REACTIVE SPECIES DOSES THROUGH GROUND RESISTANCE
MODULATION IN A SUB RADIO FREQUENCY ATMOSPHERIC PRESSURE
PLASMA JET INTERACTION WITH LIQUID: IMPLICATION ON DYE
DEGRADATION KINETICS AND CHANGES IN PHYSICOCHEMICAL PROPERTIES
OF LIQUID**

Aishik Basu Mallick, G. Veda Prakash, Satyananda Kar, Ramesh Narayanan

*Department of Energy Science and Engineering, Indian Institute of Technology Delhi,
Hauz Khas, New Delhi, India*

This study examines the role of ground side current limiting resistance (100 Ω to 1 M Ω), on the target side in regulating the transfer and dissolution of plasma generated reactive species into liquid media during atmospheric pressure plasma jet interaction with liquid. The plasma jet was operated under optimized conditions, at a pulse frequency of 30 kHz, and applied voltage of 9 kV_{pp} with argon flow of 1.5 LPM [1]. Electrical diagnostics revealed an inverse relationship between the current transfer through water with ground resistance magnitude which influences the applied power to the liquid load.

Rate of formation of hydroxyl radical (0 – 473 μ M), hydrogen peroxide (0 – 3.9 mM), and nitrate ion (0 – 139 ppm) in bulk liquid reduces with increment in resistance values for solution volume of 10 ml is observed. Subsequent effect in physicochemical parameters of the treated liquid, including pH, solution conductivity, oxidation reduction potential (ORP) was observed as a function of treatment duration provided evidence for species dissolution in liquid. Together plasma jet interacting with liquid forms an equivalent electrical network, influencing emission characteristics thereby tailoring different plasma induced radical chemistry.

References

- [1]. A.B. Mallick, G.V. Prakash, S. Kar, and R. Narayanan, *Rev. Sci. Instrum.* **94**, (2023).

PLASMA-CHEMICAL STUDY OF A NONEQUILIBRIUM MICROWAVE DISCHARGE IN DIELECTRIC POWDERS

Z.A. Zakletskii

Prokhorov General Physics Institute of the Russian Academy of Sciences

Atmospheric pressure microwave discharge is a highly efficient and economically promising method for plasma-chemical synthesis, particularly in nitrogen fixation. Its electrodeless design eliminates product contamination and extends equipment lifespan, while high electron density and spatial stability minimize heat loss by directing energy precisely into the reaction zone. The combination of hardware accessibility, energy maneuverability, and the use of subthreshold discharges results in exceptionally low energy consumption, making microwave plasma a clean and controllable tool for industrial-scale production.

The subthreshold microwave discharge mode ensures profound thermodynamic non-equilibrium, where field energy is selectively directed toward exciting nitrogen internal bonds while minimizing parasitic gas heating. The self-organization of plasma into thin filaments creates zones of extreme energy density sufficient to break the triple bond, while the surrounding cold gas provides instantaneous quenching, preventing product back-decomposition. This "structured" discharge, consisting of a network of active channels, significantly increases the reaction volume and synthesis selectivity, enabling high nitric oxide yields at low average power consumption.

Using a 0D kinetic model, we analyze the synergistic effects between a non-equilibrium microwave discharge and dispersed aluminum oxide (Al_2O_3) particles.

Plasma-catalysis, which combines non-equilibrium plasma with solid catalysts, offers a solution by enabling targeted reaction pathways. Introducing high-surface-area particles into the plasma zone amplifies surface-mediated processes, potentially improving process performance and scalability. A comprehensive kinetic model was developed, incorporating:

Homogeneous reactions: A detailed scheme for air plasma (~12000 reactions), including electron-impact processes (calculated via Boltzmann solver), ion-molecular reactions, and neutral chemistry.

Heterogeneous processes: Surface loss of active species (O, N, NO_x) on Al_2O_3 particles, parameterized using effective sticking coefficients (γ).

SPATIAL DISTRIBUTION OF ELECTRIC FIELD STRENGTH IN GAS MIXTURES WITH HELIUM IN AN ATMOSPHERIC PRESSURE GLOW DISCHARGE WITH DIFFERENT CATHODE SHAPES

A.V. Kazak, P.A. Ivanova, L.V. Simonchik, M.U. Tomkavich, A.M. Vabishchevich

B.I. Stepanov Institute of Physics of NAS of Belarus, Minsk, Belarus, p.ivanova@ifanbel.bas-net.by

Glow discharges at atmospheric pressure are of considerable interest due to their relevance for plasma-assisted technologies, surface modification and biomedical applications. However, their structure and stability remain highly sensitive to both gas composition and cathode configuration. In this work, a systematic study was carried out to clarify how admixtures of molecular gases influence the discharge characteristics under conditions of non-planar electrode topology. The effect of air and water vapor impurities on the discharge characteristics was investigated. It was found that the presence of impurities leads to morphological changes and to an increase in the electric field strength in the cathode region.

A normal self-sustained glow discharge at atmospheric pressure was ignited in an air-locked chamber between a 9 mm diameter copper rod electrode (cathode) and a slightly rounded copper anode, similar to [2]. A flow of plasma-forming helium gas was provided through the chamber at a rate of approximately 1 l/min at atmospheric pressure. Using an illumination system consisting of a single quartz lens with a focal length of 75 mm or a collimator consisting of two lenses with a focal length of 110 mm and a polarizer placed between them, the discharge image was focused 1:1 in the plane of the entrance slit (20 μm) of a high-resolution scanning monochromator MDD-500x2 (Solar) with two 1800 lines/mm diffraction gratings. In the experiment, the discharge current was 1 A, the discharge gap was 5 mm.

The experiments were performed in helium at atmospheric pressure with controlled additions of air and water vapor. Key discharge parameters, including electric field strength, spatial structure, and cathode region morphology, were analyzed. It was found that even small concentrations of impurities substantially modify the discharge behavior. The most pronounced effect was observed for helium mixtures containing water vapor, where the electric field reached its maximum values (to 70 kV/cm) compared with both pure helium (to 55 kV/cm) and helium/air mixtures (to 65 kV/cm). This behavior is attributed to changes in ionization kinetics, energy transfer processes, and the effective electron loss mechanisms associated with molecular species [1].

Significant modifications of the near-cathode region were also observed. The introduction of air resulted in a noticeable compression of the cathode layer, indicating enhanced ionization and altered sheath dynamics. In contrast, the addition of water vapor produced an opposite effect, increasing the thickness of the cathode region. Such differences suggest that various impurity species affect the balance between ionization, excitation, and recombination processes in distinct ways. The experimental observations are consistent with the expected influence of molecular gases [1] on electron energy distribution and secondary emission processes.

Furthermore, the study demonstrates that the discharge structure is strongly dependent on cathode geometry. Non-planar cathodes introduce spatial non-uniformities in the electric field, which, when combined with impurity-driven kinetic effects, lead to substantial variations in discharge morphology and stability. The results highlight the coupled role of electrode shape and gas composition in determining the properties of atmospheric-pressure glow discharges.

The obtained results allow us to understand the mechanisms governing the influence of impurities in helium discharges and can be useful for optimizing plasma sources operating under real conditions, where molecular admixtures are inevitable.

References

- [1]. Fridman A. "Plasma Chemistry". *Cambridge University Press* 2008.
- [2]. Simonchik L.V. and Kazak A.V. *J. Phys. D: Appl. Phys.* **52** 024004 (2019).

VACUUM ULTRAVIOLET RADIATION OF THE PLASMA JET

V.P. Krainov¹, B.M. Smirnov²,

¹*Moscow Institute of Physics and Technology, Dolgoprudny, Russia*

²*Joint Institute of High Temperatures, Moscow, Russia*

Hot dense plasma is the source of the VUV-radiation. The typical wavelength is determined by the atomic ionization potentials. For helium plasma the transition $\text{He}(2^1P \rightarrow 1^1S)$ with the wavelength of $\lambda = 58.4 \text{ nm}$ is the main transition resulting in VUV-radiation. We derive the radiation flux at the electron density of $N_e = 10^{17} \text{ cm}^{-3}$ and the electron temperature of $T_e = 4 \text{ eV}$. The Boltzmann density of excited atoms is $2 \cdot 10^{14} \text{ cm}^{-3}$. The width of the spectral line is of $\Gamma = 10^6 \text{ s}^{-1}$. Taking into account that $\hbar\omega \gg T_e$, one obtains the radiation flux the simple expression

$J_\omega = \frac{\hbar\omega^3\Gamma}{4\pi^3c^2} \exp\left(-\frac{\hbar\omega}{T_e}\right) = 6 \cdot 10^{-5} \text{ W/cm}^2$. Here $\hbar\omega$ is the photon energy. This is much less than the photo-recombination flux. Spectral power of the VUV-radiation due to photo-recombination of electrons and ions in the plasma:

$$P_\lambda = \frac{2}{\sqrt{\pi}} P \sqrt{\frac{\lambda_1}{\lambda} - \frac{\lambda_1}{\lambda_o}} \exp\left(\frac{\lambda_1}{\lambda} - \frac{\lambda_1}{\lambda_o}\right) \frac{\lambda_1}{\lambda^2}, \quad \lambda_1 = \frac{2\pi c\hbar}{T}, \quad \lambda_o = \frac{2\pi c\hbar}{J} > \lambda.$$

At the temperature of $T = 3 \text{ eV}$ we have the values of parameters $\lambda_1 = 414 \text{ nm}$, $\lambda_o = 50.4 \text{ nm}$.

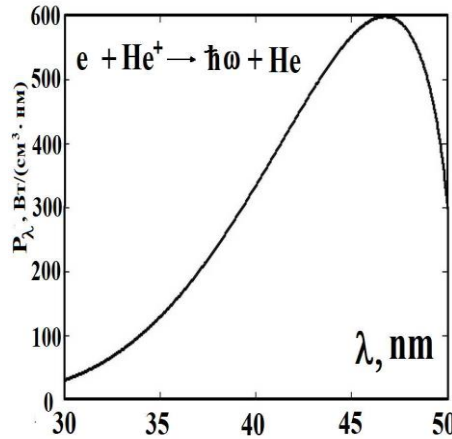


Fig. 1. The radiation power of helium plasma in the VUV spectral region.

It follows from Fig. 1 that the hot dense plasma can be a source of VUV-radiation with the wavelengths less than 50 nm. VUV-radiation determines the recombination of electrons and ions during the first evolution stage, when the plasma jet goes from the plasmatron.

References

- [1]. Krainov V.P., and Smirnov B.M. *Thermophysics of High Temperatures*, **63** (4) 475-480 (2025).

PROCESSING OF ION FLOW FOR PLASMA SEPARATION

D.D. Tiubaev, A.P. Oiler, A.V. Timofeev, R.A. Usmanov

*Joint Institute for High Temperatures of Russian Academy of Sciences, Moscow, Russia,
denistyubaev@yandex.ru*

The motion of ionized matter in crossed electromagnetic fields is studied in the context of developing plasma mass separation technology [1-3]. The specific objective of the present work is to investigate ways of generation of an ion beam several centimeters in width, drifting at velocities on the order of several km/s in a plasma, in the presence of an external magnetic field of several kG, for subsequent processing in the separation zone.

Ion trajectories are computed via numerical integration of Newton's equations. Ion-neutral collisions are simulated using Monte-Carlo method [4] with an isotropic scattering model and cross-section data from [5].

We examine configurations with non-uniform electromagnetic fields to establish the relationship between ion drift velocity and trajectory width. Comparison with the analytical solution for uniform fields reveals that, for a fixed maximum value of magnetic field and trajectory width, the drift velocity in non-uniform configurations is either comparable to or lower than that in uniform fields.

Extraction of ions from a cylindrical ionization chamber into a channel whose width is several times smaller than the chamber radius is simulated. First, the initial coordinate distribution in the ionizer is computed for two categories of ions—those passed through the channel and those deposited on the walls in case of zero initial velocity. This distribution is characterized as a function of two key parameters: the “characteristic Larmor radius” and a parameter governing the electric field profile, yielding insights for optimizing beam extraction. Second, particle flight times, are determined as a function of the ion's point of origin within the ionization chamber.

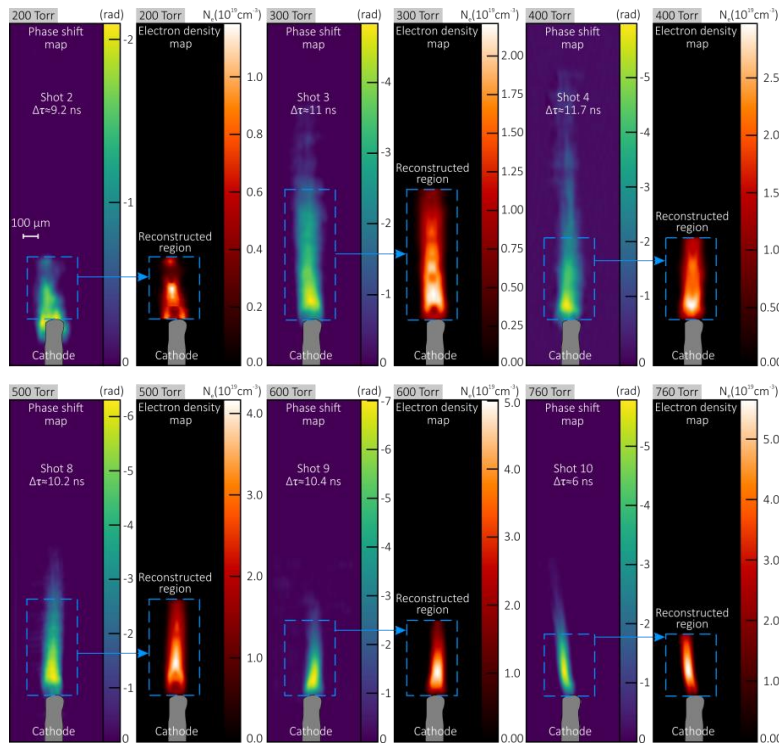
The work was supported by the Russian Science Foundation (grant №25-79-30008, <https://rscf.ru/project/25-79-30008/>).

References

- [1]. Smirnov V. P., Samokhin A. A., Vorona N. A., Gavrikov A. V. *Plasma Phys. Rep.* **39** (6) 456-466 (2013).
- [2]. Smirnov V. S., Egorov R. O., Kislenko S. A., Antonov N. N., Smirnov V. P., Gavrikov A. V. *Phys. Plasmas* **27**(11) :113503 (2020).
- [3]. Liziakin G. D., Antonov N. N., Vorona N. A., Gavrikov A. V., Kislenko S. A., Kuzmichev S. D., Melnikov A. D., Oiler A. P., Smirnov V. P., Timirkhanov R. A., Usmanov R. A. *Plasma Phys. Rep.* **48** (11) 1251-1260 (2022).
- [4]. Nanbu K. *IEEE Trans. Plasma Sci.* **28** (3) 971-990 (2000).
- [5]. Buchachenko A. A., Viehland L. A. *Int. J. Mass Spectrom.* **443** 86-92 (2019).

MECHANISM OF HIGHLY-IONIZED PLASMA FILAMENT GROWTH IN A PULSED NANOSECOND DISCHARGE IN ATMOSPHERIC AIRE. V. Parkevich¹, A. I. Khirianova¹, K. V. Shpakov¹, T. F. Khirianov¹, K.S. Vinogradova¹,
A.A. Tarasenko¹, D.V. Antonov¹, Gavrilov S.Yu.¹, and N. A. Popov²¹ *P.N. Lebedev Physical Institute of the Russian Academy of Sciences 119991, Moscow, Russia,*² *Skobeltsyn Institute of Nuclear Physics, Moscow State University, 119991 Moscow, Russia*

The dynamics of highly-ionized plasma filament formation in a pulsed nanosecond discharge in air at pressures of 100–760 Torr is studied using high spatio-temporal resolution laser diagnostics. The discharge initiation is governed by an explosive process at the cathode, generating a localized high-density plasma from which an ionization wave propagates toward the anode with a velocity of $\sim 10^6$ – 10^7 cm/s, largely independent of air pressure. This wave defines the front of the growing filament. At elevated pressures (400–760 Torr) the wave front undergoes instability, fragmenting into a system of dense microchannels (~ 20 μm in diameter, with an electron density up to $N_e \sim 5 \times 10^{19}$ cm^{-3}) which constitute the fine-scale structure of the discharge. A distinct pressure threshold is observed: microchannel formation ceases when pressure is reduced below 400 Torr, leading to the development of a homogeneous, yet still highly-ionized, filament. At lower pressures (≤ 200 Torr), plasma generation shifts to the lateral cathode surface and is dominated by electrode material vapor, while extended filament growth is suppressed due to increased characteristic filamentation times. The rapid ionization and heating are attributed to stepwise dissociation of N_2 followed by ionization of N atoms. These findings reveal critical thresholds and mechanisms governing plasma microstructure, providing essential data for refining kinetic models of high-pressure nanosecond discharges.

**Fig. 1.** Phase shift and reconstructed electron density maps of the filaments.

The study was supported by the Russian Science Foundation (project no. 24-79-10167).

References

- [1]. Parkevich E. V. et al. Phys. Rev. E, 112 (6), 065211 (2025)

FEATURES OF THE FORMATION OF A PULSED DISCHARGE IN HELIUM IN A POINT-TO-PLANE GAP

G.B. Ragimkhanov¹, A.A. Trenkin², A. N. Belonogov²

¹*Dagestan State University, Makhachkala, Russia, gb-r@mail.ru*

³*Russian Federal Nuclear Center – All-Russian Research Institute of Experimental Physics, Sarov, Russia*

The results provide reference data for modeling nanosecond discharges in helium and for comparing microstructure formation in different gases. By now, the presence of discharge microstructure—where the current-carrying channel is a superposition of a large number of microchannels (filaments)—has been established for many types of discharges in air, nitrogen, and argon over a range of pressures. At the same time, despite experimental evidence that microstructure is a widespread and intrinsic feature of gas-discharge processes, this phenomenon has received insufficient attention, and the number of publications on the topic remains quite limited.

Building on our earlier studies, we present here results on the spatial structure of a high-voltage pulsed discharge in a tip-to-plane helium gap with an interelectrode spacing of 1.5 mm. The axisymmetric needle cathode was made of stainless steel; it was 19 mm long and 14 mm in diameter, with a 36° apex angle and a radius of curvature of 0.15 mm. The plane electrode was a counter-electrode whose working surface was close in shape to a spherical segment, 4.5 cm in diameter and 1.5 cm thick.

The discharge spatial structure was investigated using shadowgraphy combined with high-speed imaging. It is shown that the discharge onset is characterized by the appearance of weakly luminous cathode spots, and that the discharge may develop in either a single-channel or a multichannel mode. The presence of a microchannel structure was detected at pressures of 1.5 atm and above. Within the pressure range studied, both single-channel and multichannel (predominantly two-channel) discharge modes were observed. At pressures of 1.5 atm and higher, discharge microstructure was recorded. The microstructure, appearing as an ensemble of microchannels, is most clearly manifested at 3 atm; however, it is less pronounced than in air and nitrogen. It is shown that discharge initiation is accompanied by weakly luminous cathode spots that are distributed stochastically from pulse to pulse over the electrode surface, while with increasing pressure their localization tends to concentrate on the needle (tip) region of the cathode.

Experimentally, changes in the morphology of the plane electrode (anode) surface fabricated from various materials and alloys (stainless steel, copper, an aluminum alloy, and brass) were examined using scanning electron microscopy and optical microscopy with elemental analysis. The results indicate a complex interaction between the spark discharge and the electrode surface and point to the important role of electrode material in energy deposition and erosion processes in dense-gas spark discharges. It is shown that discharge exposure leads to the formation of localized erosion regions with a characteristic size of about 0.9–1.2 mm, containing a large number of microcraters with sizes ranging from hundreds of nanometers to tens of micrometers.

It was found that the erosion pattern, the degree of surface melting, and the crater distribution depend strongly on the electrode material.

This research was carried out with financial support from the Russian Science Foundation through grant № 25-22-2009.

References

- [1]. K. I. Almazova et al. *Plasma Sources Sci. Technol.* 30 (9), 095020 (2021)

FORMATION OF A PULSED DISCHARGE IN ATMOSPHERIC PRESSURE HELIUM IN A PLANE-PARALLEL GEOMETRY UNDER CONDITIONS OF GAS PREIONIZATION

V.S. Kurbanismailov, G.B. Ragimkhanov, Z.R. Khalikova

Dagestan State University, Makhachkala, Russia, gb-r@mail.ru

The study of pulsed gas discharges remains highly relevant from both fundamental and applied perspectives. Despite significant progress in the development of experimental diagnostic techniques, obtaining a complete spatiotemporal picture of plasma evolution throughout the entire discharge gap remains a challenging task. In our previous works [1,2], it was shown that under conditions of gas pre-ionization, depending on the initial discharge formation conditions—namely, the magnitude of the applied electric field, gas pressure, and the concentration of pre-ionization electrons—various discharge modes can be realized, including a uniform volumetric mode, a volumetric mode with cathode spots, a constricted mode, and a high-current diffuse mode. At the same time, the discharge characteristics are also strongly determined by the parameters of the RLC circuit. In the present work, a pulsed gas discharge in atmospheric-pressure helium was investigated in a plane-parallel gap. The electrode system consisted of two parallel electrodes: a flat stainless-steel anode with a radius of $r_0=2$ cm and a mesh cathode.

Analysis of the current oscillograms revealed the existence of two stable discharge regimes—aperiodic and oscillatory—differing in the amplitude and duration of the current pulse. It was established that in the oscillatory regime, the current oscillation period is $T \approx 1.7 \mu\text{s}$ and depends neither on the voltage across the discharge capacitor in the range of 3–14 kV nor on the pressure in the discharge chamber in the range of 1–3 atm. This regime is characterized by a more uniform glow of the discharge gap without pronounced cathode and anode spots at voltages up to 11 kV.

The aperiodic regime is characterized by an almost linear dependence of the discharge current amplitude, I_{max} , on the applied voltage. The time-integrated discharge images reveal multiple diffuse channels localized near the mesh cathode. It was shown that the glow structure depends significantly on the value of the ballast resistance connected in series with the discharge gap. When the ballast resistance is reduced to 2 Ω , thin spark channels begin to form in the gap already at voltages above 7 kV.

For the numerical analysis, a discharge model was developed in COMSOL Multiphysics using the Plasma Module. The helium model included the atomic ground state, all excited states up to $n=3$, two molecular states—metastable $He_2^*(1)(a^3 \sum_u^+)$ and excimer $He_2^*(2)(A^1 \sum_u^+)$ (resonant)—as well as atomic and molecular helium ions. The plasma was described using a modified fluid model known as the local mean energy approximation (LMEA). Characteristic spatial distributions of charged and excited species in the discharge gap were obtained.

This research was carried out with financial support from the Russian Science Foundation through grant № 25-22-2009.

References

- [1]. V.S. Kurbanismailov, O.A. Omarov, *High Temperature*, **33**:3 (1995), 346–350.
- [2]. V.S. Kurbanismailov, O.A. Omarov, G.B. Ragimkhanov, D.V. Tereshonok, *Tech. Phys. Lett.*, **43** (9), 853 (2017).

INFLUENCE OF WATER VAPOR ON PLASMA PROPERTIES OF PULSE-PERIODIC DISCHARGE IN NON-UNIFORM ELECTRIC FIELD AT AIR

V.F. Tarasenko, D.V. Beloplotov, A.N. Panchenko, D.A. Sorokin

Institute of High Current Electronics SB RAS, Tomsk, 634055 Russia, yf.tarasenko@hcei.ru

Pulsed electrical discharges have various applications and are being extensively studied (see [1, 2]). In particular, much attention has been paid to the study of nanosecond pulsed-periodic discharges, including in non-uniform electric fields [3].

The objective of this study is to investigate the effect of air humidity on the spectral and optical characteristics of the radiation emitted by a pulsed-periodic discharge in a tip-to-tip gap.

The report will present new data on the emission spectra and characteristics of a discharge plasma in a non-uniform electric field. It should be noted that with a short voltage pulse front in such discharges, runaway electrons and X-ray radiation, as well as particle tracks from electrodes, are recorded [4, 5]. Specifically, it was found that relative air humidity (8–50%) during a pulsed-periodic discharge significantly affects the emission spectrum of the air between two iron needles and increases the intensity of broadband continuum emission, the H α hydrogen line, and the lines of iron atoms and ions (Fig. 1).

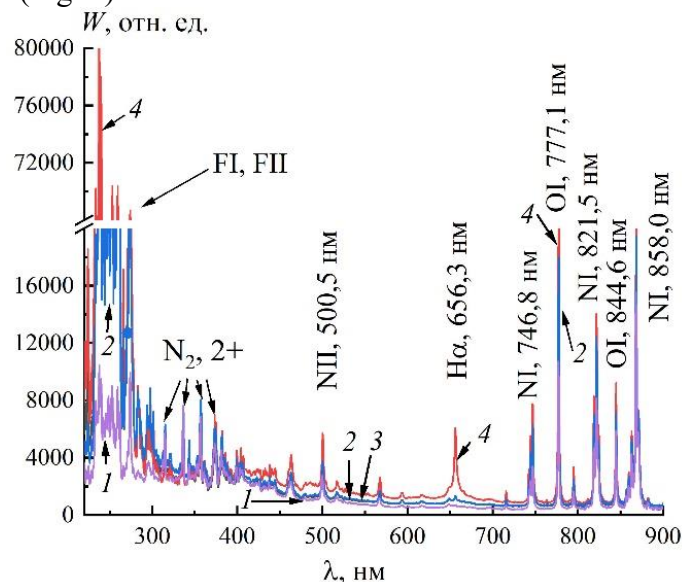


Fig. 1. Emission spectra of air with relative humidity $Y \approx 8\%$ (1), $Y \approx 25\%$ (2), air with $Y \approx 8\%$ with the addition of 1.5 Torr of hydrogen (3) and air with $Y \approx 50\%$ (4). Mixtures pressure 760 Torr. Generator GIN-50-1. $f = 10$ Hz. $U_0 = 16$ kV. $T = 23^\circ\text{C}$.

It is assumed that the broadband continuum that appears during discharge contraction is caused by the emission of molecular hydrogen during the transition $\text{H}_2(a^3\Sigma_g^+) \rightarrow \text{H}_2(b^3\Sigma_u^+)$.

State assignment of the IHSE SB RAS (project no. FWRM-2026-0008) supported this study.

References

- [1]. Wang D., Namihira T. *Plasma Sources Science and Technology* **29** (2) 023001 (2020).
- [2]. Shao T., Zhang C. (eds.) "Pulsed Discharge Plasmas: Characteristics and Applications." *Singapore: Springer Nature* (2023).
- [3]. Gavrilov S.Y., Parkevich E.V., and Khirianova A.I. *Bulletin of the Lebedev Physics Institute*. **52** (Suppl 4) S474-S482 (2025).
- [4]. Tarasenko V.F., Beloplotov D.V., Panchenko A.N., and Sorokin D.A. *Surfaces* **6** (2) 214–226 (2023).
- [5]. Tarasenko V.F., Beloplotov D.V., Panchenko A.N., and Sorokin D.A. *Plasma Science and Technology* **26** (9) 094003 (2024).

TRANSPORT PROPERTIES OF ELECTRON DRIFT IN A MIXTURE OF XENON AND WATER VAPOR

S.A. Maiorov¹, G.B. Ragimkhanov², R. I. Golyatina³

¹*Joint Institute for High Temperatures of the Russian Academy of Sciences, Moscow, Russia, mayorov_sa@mail.ru*

²*Dagestan State University, Makhachkala, Russia*

³*Prokhorov General Physics Institute of Russian Academy of Sciences, Moscow*

Small admixtures of molecular gases in heavy noble gases can qualitatively change electron transport and may produce negative differential conductivity (NDC), i.e., a decrease of the drift velocity with increasing reduced electric field E/N . In xenon this effect is closely related to the Ramsauer-Townsend minimum of the elastic momentum-transfer cross section around 0.6 eV. Water vapor is a common impurity in xenon-based discharge and detector systems; therefore, quantitative transport data for Xe-H₂O mixtures are required for discharge modeling and for assessing the impact of humidity contamination.

We calculated electron transport coefficients in Xe-H₂O under a uniform steady electric field by solving the Boltzmann kinetic equation in the two-term approximation. Cross sections for electron scattering in Xe were taken from the LXCat/TRINITY database, while for H₂O the Hayashi set was used with rotational excitation channels included. The drift velocity v_{dr} , mean electron energy ε , mobility μ , transverse diffusion coefficient DT , and the first Townsend ionization coefficient αT were obtained for $E/N = 0.1-100$ Td and H₂O molar fractions $\chi = 10^{-5}-10^{-1}$ (0.001%-10%).

The calculations show that even trace amounts of H₂O strongly affect electron drift in xenon. At low and moderate E/N , adding H₂O increases v_{dr} by several times compared with pure Xe, despite a reduction in ε ; for $\chi \lesssim 1\%$ the ionization coefficient αT remains nearly unchanged in the considered field range. A pronounced NDC region ($dv_{dr}/d(E/N) < 0$) is formed already at $\chi \sim 10^{-5}-10^{-4}$, and the turning point $dv_{dr}/d(E/N) = 0$ corresponds to $\varepsilon \approx 0.6$ eV for all χ , indicating that NDC is governed by the Xe Ramsauer minimum. The nonmonotonic behavior is explained by the competition between (i) redistribution of the electron energy distribution towards the Ramsauer minimum due to the increased momentum-transfer cross section of H₂O at these energies and (ii) enhanced energy losses and angular scattering once rotational/vibrational excitation channels of H₂O become active at higher E/N . The results provide reference data for kinetic modeling of xenon discharges and for benchmarking electron-H₂O cross-section sets.

References

- [1]. Petrovic Z. Lj., Crompton R. W., and Haddad G. N. *Aust. J. Phys.* 37, 23 (1984).
- [2]. Patrick E. L., Andrews M. L., and Garscadden A. *Appl. Phys. Lett.* 59, 3239 (1991).
- [3]. de Urquijo J., Basurto E., Juarez A. M., Ness K. F., Robson R. E., Brunger M. J., and White R. D. *J. Chem. Phys.* 141, 014308 (2014).
- [4]. LXCat: electron scattering cross section database (TRINITY and Hayashi sets), lxcatt.net (accessed May 20, 2023).

CREATION OF LUMINOUS CHARGED PARTICLES USING CAPILLARY AND CORONA DISCHARGES

V. L. Bychkov, A.A. Logunov, K.N. Kornev, D.V. Bychkov, O.S. Surkont

M. V. Lomonosov Moscow State University, Moscow, 119991, RF, bychvl@gmail.com

In this work, we investigate the combined effect of capillary discharge action on metal in the presence of ions formed by the corona discharge. At the same time, we consider the issue of the electric charging of the obtained particles. Experiments on the capillary plasma generator's jet formation of autonomous long-lived luminous particles of lead, tin or solder up to 5-7 mm in size and their charging using ions created using a corona discharge were carried out. The capillary plasma generator interacted with the energy of 1176, 1472 J inputted in the discharge. Formed metal compact long-lived luminous formations were charged by ions in the field of the corona discharge. The applied voltage to the corona discharge ranged from 5 to 15 kV, and the discharge current was in the range of 10-100 μA . At that, the sign of the ions coincided with the sign of the corona discharge. In the case of a negative corona using under experimental conditions, neutral particles were charged to a value of about $1.3 \cdot 10^{-7}$ C. Produced objects have properties similar to those of real ball lightning.

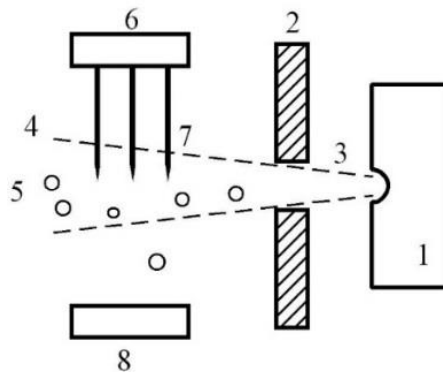


Fig.1 Experimental scheme. 1-Capillary plasma generator, 2 – metal strip, 3 - plasma jet, 4 - neutral gas jet, 5 - macroscopic particles, 6 - corona discharge electrode, 7 - corona discharge electrode needles, 8 – corona discharge electrode.



Fig.2 Spheres with a visible diameter of up to 7 mm, realized in a capillary discharge.

ON MECHANISM PROVIDING THE TRAJECTORY TWIST OF SURFACE STREAMER IN A BARRIER DISCHARGE UNDER TRANSVERSE MAGNETIC FIELD

Yu. Akishev, N. Dyatko, V. Karalnik, I. Kochetov, A. Petryakov

State Research Center of Russian Federation - Troitsk Institute for Innovative and Fusion Research, Joint-Stock Company, Moscow, Troitsk, Russia, akishev@triniti.ru

Barrier discharge is widely used to create nonequilibrium plasma enriched with bio-chemically reactive species and UV radiation. The transverse magnetic field has the great effect on spatial configuration of streamers and specific energy delivered into plasma with discharge. The experiment shows that surface streamers in a transverse magnetic field propagate by swirling trajectories [1, 2] (Fig. 1a). This report describes new mechanism of the trajectory twisting of a positive streamer in a surface barrier discharge by a transverse magnetic field.

Note the streamer body doesn't move aside due to Ampere force, that is, the streamer trajectory is determined by the direction of its head movement. The cause of streamers swirling is the seed electron behavior in a transverse magnetic field. Seed electrons occur ahead the streamer's head due to photoemission from a barrier and create e-avalanches during their movement towards the head. The created electrons are deflected by transverse magnetic field by the Lorentz force to the left regarding to the electric force direction. The resulting trajectories are shown in Fig. 1. Due to this deflection, the maximum of electron avalanches flux entering the streamer head will shift to a right side. This effect shifts the maximum of positive charge at the head as well and therefore changes the streamer movement direction.

We used the model positive space charge distribution located at the positive streamer head. To calculate the 3D electron trajectories in the presence of a magnetic field, it was necessary to determine three electron mobilities: μ , μ_{\perp} , μ_{\times} . The electron drift velocity is determined as [3, 4]:

$$\mathbf{V}_e = \mu(\mathbf{E} \cdot \mathbf{b})\mathbf{b} + \mu_{\perp}(\mathbf{E} - (\mathbf{E} \cdot \mathbf{b})\mathbf{b}) - \mu_{\times}\mathbf{E} \times \mathbf{b}, \quad \mathbf{b} = \mathbf{B}/B,$$

\mathbf{E} – electric field vector; \mathbf{B} – magnetic field induction vector.

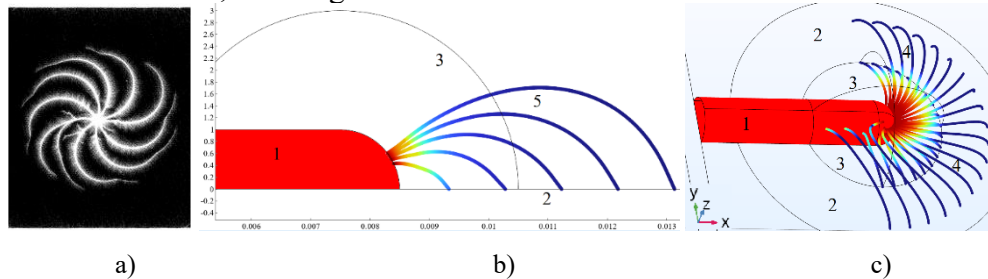


Fig. 1. a) Photo of swirling streamers [1]. b) Sketch of the 3D electric field distribution around the streamer head (z-x plane). c) Sketch illustrating the swirled electrons trajectories in front of streamer head in transverse magnetic field. The magnetic field is directed upward. The used Cartesian coordinate system is shown as well. 1 is the streamer body; 2 is the boundary of the e-emitting surface on the dielectric barrier; 3 are the lines showing the UV-emitting volume around the streamer head; 4 are the e-trajectories; 5 are the E-field streamlines.

The resulting electric field 3-D distribution and the obtained trajectories are presented in Fig. 1b, 1c. One can see that trajectories are shifted to the right side regarding to the longitudinal streamer axis. Thus, the mechanism proposed explains the streamer swirling phenomenon observed in the experiments.

This work was supported by the Russian Science Foundation under grant no. 25-49-00039

References

- [1]. P. Uhlig, J. C. Maan, and P. Wyder. *PHYS REV LETTERS* Vol 63, # 18, 1989
- [2]. A. Petryakov et al, *Proc. of the PPPT-11*, Minsk, 2025
- [3]. G. J. M. Hagelaar and L. C. Pitchford, *Plasma Sources Sci. Technol.* 14, 722-733 (2005)
- [4]. TRINITY database, www.lxcat.net, retrieved on December 17, 2025.

EXPERIMENTAL INVESTIGATION OF THE X- AND O-MODE ANOMALOUS ABSORPTION IN THE PLASMA FILAMENT

M.S. Usachonak¹, L.V. Simonchik¹, A.Yu. Popov², E.Z. Gusakov²

¹*Stepanov Institute of Physics of NAS of Belarus, Minsk, Belarus,*
m.usachonak@dragon.bas-net.by

²*Ioffe Institute, St-Petersburg, Russia*

A decade and a half ago, the effect of anomalous backscattering of pump power was observed in X2-mode electron cyclotron resonance heating (ECRH) experiments at TEXTOR [1]. The observed phenomenon has been explained as a consequence of two upper-hybrid plasmon parametric decay (TUHPD) instability [2], which has a very low threshold due to the trapping of daughter waves in the vicinity of the density maximum. This makes every region that has a local density maximum potentially unfavorable for the microwave beam as it passes from the launching antenna to its destination at the 2nd harmonic ECR. This was confirmed experimentally on the ASDEX-Upgrade and TCV tokamaks, as well as at the Wendelstein 7-X and L-2M stellarators. Moreover, the model experiments on interaction of microwaves with inhomogeneous filament plasma have demonstrated strong anomalous absorption related to the decay parametric instabilities not only for the X-mode [3,4], but for O-mode [5] as well. This work presents the comparable results of anomalous absorption for ordinary and extraordinary (O-and X-mode) pump waves in a plasma filament.

The experiments were performed under well-controlled plasma conditions at the linear facility «Granite» in Institute of Physics of NAS of Belarus. In these experiments, the effect of strong anomalous absorption of the X- and O-mode pump at frequency $f_0 = 2.38$ GHz was observed. The maximum average density of an argon plasma at a pressure of about 1-2 Pa in the filament was approximately 10^{10} cm⁻³, with the electron temperature reaching up to 1 eV. These investigations were performed at the electron density less than the critical one and in a magnetic field below the electron cyclotron resonance for the pump frequency f_0 .

The observed absorption has a threshold character. The thresholds are measured to be 100-200W and depend on both the magnetic field and the initial plasma density. The absorption efficiencies are found to be approximately 50% and 80% for the O- and X-mode waves, correspondingly. The absorption is accompanied by an increase in the electron energy up to ~5-8 eV and an increase in the electron density by more than one order of magnitude. The microwaves absorption is localized in a ring layer, expanding towards the edge of the plasma column. Scenarios for the pump wave decay are proposed. The agreement between the calculated values of the absorption thresholds and the experimental values is shown.

References

- [1]. Westerhof E., Nielsen S.K., Oosterbeek J.W. et al., *Phys. Rev. Lett.* **103** (2009) 125001.
- [2]. Gusakov E.Z., Popov A.Yu., *Plasma Phys. Control. Fusion* **57** (2015) 025022
- [3]. Altukhov A. B., Arkhipenko V. I., Gurchenko A. D., Gusakov E. Z., Popov A. Yu., Simonchik L. V. and Usachonak M. S. // *Europhys. Lett.* 2019. V.126. P.15002.
- [4]. Gusakov E. Z., Popov A.Yu., Simonchik L.V., Usachonak M.S. *Physics of Plasmas* **32**, (2025) 092101.
- [5]. Usachonak M.S., Popov A.Yu., Simonchik L.V., Gusakov E.Z., Tretinnikov P.V. *Plasma Physics Reports*, **52** (2026) 15–29.

EXPERIMENTAL DEMONSTRATION OF TEMPORAL COMPRESSION OF HIGH-CURRENT PULSED ELECTRON BEAM IN THE SYSTEM WITH VIRTUAL CATHODE

D.A. Adamiants, A.E. Donets, V.I. Rogozhin, A.A. Ravaev, A.B. Buleyko,
O.T. Loza, I.R. Muftakhov

JSC "SCR RF TRINITI", Moscow, Russia, d.adamiants@gmail.com

The paper studies the development of the coaxial system with virtual cathode (VC) in the axially symmetrical configuration of magnetically insulated diode [1]. Such a system allows flexible parameters adjustment of the VC created with the use of a spherical electrode in a hollow grounded liner (Fig.1).

Systems with high-current relativistic electron beam require a spatially non-uniform transport region to create VC. Typically, the radius of a hollow grounded liner increases at a certain distance from the cathode. However, this method makes flexible parameters adjustment of the VC impossible for fixed electron energy and beam current, because it requires the liner and/or solenoid resizing.

The optimal parameters of the VC were calculated for a system with strong (1 T) magnetic field. Then, the cathode with coaxial internal spherical electrode on the rod was installed in the liner (Fig.1).

The experimental results are shown in the Fig.2: cathode potential (a) and currents in the layout without VC (b) and with VC (c). In the presence of the VC the phenomenon of the electron beam compression was observed: amplitude increase while duration decrease.

The work was performed under State Contract no. H.4κ.241.09.25.1066 dated 20.05.2025.

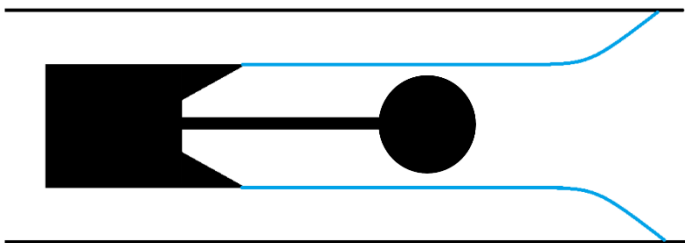


Fig. 1. Magnetically insulated coaxial diode with an inner electrode

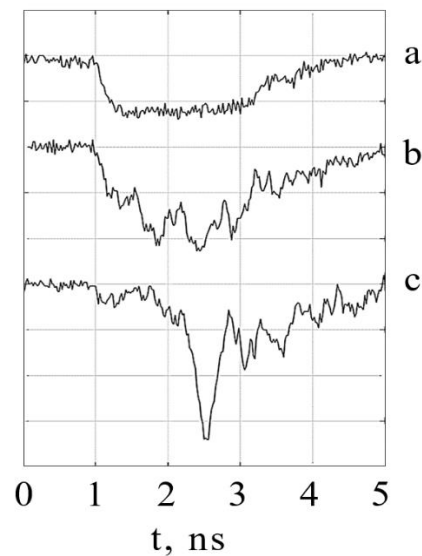


Fig. 2. Oscillograms: cathode (a) and currents in the layout without (b) and with VC (c)

References

- [1]. Donets A.E., Rogozhin V.I., Ravaev A.A. // All-Russian Youth Conference on Controlled Fusion, Plasma Technologies and High-Tech Medicine (VMKT-2025). Moscow, Troitsk, 2025. P. 161–162. (*in Russian*)

THE INFLUENCE OF THE INTRINSIC NOISE OF A RELATIVISTIC ELECTRON BEAM ON THE PARAMETERS OF ITS PROPAGATION

S.E. Andreev, I.L. Bogdankevich, N.G. Gusein-zade

*Prokhorov General Physics Institute of the Russian Academy of Sciences, Vavilova st., 38,
Moscow, 119991, Russian Federation, E-mail ira.bogdankevich@mail.ru.*

One of the pressing challenges of modern relativistic plasma microwave electronics is the creation of a source of powerful ultra-wideband radiation. A promising candidate for the implementation of such a source is a plasma maser, the operation of which is based on the Cherenkov interaction of a high-current relativistic electron beam (REB) with a preformed plasma. Depending on the operating mode, the maser is capable of amplifying either an external signal - in this case it operates as a plasma relativistic amplifier (PRA) - or the system's own noise (plasma relativistic noise amplifier, PRNA) when there is no external signal. In the latter mode, the noise microwave radiation at the output is formed by amplifying the fluctuations initially inherent in the electron beam [1]. In this regard, the study of the radiation parameters of a relativistic electron beam in a vacuum and their influence on the spectral characteristics of plasma masers is of particular importance. In [2], the plasma maser operated in the mode of an amplifier of the electron beam's own noise; feedback was absent due to the short duration of the REB current pulse, which was 2 ns. The power of the input noise signal, estimated based on the dependence of the output power of the PRNA on the length of the plasma-beam interaction region, reached 5 MW. In [3], based on the concepts of the ectonic nature of the emission of an explosive emission cathode [4], a numerical simulation of input noise was performed. The impact of ectons on the dynamics of the REB was taken into account by introducing a noise component with a uniform distribution and variable amplitude into the smooth current pulse. The current magnitude in [3] did not exceed a few kA. To increase the efficiency of plasma-beam interaction, it is advisable to use REB currents approaching the maximum permissible values for a given electrodynamic system. It is shown in [5] that the use of high-density, nanosecond-duration electron beams can be accompanied by the development of critical explosive electron emission, which manifests itself in the form of random high-amplitude current pulses. In the present work, the influence of the initial noise component on the propagation characteristics of a relativistic electron beam was studied numerically in a three-dimensional version of the KARAT code [6]. The input noise parameters and the magnitude of the REB current varied over a wide range, including the region of maximum permissible values. During the analysis, time realizations of the output power, the corresponding spectral characteristics, as well as the correlation coefficients between the shape of the REB current and the output radiation signal were obtained. A strong correlation was found between the shape of the REB current pulse and the instantaneous radiation power generated in the chamber during the passage of relativistic electrons. The obtained correlation coefficient decreases as the current increases and approaches the limit. Also, due to the unevenness of the reflection coefficient from the collector over frequency, there is a noticeable correlation of these parameters in the output coaxial waveguide.

References

- [1]. Strelkov P.S., Ivanov I.E. and Shumeiko D.V. *Plasma Phys. Rep.* **42** (7) 644-648 (2016).
- [2]. Buleyko A.B., Ponomarev A.V., Loza O.T., Ulyanov D.K., Sharypov K.A., Shunailov S.A., Yalandin M.I. *Physics of plasmas*, 28, 023304, (2021) DOI: 10.1063/5.0031432.
- [3]. Bogdankevich, I.L., Andreev, S.E., Loza, O.T. *et al. Phys. Wave Phen.*, 33, 247-252 (2025).
- [4]. Mesyats G.A., *Bulletin of the RAS*, 2014, V .84, (7), 579-589.
- [5]. Tverdohklebov S.I., Tukhfatullin T.A., *Izvesnia TPU*, 2000, №3, 32-50.
- [6]. Tarakanov V. P. "User's manual for code KARAT." *Springfield: BRA* 2012 (1992).

CALCULATION OF NONLINEAR SPECTRA OF CHERENKOV INSTABILITIES OF DENSE ELECTRON BEAMS IN ELECTRODYNAMIC SYSTEMS OF PLASMA MICROWAVES

A.V. Ershov, M.V. Kuzelev

Faculty of Physics, Lomonosov Moscow State University, Leninskie Gory, 1-2, Moscow, 119991, Russia, ershov.av17@physics.msu.ru

The multi-wave interaction of a thin-walled tubular rectilinear electron beam with delayed electromagnetic waves of a cylindrical electrodynamic system with plasma filling is considered. General nonlinear equations of the multi-wave regime of Cherenkov beam instability are obtained.

$$\begin{aligned} \frac{dE_s(t, r_b)}{dt} &= -\theta_s \left(\frac{\partial D_0}{\partial \omega_{ws}} \right)^{-1} \frac{\Omega_{bs}^2}{s k_0^2 u^2} \exp(i\Delta_s t) \rho_{bs}, \\ \frac{dy}{dt} &= k_0 u \eta, \\ \frac{d\eta}{dt} &= k_0 u \left(1 - 2\gamma^2 \frac{u^2}{c^2} \eta \right)^{3/2} \frac{1}{2} \sum_{s=S_{\min}}^{S_{\max}} \left(E_s \exp(-i\Delta_s t + isy) - i \frac{\Omega_{bs}^2}{s k_0^2 u^2} \rho_{bs} \exp(isy) + C.C. \right), \\ \rho_{bs} &= \frac{1}{\pi} \int_0^{2\pi} \exp[-isy(t, y_0)] dy_0, \end{aligned} \quad (1)$$

For the case of the collective forced Cherenkov effect, multi-wave equations with cubic nonlinearity are obtained. The nonlinear dynamics of the spectrum of waves excited by a beam in a plasma waveguide is studied, the results are shown in Fig. 1.

It is shown that there is a broadening of the instability spectrum in the regime of the collective forced Cherenkov effect due to the mechanism of collective nonlinear deceleration of the electron beam during its interaction with many modes of delayed electromagnetic waves. The efficiency of the transfer of the kinetic energy of the beam into radiation can be estimated using the formula [1] $\eta = 2\gamma^2 (u^2/c^2)(\Delta u/u)$, which in our case is about 30%.

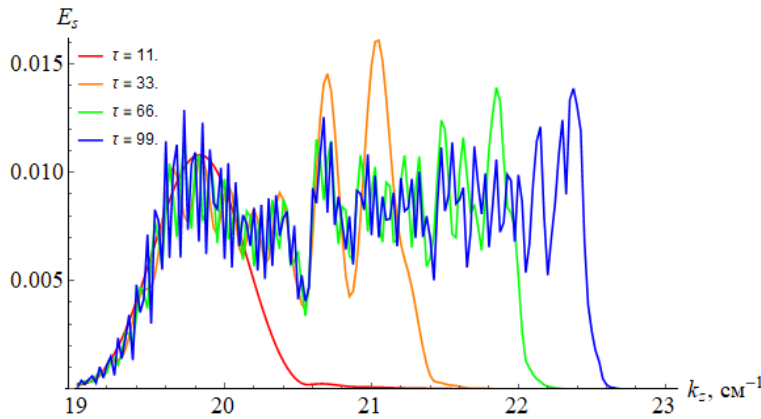


Fig. 1 Dynamics of the surface wave spectrum of a coaxial plasma waveguide under the collective stimulated Cherenkov effect

References

- [1]. Kuzelev M.V., Rukhadze A.A., Strelkov P.S., Shkvarunets A.G. "Relativistic plasma UHF electronics" *Sov. Phys. Usp.* 28 724–726 (1985).

SELF-EXCITATION OF A PLASMA MICROWAVE AMPLIFIER USING AN NON-UNIFORM ABSORBER

I.N. Kartashov, M.V. Kuzelev, A.V. Tumanov

Moscow State University, Moscow, Russia, avtumanow@gmail.com

The beam-plasma instability development in a plasma microwave amplifier with an absorber non-uniform along the length of the system is considered. The addition of an absorber to the system is due to the need to suppress parasitic feedback. In this case, the presence of an absorber leads to a modification of the system's electrodynamic properties. Beam-plasma instability spatial dependency of increments are calculated, parameter regions are determined when self-excitation of the amplifier does not occur. Efficiency modification of conversion of electron energy into energy of amplified wave and effect of absorber on it are estimated.

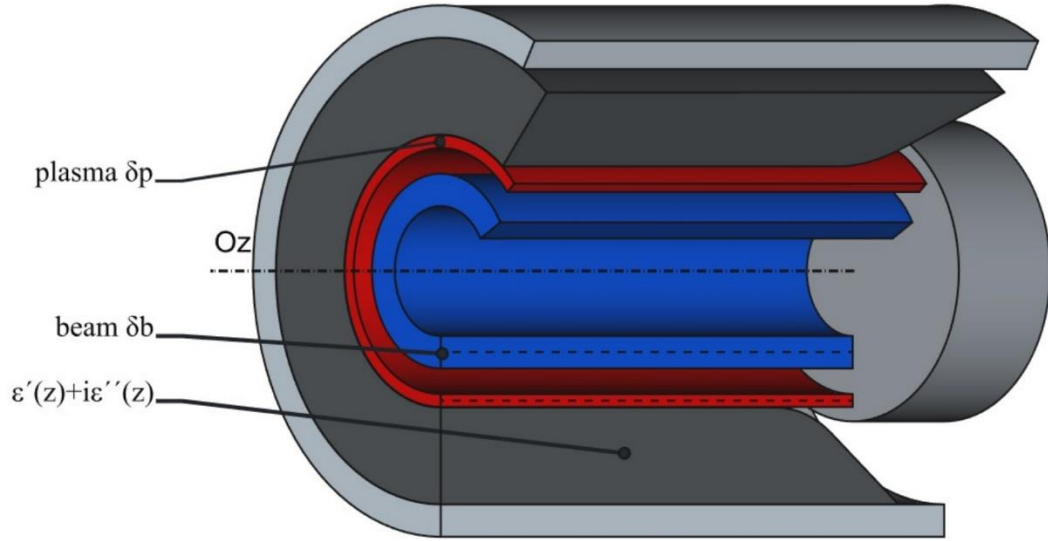


Fig. 1. A schematic of the microwave plasma amplifier: absorber is located unevenly along the beam-plasma interaction area

In such a system, there is a well-known dispersal equation [1,2], that can be written for each position along the z-axes, considering absorber permittivity.

$$\left[\omega^2 - \omega_p^2 \frac{\chi_0^2}{k_{\perp p}^2} \right] \left[(\omega - k_z u)^2 - \omega_b^2 \gamma^{-3} \frac{\chi_0^2}{k_{\perp p}^2} \right] = \Theta \omega_p^2 \frac{\chi_0^2}{k_{\perp p}^2} \omega_b^2 \gamma^{-3} \frac{\chi_0^2}{k_{\perp p}^2}.$$

The absorber permittivity dependence on the longitudinal coordinate is assumed to be slow, so the geometrical optics approximation is applicable, with $\text{Im} \varepsilon \approx \text{Re} \varepsilon$. By determining the increments dependence of the forward and backward waves, one can check whether the self-excitation condition of the system is met.

$$|\kappa_{14} \kappa_{41}| \exp \left[\int_0^L (-\text{Im} k_{z1}(z) + \text{Im} k_{z4}(z)) dz \right] > 1$$

This work was supported by the Theoretical Physics and Mathematics Advancement Foundation "BASIS"

References

- [1]. I.N. Kartashov, M.V. Kuzelev and A.V. Tumanov, *Phys. Plasmas* 32, 023103 (2025)
- [2]. I.N. Kartashov and M.V. Kuzelev, *Plasma Physics Reports* 50 (5), 597-602 (2024).

POSSIBILITIES OF ATOMIC-LAYER ETCHING IN INDUCTIVELY COUPLED PLASMA FOR THE CREATION OF NANOELECTRONIC DEVICES

A.V. Miakonkikh, R.R. Khalilullin, V.O. Kuzmenko

NRC "Kurchatov institute" - Valiev IPT, Nakhimovsky Prospect, 36/1, Moscow, Russia, E-mail: miakonkikh@ftian.ru

The dimensions of individual integrated circuit components are approaching the atomic scale, necessitating new manufacturing technologies that ensure high precision and reproducibility in the formation of functional nanostructures. This requires additive and subtractive methods for component formation with maximum precision, scalable to large wafer sizes of up to 300 mm. Although Plasma assisted atomic layer etching (ALE), was proposed several decades ago, its implementations still lack some of the expected advantages of the atomic layer process, such as ideal etch rate control, uniformity over a large wafer, and a synergy level close to 1. While the synergy effect and atomic-scale etch rate control achieved with the neutral beam approach were quite good, significant efforts are being made to tune ALE for use in equipment with a wide-aperture plasma source. Technological interest is focused on plasma assisted atomic layer etching processes that could be performed in currently common plasma etching systems, one of the advantages of which is the ease of scaling to wafer sizes up to 300 mm. Currently, various materials are being studied for the feasibility of implementing the ALE process, with etch selectivity being one of the key optimization areas.

The cyclic process of atomic layer plasma-chemical etching is organized as a "reverse" of the ALD process, in which the first step of the cycle involves chemisorption of a monolayer of active precursor on the surface, followed by removal of excess precursor from the reactor chamber, and, in the next step, activation of the reaction between the substrate and the adsorbate monolayer (etching reaction) by bombarding the surface with plasma ions of chemically inert gases with energies <40 - 60 eV. The ion flux also facilitates the desorption of volatile reaction products [1, 2]. A prerequisite for selecting a specific reaction for atomic layer etching is the absence of spontaneous reaction in the absence of ion stimulation. Using the example of the ALD process for thin silicon layers, the process's ultimate capabilities in terms of minimum layer thickness removal per cycle, close to a monoatomic silicon layer, are demonstrated, as well as the record-breaking selectivity of the atomic layer etching process for underlying layers of other materials. Potential applications of ALD and ALE processes are demonstrated, which can significantly improve the performance of modern nanoelectronic structures and create promising nanoelectronic devices [3,4].

All these challenges are closely related to the need to obtain a controlled ion energy distribution function (IEDF). The ion energy profile determines how closely the process adheres to the "ALE window"—a narrow energy range in which the modified surface layer is completely removed, while the unmodified material remains defect-free. In ICP reactors, the energy spectrum of ions reaching the wafer surface is controlled by applying a high-frequency (HF) bias voltage to the substrate, which generates an electric field. The report will examine the possibilities of forming a narrow energy distribution of the IEDF.

The research was carried out within the State assignment of the National Research Center "Kurchatov Institute".

References

- [1]. Miakonkikh A.V., Kuzmenko V.O., Efremov A.M., Rudenko K.V. *Russ. Microelectron.* **53(1)** 70-78 (2024)
- [2]. Miakonkikh A., Kuzmenko V., Efremov A., Rudenko K. *Vacuum* **234** 114044 (2025)
- [3]. Kuzmenko V., Lebedinskij Y., Miakonkikh A., Rudenko K. *Vacuum* **207** 111585 (2023)
- [4]. Kuzmenko V., Melnikov A., Isaev A., Miakonkikh A. *J. Vac. Sci. Technol. A* **42(5)** 052602 (2024)

NUMERICAL INVESTIGATION OF CLAMP EFFECT ON SPACE CHARGE LAYER FORMATION AND IMPACT ON ETCH UNIFORMITY

R.R. Khalilullin ^{1,2}, V.O. Kuzmenko ¹, A.V. Miakonkikh ¹

¹*NRC “Kurchatov institute” – Valiev IPT, Moscow, Nakhimovsky Prospect, 36/1, Moscow, Russia, E-mail: khalilullin.rr@phystech.edu*

²*Moscow Institute of Physics and Technology, 9 Institutskiy Pereulok, Dolgoprudny, Russia.*

Modern semiconductor manufacturing demands etching processes with atomic-scale precision and minimal unintended material removal. Contemporary fabrication requirements necessitate minimization of physical sputtering during plasma processing while maintaining high throughput across large-diameter wafers, which is also necessary for ALE [1]. Inductively coupled plasma (ICP) reactors provide the capability for independent control of plasma density and ion energy via two independent generators, making them essential for advanced micro- and nanoelectronic device fabrication [2]. However, the mechanical constraints of wafer handling, particularly the clamping mechanism, introduce subtle but significant variations in plasma-surface interactions that are often overlooked in process optimization and this is why understanding space charge layer dynamics is important for achieving uniform processing results and reducing parasitic sputtering effects.

Our approach combines two diagnostic techniques to capture both plasma bulk properties and surface effects. Spectral ellipsometry provides monitoring of surface layer thickness before and after plasma exposure, revealing how ion bombardment varies across the wafer. In addition, we use Langmuir probe measurements for electron temperature and density in the plasma volume and we use plane multiprobe for density measurements near the surface of the plate.

A two-dimensional hydrodynamic model of the plasma chamber was developed using COMSOL Multiphysics software that specifically accounts for the physical constraints of industrial wafer handling. Unlike simplified models that treat the substrate as an ideal infinite plane, our simulation incorporates the exact geometry of the ceramic glass clamp used in production reactors. The model includes field-dependent ion mobility corrections to handle the high electric fields present in the sheath region, and tracks how the clamp's edge disrupts the natural formation of the space charge layer. In this work, we validated our model using experimental data from Langmuir probe measurements under different conditions and carried out a final comparison of the sputtering rate with the model results, which allows us to conclude that the modeling results are similar in an area inaccessible to experimental research.

Our key finding in this work reveals how the mechanical clamp affect the space charge layer. The ceramic clamp creates a sharp discontinuity that forces equipotential surfaces to rise near the holder edge. This geometric constraint causes the vertical electric field component to vary along the wafer radius because in the pre-sheath region near the clamp, the field intensifies while within the sheath itself it weakens. These field variations produce different ion energy distributions at different radial positions and this explains why etch rates and profiles often vary across production wafers despite apparently uniform plasma conditions and this is why it's necessary to have understanding of effects that happen in space charge layer as well as holder geometry optimization.

This work was performed under the state assignment of the NRC "Kurchatov Institute".

References

- [1]. Gottlieb S, et al. *Jour. of Vac. Sci. and Technol.*, **42** 1-53 (2024).
- [2]. Bogdanova, D., et al. *Plasma Sources Sci. Technol* **30** (7) 1-31 (2021).

MICROWAVE GYROTRON-INDUCED COATING FORMATION ON TUNGSTEN PLATES FROM METAL AND DIELECTRIC POWDERS

T.E. Gayanova¹, E.A. Obraztsova^{1,2}, A.V. Stepanova³, A.S. Sokolov¹, E.V. Voronova¹,
V.D. Stepakhin¹, N.N. Skvortsova¹

¹*Prokhorov General Physics Institute of the Russian Academy of Sciences, Moscow, Russia*

²*Moscow Institute of Physics and Technology (National Research University), Dolgoprudny, Russia*

³*Mendeleev University of Chemical Technology of Russia, Moscow, Russia*

Tungsten has been approved as the preferred material for the first wall and divertor core of the ITER international fusion reactor. Currently, a grade of tungsten (W-VMP), having undergone industrial manufacturing and assembly, is already being used as the divertor material. However, surface modification and mass transfer mechanisms under extreme thermal loads remain poorly understood [1,2]. This paper examines the interaction of plasma generated by microwave radiation from a gyrotron (power up to 0.5 MW, frequency 75 GHz) with a metal/dielectric powder mixture and V-MP tungsten plates.

An experimental study was conducted using powder systems based on tungsten and boron-containing dielectric materials (B, B₄C). In some experiments, activating additives such as magnesium or carborane were added to the mixtures to intensify plasma-chemical processes.

The test samples were exposed to pulsed microwave radiation from a gyrotron with a power of 400 kW and a pulse duration of 8 ms. As a result of plasma-chemical synthesis, the deposition of plasma-dust condensate particles on tungsten plates was observed. It was found that the maximum deposition intensity was achieved using mixtures containing magnesium or carborane.

The plasma-chemical reactions under study occur under high-temperature heating of the powder material surfaces, a gaseous environment, and plasma. Specifically, the surface temperature, determined using Planck radiation for the Al₂O₃+Ni/W (1:4) system, ranged from 3500 to 4700 K (with an error of ±400 K). Under the influence of microwave discharge, the formation of crystalline structures was observed in the studied systems, as documented by scanning electron microscopy (SEM) and energy-dispersive X-ray spectroscopy (EDX). The resulting EDX maps, demonstrating the particle distribution on the wafer surfaces after the experiment, are shown in Fig 1.

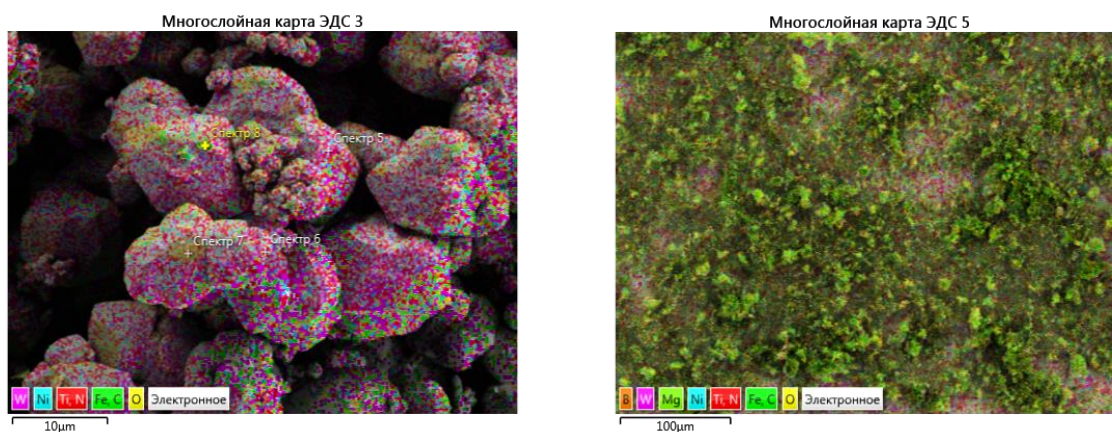


Fig. 1. Raw tungsten powder and the surface of the tungsten plate is coated with W and B₄C

References

- [1]. www.iter.org
 [2]. Будаев В.П. // ВАИТ. Сер. Термоядерный синтез, 2015, т. 38, вып. 4

SYNTHESIS OF SODIUM-MANGANESE OXIDE MATERIALS VIA MICROWAVE DISCHARGE: FIRST EXPERIMENTAL RESULTS

M. E. Donets^{1*}, T. E. Gayanova², N.N. Skvortsova², N. S. Akhmadullina³, D. V. Malakhov², V. D. Stepakhin², E. A. Korneeva¹, N. Yu. Samoylova¹

¹Joint Institute for Nuclear Research, 6 Joliot-Curie St, Dubna, Moscow Region, Russia 141980, *mdonets@jinr.ru

²Prokhorov General Physics Institute of the Russian Academy of Sciences, Moscow, Russia

³A.A. Baikov Institute of Metallurgy and Material Science of the Russian Academy of Sciences, Moscow, Russia

Sodium-ion batteries are attractive for grid-scale storage because sodium is abundant and chemically similar to lithium. P2-layered sodium-manganese oxide Na_{0.7}MnO₂ (NMO) cathodes combine low cost, good ion diffusion, and stability. Electrochemical performance correlates with particle size and morphology. The smaller particle size leads to shorter diffusion paths and larger active surface area and as a result it boosts capacity and cycling rate [1–4].

In [5], NMO was synthesized via microwave synthesis (2.45 GHz, 500 W) yielding the material with sub-1 μm particles and a capacity of 200 mAh/g at 1/12C. Non-uniform irradiation limited the process, prompting tests with more powerful, uniform radiation.

Two series of plasma-chemical synthesis experiments were performed using a gyrotron at the MIG-3 experimental stand. The starting mixtures comprised the following compositions: Na₂CO₃/Mn₂O₃ and NaOH/NaNO₃/Mn₂O₃. In both cases graphite (TIMCAL SUPER C45) was added as a conductive additive. The mixtures were placed into the plasma-chemical reactor and treated with pulses of MW irradiation (200 kW and 300kW, 4 ms). Particles of spherical morphology with a diameter ranging from 20 to 100 μm were discovered via SEM (Fig. 1). Elemental analysis and XRD were also used to analyze the obtained materials.

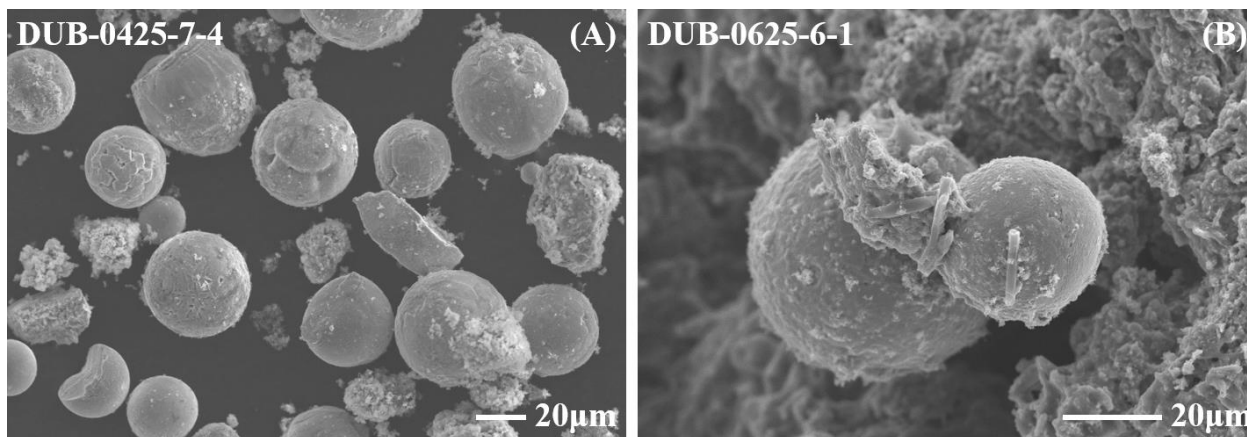


Fig. 1. SEM images of the samples prepared via plasmochemical method from (A) Na₂CO₃/Mn₂O₃ + 10% C and (B) NaOH/NaNO₃/Mn₂O₃ + 10% C under oxygen atmosphere.

References

- [1]. Yamada, A., Chung, S. C., Hinokuma, K., *Journal of the electrochemical society*, 148(3), A224 (2001).
- [2]. Ni, J., Kawabe, Y., Morishita, M., Watada, M., Sakai, T., *Journal of Power Sources*, 196(19), 8104-8109 (2011).
- [3]. Zhang, H., Xu, Y., Liu, D., *RSC Advances*, 5(15), 11091-11095 (2015).
- [4]. Samoylova, N. Y., Donets, M. E., Vasin, R. N., *et al. Nano Research*, 18(4), 94907280 (2025).
- [5]. Matsumae, Y., Suzuki, R., Komiya, K., & Higuchi, M., *Journal of the Ceramic Society of Japan*, 128(8), 544-546, (2020).

EFFECTIVE LENGTH OF A PLASMA ANTENNA ON A PLASMA COLUMN

I.M. Minaev, V.I. Zhukov, O.V. Tikhonovich, D.M. Karfidov, I.L. Bogdankevich

*Prokhorov General Physics Institute of the Russian Academy of Sciences, Moscow, Russia,
E-mail: minaev1945@mail.ru*

The frequency range of plasma vibrator antennas can be extended by controlling the length of the plasma antenna (plasma column) [1]. A plasma column in a gas-discharge tube is produced by a surface wave excited by a high-frequency generator with power P_1 and frequency ω_1 , whereas radiation is generated at another frequency ω_2 by a second source with power P_2 . The plasma column length is governed by ω_1 and P_1 . Since the efficiency of plasma antennas increases with the ratio of the plasma frequency to the radiation frequency [2], it is advantageous to form a plasma column at $\omega_1 > \omega_2$ whose length L corresponds to the resonant antenna length at ω_2 . The surface-wave discharge exists while the wave energy is sufficient to maintain the electron density n_e above the critical value n_{ecr} . When n_e decreases to n_{ecr} , the plasma column passes into a decaying plasma region (deionization region), as shown in Fig. 1a.

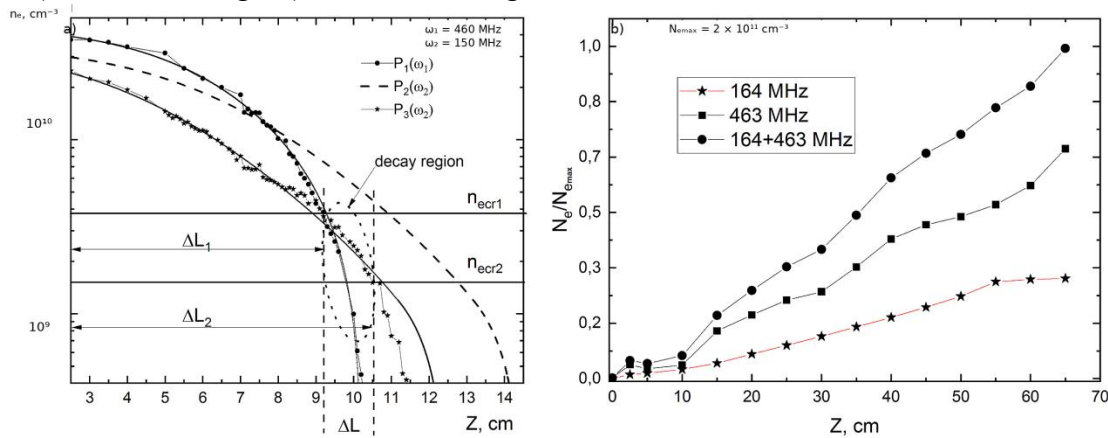


Fig. 1. Axial distribution of electron density along the plasma column; (a) $P_1 = 7$ W, $P_2 = 5$ W, $P_3 = 7$ W; (b) 164 MHz – 10 W, 463 MHz – 15 W.

At the operating frequency ω_2 , a surface wave can also propagate along the plasma column, causing an additional increase in n_e and a shift of the critical point n_{ecr} , which corresponds to a new effective antenna length. For $P_2 < P_1$, the plasma column length increases by ΔL . For $P_2 > P_1$, the surface wave at ω_2 can propagate along a part of the decaying plasma region and further, until P_2 becomes insufficient to sustain n_e above the critical value for wave propagation at ω_2 . In this case, a plasma column of another length is formed. Thus, the discharge behavior and the effective antenna length in the presence of the second surface wave are determined by the plasma parameters in the deionization region, as well as by P_2 and ω_2 . For this purpose, an electrodynamic model was developed in the electromagnetic code KARAT [3] with Particle-in-Cell (PiC) method, enabling simulation of discharge ignition and sustainment at two frequencies, 460 MHz and 150 MHz. The aim of this work is to study the influence of the deionization region on the operating characteristics of a plasma antenna. Analytical estimates and numerical calculations show that this region determines such characteristics of a plasma antenna as the radiated power and the effective length.

References

- [1]. Minaev I.M., Tikhonovich O.V., Vekshin Y.E. *Journal of Communications Technology and Electronics* **69** (3), 227-232 (2024).
- [2]. Istomin E.N., Karfidov D.M., Minaev I.M., Rukhadze A.A., Tarakanov V.P., Sergeichev K.F., Trefilov A.Yu. *Plasma Physics Reports* **32** (4), 388-400 (2006).
- [3]. V. P. Tarakanov, User's Manual for Code KARAT (BRA Inc., VA, USA, 1992).

STRUCTURE AND DYNAMICS OF A SURFACE-WAVE-SUSTAINED MICROWAVE DISCHARGE IN LOW-PRESSURE ARGON

V.P. Stepin, V.I. Zhukov, D.M. Karfidov, S.E. Andreev, I.L. Bogdankevich,
 N.N. Bogachev

*Prokhorov General Physics Institute of the Russian Academy of Sciences, Moscow, Russia,
 s.stepin@physplasm.ru*

Surface-wave-sustained discharges in dielectric tubes are used to produce extended plasma columns and are applied in plasma antennas, gas-discharge lasers, and material processing technologies [1]. In this work, an experimental and numerical study of a microwave surface-wave discharge in argon at pressures of 0.02–6 Torr ($v_{en} \ll \omega$) is carried out.

The discharge was excited by a waveguide applicator (2.45 GHz, up to 850 W) in a 2-m-long quartz tube. Numerical simulations were performed using the electromagnetic PiC code KARAT [2], reproducing the experimental conditions. The relative plasma density n_e , averaged over the cross-section, was determined from the signal I of a collimated photodetector assuming $I \propto n_e \pi r T_e = \text{const}$ [3]. Radial density profiles were obtained from transverse images using Abel inversion. The propagating discharge is shown to consist of an ionization front and a stabilized region. In the stabilized part, a linear axial electron density profile is formed; n_e exceeds the critical density $n_c = 7.5 \cdot 10^{10} \text{ cm}^{-3}$ for 2.45 GHz and increases with pressure. In the front region at $n_e \approx n_c$ microwave field enhancement due to plasma resonance occurs, accompanied by nonlocal electron heating [4].

The radial plasma structure depends on pressure: at low pressures a Bessel-type profile is formed, whereas at higher pressures a density depression appears on the tube axis. The pressure dependence of the ionization-front velocity obtained in the experiment and in the simulations shows the same behavior. This combined experimental–numerical characterization of axial and radial structure, ionization-front dynamics, and resonance at $n_e \approx n_c$ provides a consistent picture of surface-wave discharges in argon and supports optimization of surface-wave plasma sources and plasma antennas.

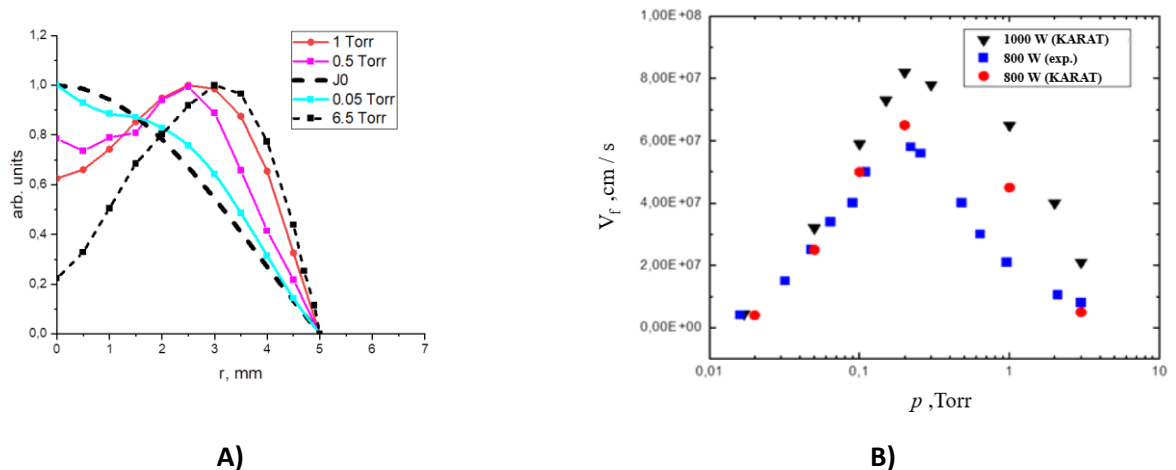


Fig.1. A) Experimental radial plasma density profiles at $z = 5$ cm from the excitation point; Bessel-type profile - $J_0 \sim J_0(2.4r/a)$. B) Experimental and KARAT-calculated dependences of the ionization-front velocity V_f on pressure p .

References

- [1]. Istomin E.N., Karfidov D.M. et al. *Plasma Physics Reports* **32** (4), 388-400 (2006)
- [2]. Tarakanov V. P. User's Manual for Code KARAT//BRA Inc., VA, USA. 1992.
- [3]. Zhukov V.I., Karfidov D.M., Sergeichev K.F. *Plasma Physics Reports* **46** (8) 837-845 (2020).
- [4]. Aliev Yu.M., Maximov A.V., Schlüter H. // *Phys. Scr.* 1993. V. 48. № 4. P. 464-466. +

PLASMA SCIENCE AND TECHNOLOGY IN BRAZIL: FOUR PILLARS FROM FUSION AND SPACE PLASMAS TO ATMOSPHERIC-PRESSURE APPLICATIONS

R.S. Pessoa, G. Petraconi Filho, D.M. Leite, A.L.J. Pereira, A.S. da Silva Sobrinho,
H.S. Maciel

*Plasmas and Processes Laboratory (LPP), Aeronautics Institute of Technology (ITA),
Departamento de Ciência e Tecnologia Aeroespacial, São José dos Campos (SP), Brazil.*

Brazilian plasma science has grown from mid-20th-century roots into a multi-institutional field spanning fundamentals, space plasmas, and technology. This invited report reviews four pillars: (i) fusion and magnetic confinement; (ii) technological plasmas (vacuum/high-temperature) for thin films, surface engineering, propulsion, and microelectronics; (iii) basic plasma physics supporting modeling and diagnostics; and (iv) space/astrophysical plasmas, strengthened by Brazil's equatorial location and long-term programs on ionospheric irregularities, scintillation, and space-weather services. Emphasis is placed on the atmospheric-pressure revolution—cold atmospheric plasmas and plasma-activated liquids—enabling applications in medicine/dentistry, agriculture, and environmental remediation. The report concludes with challenges and mission-oriented opportunities for scale-up and impact.

PLASMA TECHNOLOGIES IN AERODYNAMICS

S.V. Ryzhkov, V.V. Kuzenov

*Bauman Moscow State Technical University (BMSTU). Moscow, Russia,
E-mail: svryzhkov@bmstu.ru*

The development of rocket and space technology using new technical solutions, laser and electron-ion-plasma technologies stimulate active research of gas-dynamic and thermophysical processes in a wide range of parameters and various gas-vacuum conditions in the world's leading scientific centers. The use of plasma technologies in aerodynamics is of constant interest. This interest is primarily related to the potential impact on the integral and local characteristics of body flow: modification of the shape and intensity of compaction surges, control of boundary layers and areas of flow separation, effects on vortex structures in the flow, cavity, and others. It is important to note here that the possibility of experimentally studying such flows near the surface and inside the structure of promising aircraft is fraught with many technical difficulties and requires high financial costs. Therefore, the study of the possibilities of magnetoplasma flow control methods, plasmophysical characteristics of pulsed plasma jets (generated by various types of plasma discharges) It requires the development of physico-mathematical and computational models suitable for the analysis of magnetohydrodynamic flows in high-speed, radiating, nonequilibrium gas and plasma flows under conditions of strong heterogeneity of the properties of the medium. However, in this case, high accuracy of the obtained numerical results is necessary (especially when finding temperature and heat flux distributions), strict requirements are imposed on the software package and numerical methods that simulate high-speed gas-plasma flows near bodies of complex geometric shape [1-10].

This research has been supported by the Ministry of the Science and Higher Education of the Russian Federation (Russian Minobrnauki), Project No. FSFN-2024-0011.

References

- [1]. Kuzenov V. V., Ryzhkov S. V. *Journal of Physics: Conference Series* **815**, 012024 (2017). doi: 10.1080/15361055.2022.2112037
- [2]. Kuzenov V. V., Varaksin A. Yu., Ryzhkov S. V. *Symmetry* **16**, 1200 (2024), doi: 10.3390/sym16091200.
- [3]. Polyanskiy A. G., Ryzhkov S. V. *AIP Conference Proceedings* **3177**, 060005 (2025), doi: 10.1063/5.0295139.
- [4]. Kuzenov V. V., Ryzhkov S. V. *Technical Physics* (2025), doi: 10.1134/S1063784225700392.
- [5]. Kuzenov V. V., Ryzhkov S. V. *Fusion Science and Technology* **81**, 789-799 (2025). doi: 10.1080/15361055.2025.2512616.
- [6]. Varaksin A. Yu., Ryzhkov S. V. *Aerospace* **11**: 800 (2024).
- [7]. V.Yu. Khomich, V.A. Yamshchikov, V.V. Kuzenov, S.V. Ryzhkov, E.V. Shakhmatov. *Technical Physics Letters* **51**, 262-269 (2025).
- [8]. Varaksin A. Yu., Ryzhkov S. V. *Mathematics* **11**: 3290 (2023).
- [9]. Shumeiko A., Telekh V., Ryzhkov S.V. *Chinese Journal of Aeronautics*. **38**, issue 6. P. 103401. <https://doi.org/10.1016/j.cja.2025.103401> (2025).
- [10]. Varaksin A. Yu., Ryzhkov S. V. *Aerospace* **12**: 894 (2025).

INTERACTION OF POWERFUL HIGH-FREQUENCY RADIO EMISSION WITH PLASMA IN THE LOWER AND UPPER IONOSPHERE - EXPERIMENTAL RESULTS

N.V. Bakhmetieva, I.N. Zhemyakov, E.E. Kalinina, O.K.Khromin

Radiophysical Research Institute Nizhny Novgorod State University, 25/12a Bol'shaya Pecherskaya Str., Nizhny Novgorod, 603950, Russia, nv_bakhm@nirfi.unn.ru

Under the influence of powerful high-frequency radio emission from ground-based heating facilities, artificial plasma irregularities along the geomagnetic field with transverse scales from cm to tens of kilometers are formed in the disturbed region of the ionosphere [1]. The causes of the formation these irregularities differ in different regions of the ionosphere. Vertical and oblique probing of the disturbed region using ionosondes and specially created diagnostic facilities makes it possible to study the features of the occurrence of these irregularities far from the region of resonant interaction of powerful radio emission with the ionospheric plasma of the F-region. The report presents and discusses the results of experiments with ionospheric plasma disturbance by power radiation from the SURA mid-latitude heating facility (56.15°N, 46.11°E). The basis of the initial experiments was the creation of a disturbed region in the ionospheric plasma by emitting radio waves of ordinary or extraordinary polarization at a frequency of 4.300 MHz from the heating facility for several seconds or several minutes. Depending on the time and frequency of the impact on the ionosphere near the altitude of the upper hybrid resonance, artificial inhomogeneities in temperature and electron concentration arose. Using the method of vertical probing of the disturbed region with test radio waves at a frequency of 2.95 MHz on the base of a partial reflection technique it was established that during the operation of the heating facility, not only signals specularly reflected from the ionosphere were recorded, but also additional signals from altitudes both above and below the height of specular reflection of the test wave. The additional signal had a pronounced diffuse character [2]. This means that the artificial disturbance manifests itself at altitudes significantly below the reflection altitude of the powerful radio wave. Recent experiments are conducted in July and October 2025, when irradiating the ionosphere with a powerful radio wave of the ordinary polarization at 5.828 MHz and probing it with test radio waves at 4.300 MHz, yielded similar results. The difference was that in the first experiments, the additional signal was received primarily from altitudes in the E-layer (100–130 km), while in the more recent experiments; it was received most often from altitudes of the lower part F2-layer (140–170 km). The report discusses the physical causes of the propagation of the artificial disturbance from the altitude of the resonant interaction of powerful radiation with ionospheric plasma to altitudes in the lower ionosphere.

The work was supported by Russian Science Foundation under project No. 25-27-00031.

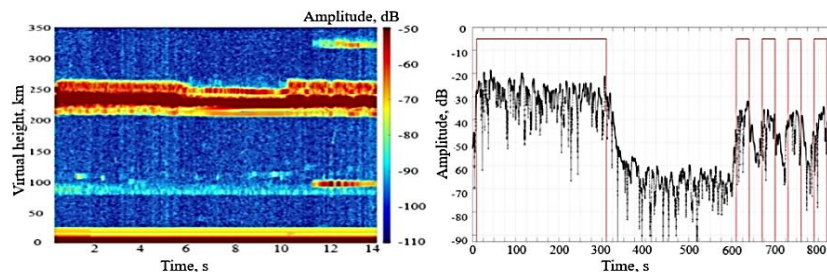


Fig. 1. An example of an additional signal appearing at the virtual altitude of 237 km during the operation of the SURA facility in October 8, 2025. The red lines indicate the heating intervals.

References

- [1]. Gurevich, A. V. "Nonlinear Phenomena in the Ionosphere". Springer-Verlag, Berlin and Heidelberg GmbH & Co. K, Berlin, Germany (2012).
- [2]. Bakhmetieva N. V., et al. *Advances in Space Research* **61** (7) 1919-1930 (2018).

**INVESTIGATION OF SPORADIC E-STRUCTURES AND WAVE PHENOMENA IN THE EARTH'S
LOWER IONOSPHERE BASED ON ANALYSIS OF RADIO OCCULTATION
MEASUREMENTS**

V.N. Gubenko, I.A. Kirillovich, V.E. Andreev

Kotel'nikov Institute of Radio Engineering and Electronics of the RAS, Fryazino, Moscow region, Russia, E-mail: vingubenko@gmail.com; gubenko@fireras.su.

Sporadic E-layers (E_s) are thin layers of increased ionization at heights of ~90 to ~130 km in the Earth's ionosphere. The study of effects associated with E_s -structures is important for ensuring smooth operation of radio communication and navigation systems. The wind shear theory of E_s -layer formation at middle latitudes has been confirmed by many studies. It has been found that the E_s -layers at middle latitudes are very thin (their thickness is several hundred meters), distributed horizontally over hundreds of kilometers, dense (with density as high as several units $\times 10^6 \text{ cm}^{-3}$), and consist of metal atoms [1]. In the presence of inclined geomagnetic fields, ion coalescence in the E-region of the ionosphere can be caused by shear of both zonal and meridional winds. The zonal wind shear is, however, considered as the primary driver of ion convergence in middle latitudes at heights of ~115 km and below [2]. Electrons associated with the coalescence of positive ions into a thin layer move along geomagnetic field lines to neutralize the positive charge.

At high latitudes ($>60^\circ$), since the magnetic field is directed almost vertically to the local horizon, the mechanism for E_s -layer formation through wind shear is not as effective as that at middle latitudes. The large-scale horizontal plasma structure in the auroral E-region is determined by the spatial distribution of sources of solar radiation and particle precipitation. Internal gravity waves (IGWs) at high latitudes are less important as the mechanism for vertical structuring of the layers due to a large angle ($\sim 90^\circ$) of magnetic field inclination with respect to the local horizon [3]. Nevertheless, the small angle of magnetic field inclination from vertical is very considerable here due to the large electric fields perpendicular to the magnetic field. At high latitudes, convective electric fields are important drivers of ion convergence or divergence [1, 4].

We have used radio occultation (RO) measurements to study E_s -layers in Earth's ionosphere. Parameters of the ionospheric structures are determined by analyzing vertical variations of RO-signal phase path (eikonal) and intensity at frequency $f_1=1575.42$ MHz of the global positioning system (GPS). The time resolution of phase and intensity measurements of the radio signal received is 0.02 s, which corresponds to a sampling frequency of 50 Hz. The analyzed data indicates the presence of significant quasi-regular variations in radio wave intensity and phase. In the RO studies of Earth's ionosphere, not only discrete (single) E_s -layers were observed but also more complex structures such as double E_s -peaks and even rectangular sporadic layers [5].

Propagation of the IGWs at ionospheric heights leads to the formation of ionization irregularities [6]. It is now known that internal atmospheric waves generate traveling ionospheric disturbances (TIDs) and sporadic E-irregularities of several types. It has been established that TIDs feature a pronounced inclination of equal phase surfaces, whereas E_s -layers exhibit nearly horizontal phase surfaces. This is due to the fact that E_s -layers are formed by atmospheric tides and long-period buoyancy waves, which decay in the F-region of the ionosphere owing to dissipative effects [7]. The internal atmospheric wave propagating through the ionosphere leads to the formation of a wave node of ionization due to collisions between charged and neutral particles. Kato et al. [8] have shown that the wave propagating through the E-region generates wave-like electron density variations, which have the same frequency and wave number as the initial IGW in the absence of boundaries or irregularities in the surrounding plasma.

A method for determining characteristics of internal atmospheric waves based on the use of inclined sporadic E-layers of Earth's ionosphere as a detector has been developed [9-11]. The idea of this method is as follows: a small-scale internal wave propagating through the E-region causes a sporadic layer to incline, by turning its ionization plane parallel to the phase front of the internal wave. We have used radio occultation satellite measurements to examine sporadic E-layers in Earth's high-latitude and near-equatorial ionosphere. This method gives the possibility to establish relationships between small-scale IGWs and sporadic layers in Earth's ionosphere.

The work was carried out within the framework of the state order of the Kotel'nikov Institute of Radio Engineering and Electronics of the RAS.

References

- [1]. Kirkwood S., Nilsson H. *Space Sci. Rev.* **91** 579-613 (2000).
- [2]. Haldoupis C. *Space Sci. Rev.* **168** 441-461 (2012).
- [3]. Kelley M. C. "The Earth's Ionosphere: Plasma Physics and Electrodynamics." *Second Edition. San Diego. Academic Press* (2009).
- [4]. Nygren T., Jalonen L., Oksman J., Turunen T. *J. Atmos. Terr. Phys.* **46** 373-381 (1984).
- [5]. Yue X., Schreiner W. S., Zeng Z., Kuo Y.-H., Xue X. *Atmos. Meas. Tech.* **8** 225-236 (2015).
- [6]. Hines C. O. *Can. J. Phys.* **38** 1441-1481 (1960).
- [7]. Gossard E. E., Hooke W. H. "Waves in the Atmosphere" Amsterdam, Oxford, New York, Elsevier Scientific Publishing Co (1975).
- [8]. Kato S., Reddy C. A., Matsushita S. *J. Geophys. Res.* **75** 2540-2550 (1970).
- [9]. Gubenko V. N., Pavelyev A. G., et al.-A. *Advances in Space Research.* **61**(7) 1702-1716 (2018).
- [10]. Gubenko V. N., Kirillovich I. A. *Solar-Terrestrial Physics.* **5**(3) 98-108 (2019).
- [11]. Gubenko V. N., Kirillovich I. A. *Cosmic Research.* **58**(3) 139-149 (2020)

Prokhorov General Physics Institute of the Russian Academy of Sciences
(Moscow, Russia)

Complex Systems of Charged Particles and their Interaction with Electromagnetic Radiation

22th INTERNATIONAL WORKSHOP, April 6-10, 2026

<http://cscpier.org/>

The Russian Ministry for Science and Education
The Russian Academy of Sciences

Advisory Committee

Sergey Garnov	Chairman	GPI RAS, Moscow, Russia		
Sergey Garanin	Co-Chair	FSUE RFNC - VNIIEF, Sarov, Russia		
Oleg Petrov	Co-Chair	JIHT RAS, Moscow, Russia		
Tlekkabul Ramazanov	Co-Chair	Al-Farabi KazNU, Almaty, Republic of Kazakhstan		
Vladimir Krainov	Co-Chair	Moscow Institute for Physics and Technology, Moscow, Russia		
Namik Gusein-zade	Co-Chair	GPI RAS, Moscow, Russia		
Werner Ebeling		Humboldt University, Berlin, Germany		
Boris Chichkov		Leibniz Universität Hannover, Hannover, Germany		
Sergey Popel		IKI, Moscow, Russia		
Alexander Ignatov		GPI RAS, Moscow, Russia		
Michael Kalashnikov		Max-Born-Institut, Berlin-Adlershof, Germany		
Genri Norman		HSE, Moscow, Russia		
Gerd Roepke		Rostock University, Rostock, Germany		
Sergey Trigger		JIHT RAS, Moscow, Russia		
Sergey Pikuz		MEPhI, Moscow, Russia		
Viktor Karasev		SPbU, St Petersburg, Russia		
Sergey Popruzhenko		MEPhI, Moscow, Russia		
Maratbek Gabdullin		Kazakh-British Technical University, Almaty, Republic of Kazakhstan		
Leonid Simonchik		B.I. Stepanov Institute of Physics of NAS of Belarus, Minsk, Republic of Belarus		
Michael Romanovsky		PI "Science and Innovations", RosAtom, Moscow, Russia		
Babak Shokri		Shahid Beheshti University, Tehran, Iran		
Valiantsin Astashynski		A.V. Luikov Heat and Mass Transfer Institute of NAS of Belarus, Minsk, Republic of Belarus		
Bratislav M. Obradović		Faculty of Physics, University of Belgrade, Belgrade, Serbia		
Rodrigo Sávio Pessoa,		Aeronautics Institute of Technology, São José dos Campos, Brasil		

Organizing Committee

Contact: cscpier@mail.ru

Namik Gusein-zade	Chair	GPI RAS, Moscow, Russia	Sergey Andreev	GPI RAS, Moscow, Russia
Nikolai Bogachev	Scientific Secretary	GPI RAS, Moscow, Russia	Vyacheslav Stepin	GPI RAS, Moscow, Russia
Elena Tarakanova	Technical Secretary	GPI RAS, Moscow, Russia	Oleg Fomichev	GPI RAS, Moscow, Russia
			Alexander Khudov	GPI RAS, Moscow, Russia

Sections

1. Basic Aspects of Plasma Science
2. Complex Plasmas
3. Laser Plasmas
4. General Plasmas
5. Solid State Plasmas

Venue

The CSCPIER-2026 will be held at Prokhorov General Physics Institute of the Russian Academy of Sciences, Vavilov street 38, Moscow, Russia



ISBN 978-5-6048157-4-8



9 785604 815748

Подписано в печать 27.03.2026
Тираж 110 экз.
Заказ № 6739
Типография onlinescopy
г. Москва, Лефортовский пер., дом 8, строение 2
E-mail: info@onlinescopy.ru